

THE DENSITIES OF LIQUID SILICATES
CONTAINING IRON OXIDE

THE DENSITIES OF LIQUID SILICATES
CONTAINING IRON OXIDE AT 1410°C

by

DAVID ROBERT GASKELL, B.Sc.

A Thesis

Submitted to the Faculty of Graduate Studies
in Partial Fulfilment of the Requirements
for the Degree
Doctor of Philosophy

McMaster University

June 1967

DOCTOR OF PHILOSOPHY (1967)
(Metallurgy)

McMASTER UNIVERSITY
Hamilton, Ontario

TITLE: The Densities of Liquid Silicates Containing Iron Oxide at 1410°C.

AUTHOR: David Robert Gaskell, B.Sc. (University of Glasgow)

SUPERVISORS: Professors R. G. Ward and A. McLean

NUMBER OF PAGES: (xiv); 145

SCOPE AND CONTENTS:

Using the maximum bubble pressure method of density determination, the density-composition relationship of iron silicates in contact with solid iron at 1410°C has been determined. The "iron oxide" in an iron silicate has been replaced by calcium oxide, manganous oxide, cobaltous oxide, nickel oxide and calcium fluoride and the density-composition relationships occurring have been obtained. The calculated oxygen density-composition relationships have been interpreted in terms of the effects of silica concentration and cationic species on the anionic configuration occurring in the melts and this interpretation has been correlated with recently-developed thermodynamic models of silicate anion configuration in basic binary silicate systems.

ACKNOWLEDGEMENTS

The author is greatly indebted to his supervisors, Dr. R. G. Ward and Dr. A. McLean for their advice and encouragement throughout the course of the work. The problem was suggested by Dr. R. G. Ward.

The generous financial assistance of the Dominion Foundries and Steel Company, Ltd. of Hamilton, Ontario, during the early stages of the work and The International Nickel Company of Canada, Ltd. and The Department of University Affairs during the later stages is gratefully acknowledged.

The author also wishes to thank the staff and graduate students of the McMaster Metallurgy Department for their help and stimulating discussions. In particular, thanks are due to Mr. H. Neumeyer for his invaluable advice and help during the initial stages of the work, and to Mr. G. Deboer of the Engineering Machine Shop for his advice and help in the fabrication of the experimental apparatus. Acknowledgement is also made to Mr. P. L. Sachdev, who built the original apparatus.

Finally, acknowledgement is made to Miss Marilyn Stewart for her expert and rapid typing of this thesis.

TABLE OF CONTENTS

| | | |
|-----------|---|----|
| CHAPTER 1 | INTRODUCTION | 1 |
| CHAPTER 2 | THE STRUCTURES OF LIQUID SILICATES - A LITERATURE REVIEW | 3 |
| 2.1 | Physical Properties of Liquid Silicates | 3 |
| 2.1.1. | Electrical Conductivity | 3 |
| 2.1.2. | Viscosity | 10 |
| 2.1.3. | Density | 19 |
| 2.1.4. | Surface Tension | 25 |
| 2.1.5. | Phase Relationships | 31 |
| 2.1.6. | Discussion of the interpretation of the physical behaviour of liquid silicates | 37 |
| 2.2 | Thermodynamic Properties of Liquid Silicates | 42 |
| 2.2.1. | Molecular models | 42 |
| 2.2.2. | Ionic models | 45 |
| 2.2.2.1. | The Toop and Samis Ionic Model | 46 |
| 2.2.2.2. | The Flood and Knapp Ionic Model | 51 |
| 2.2.2.3. | The Masson Ionic Model | 54 |
| CHAPTER 3 | THE CONSTITUTION AND STRUCTURE OF IRON SILICATES | 68 |
| CHAPTER 4 | THE MAXIMUM BUBBLE PRESSURE METHOD OF DENSITY DETERMINATION | 77 |
| 4.1 | Theory | 77 |
| 4.2 | Corrections required for density calculation | 78 |
| 4.3 | Systematic errors | 79 |

| | | |
|-----------|---|----|
| 4.4 | Previous work | 80 |
| CHAPTER 5 | EXPERIMENTAL - THE DENSITIES OF IRON OXIDE AND IRON SILICATES | 83 |
| 5.1 | Experimental apparatus | 83 |
| 5.1.1 | Furnace assembly | 83 |
| 5.1.2 | Crucible assembly | 84 |
| 5.1.3 | Furnace atmosphere gas | 84 |
| 5.1.4 | Temperature control | 85 |
| 5.1.5 | Blowing gas arrangement | 85 |
| 5.1.6 | Pressure measurement | 85 |
| 5.1.7 | Temperature profile of the furnace | 86 |
| 5.2 | Preparation of materials | 86 |
| 5.2.1 | Preparation of wustite | 86 |
| 5.2.2 | Preparation of silica | 87 |
| 5.3 | Preliminary attempts to measure the density of liquid iron oxide | 88 |
| 5.4 | Equilibrium requirements of the system Fe (solid)-FeO(liquid) and causes of iron precipitation | 89 |
| 5.5 | The effect of the occurrence of iron precipi- tation on the measured density | 90 |
| 5.6 | Modifications to the apparatus | 93 |
| 5.7 | Determination of the density of liquid iron oxide and liquid iron silicates with the modified apparatus | 95 |
| 5.7.1 | Sampling of the melt | 96 |

| | | |
|-----------|---|-----|
| CHAPTER 6 | EXPERIMENTAL - THE DENSITIES OF TERNARY SILICATES CONTAINING IRON OXIDE | 98 |
| 6.1 | The replacement of iron oxide silicates by oxides more stable than "FeO" | 98 |
| 6.1.1 | Introduction | 98 |
| 6.1.2 | The system CaO-"FeO"-SiO ₂ | 99 |
| 6.1.2.1 | Materials preparation | 99 |
| 6.1.2.2 | Experimental procedure | 100 |
| 6.1.3 | The system MnO-"FeO"-SiO ₂ | 100 |
| 6.1.3.1 | Preparation of manganous oxide | 101 |
| 6.1.3.2 | Experimental procedure | 101 |
| 6.1.4 | The system CaF ₂ -"FeO"-SiO ₂ | 102 |
| 6.2 | The replacement of iron oxide in iron silicates by oxides less stable than "FeO" | 102 |
| 6.2.1 | Introduction | 102 |
| 6.2.2 | Crucibles | 103 |
| 6.2.3 | Blowing tubes | 104 |
| 6.2.4 | The system CoO-"FeO"-SiO ₂ | 106 |
| 6.2.4.1 | Preparation of cobaltous oxide | 106 |
| 6.2.4.2 | Experimental procedure | 107 |
| 6.2.5 | The system NiO-"FeO"-SiO ₂ | 107 |
| 6.2.5.1 | Experimental procedure | 108 |
| CHAPTER 7 | EXPERIMENTAL RESULTS | 109 |
| 7.1 | "FeO" | 109 |
| 7.2 | The system "FeO"-SiO ₂ | 109 |
| 7.3 | The system CaO-"FeO"-SiO ₂ | 109 |

| | | |
|------------|---|-----|
| 7.4 | The system MnO-"FeO"-SiO ₂ | 110 |
| 7.5 | The system CaF ₂ -"FeO"-SiO ₂ | 110 |
| 7.6 | The system CoO-"FeO"-SiO ₂ | 111 |
| 7.7 | The system NiO-"FeO"-SiO ₂ | 111 |
| CHAPTER 8 | DISCUSSIONS | 119 |
| 8.1 | The systems "FeO" and "FeO"-SiO ₂ | 119 |
| 8.2 | The oxygen density | 120 |
| 8.3 | The oxygen density deviation | 123 |
| 8.4 | The Masson model | 124 |
| 8.5 | Comparison between actual and predicted behaviour | 127 |
| 8.6 | The activity of free oxygen ions and the oxygen density | 128 |
| 8.7 | The activities of metal oxides in ternary silicate melts | 129 |
| 8.8 | Ionic interactions in binary and ternary silicate melts | 131 |
| 8.9 | The activity of silica in ternary silicate melts | 135 |
| 8.10 | The effect of temperature on polymerisation | 135 |
| 8.11 | The constancy of oxygen density | 136 |
| 8.12 | The effect of CaF ₂ additions to iron silicates | 136 |
| CHAPTER 9 | SUMMARY | 138 |
| REFERENCES | | 140 |

LIST OF TABLES

| <u>TABLE</u> | <u>TITLE</u> | <u>PAGE</u> |
|--------------|---|-------------|
| I | Variation of the Free Energy for Electrical Conduction ΔG^* with the ion-oxygen attraction I for various cations and silicate compositions. | 8 |
| II | Anions present in liquid silicates at compositions between 10 and 50 mole per cent metal oxide | 14 |
| III | Values of the equilibrium constant k for various binary silicate melts | 49 |
| IV | Values of the equilibrium constant k for various binary silicate melts. | 62 |
| V | Estimated values of $k_{1,1}$ for the system CaO-SiO ₂ at various temperatures | 66 |
| VI | The density of liquid iron oxide in contact with iron at 1410°C obtained bubbling helium, nitrogen and argon. | 112 |
| VII | The densities of iron silicate melts in contact with iron at 1410°C. | 113 |
| VIII | The analyses of iron oxide melt samples | 114 |
| IX | The densities of calcium iron silicate melts in contact with iron at 1410°C. | 115 |
| X | The densities of manganese iron silicate melts in contact with iron at 1410°C. | 116 |
| XI | The densities of calcium iron fluorosilicate melts in contact with iron at 1410°C. | 117 |
| XII | The densities of cobalt iron silicate melts at 1410°C. | 117 |

| <u>TABLE</u> | <u>TITLE</u> | <u>PAGE</u> |
|--------------|---|-------------|
| XIII | The densities of nickel iron silicate melts at 1410°C. | 118 |
| XIV | The mole fractions of anions theoretically present in various binary silicate systems at $N_{\text{SiO}_2} = 0.29$. | 126 |

LIST OF ILLUSTRATIONS

| <u>FIGURE</u> | <u>TITLE</u> | <u>PAGE</u> |
|---------------|---|-------------|
| 1 | Activation energy for electrical conduction as a function of composition in binary silicate melts. | 6 |
| 2 | Free energy of electrical conduction as a function of ion-oxygen attraction in binary silicate melts. | 6 |
| 3 | Energies of activation for viscous flow as a function of composition in alkali and alkaline earth silicate melts. | 12 |
| 4 | Comparison of the effects of CaO with the hypothetical effect of CaF ₂ on the silicate network. | 16 |
| 5 | Hypothetical solvating effect of the addition of CaF ₂ to silicate melts | 16 |
| 6 | Thermal expansivity as a function of composition in alkali silicate melts. | 21 |
| 7 | Two-dimensional representation of the cage occurring in alkali silicates at $N_{M_2O} = 0.12$ | 21 |
| 8 | Relationship between F and Z/R in binary silicates | 27 |
| 9 | Surface tension as a function of composition in binary silicates melts. | 27 |
| 10 | Temperature coefficients of surface tension as a function of composition in binary silicate melts. | 29 |
| 11 | Temperature coefficients of surface tension as a function of Z/R in binary meta-silicate melts | 29 |
| 12 | Silica saturation surfaces in various binary silicate systems. | 34 |

| <u>FIGURE</u> | <u>TITLE</u> | <u>PAGE</u> |
|---------------|---|-------------|
| 13(a) | Equilibrium values of (O^-) , (O^0) and (O^{2-}) as a function of silica concentration for $k = 0.06$ (Toop and Samis). | 48 |
| 13(b) | Equilibrium values of (O^0) , (O^-) and (O^{2-}) as a function of silica concentration for $k = 0.0$ (Toop and Samis). | 48 |
| 14 | Calculated free energy of mixing curves for various values of k (Toop and Samis). | 50 |
| 15(a) | Constituent anions as a function of composition in lead silicate melts. | 53 |
| 15(b) | Distribution of silicon atoms present in anions as a function of composition in lead silicate melts. | 53 |
| 16 | Theoretical curves of $N_{SiO_4}^{4-}$ against $N_{O^{2-}}$ for various values of k (Masson). | 58 |
| 17 | Theoretical curves of $N_{Silicate}$ against $N_{O^{2-}}$ for $k = 1$ (Masson). | 59 |
| 18 | Theoretical curves of activity against mole fraction of metal oxide for various values of k (Masson). | 63 |
| 19 | Experimentally determined activities of iron oxide as a function of composition in iron silicate melts. | 69 |
| 20 | Calculated activities of stoichiometric iron oxide as a function of composition in iron silicate melts. | 69 |
| 21 | Heat of mixing diagram and phase diagram for iron silicates. | 72 |
| 22 | Percentage ionic conduction in iron silicate melts as a function of composition. | 74 |
| 23 | Viscosities of iron silicates as a function of composition and temperature. | 74 |

FIGURE

TITLE

The following illustrations are located at the end of the thesis.

- 24 Previous determinations of the density-composition relationship of iron silicates melts in contact with solid iron.
- 25 Measured density of liquid iron oxide as a function of the atomic number of the blowing gas.
- 26 Temperature profiles and crucible location in the furnace.
- 27 The tips of blowing tubes after:
- (a) bubbling liquid iron oxide with highly deoxidised gas
 - (b) bubbling liquid iron oxide with gas containing the equilibrium partial pressure of oxygen for contact with liquid iron oxide and solid iron at 1410°C.
 - (c) bubbling liquid iron oxide with gas containing the equilibrium partial oxygen pressure for contact with liquid iron oxide and solid iron at 1410°C followed by bubbling with highly deoxidised gas.
- 28 Typical ring of iron formed at the melt surface due to heat abstraction.
- 29 Construction of the heating element.
- 30 The density-composition relationship of iron silicates in contact with iron at 1410°C.
- 31 The liquid phase field in the system CaO-"FeO"-SiO₂ at 1410°C.
- 32 Composition paths studied in the system CaO-"FeO"-SiO₂.
- 33 The density-composition relationships in the system CaO-"FeO"-SiO₂ at 1410°C.
- 34 The liquid phase field in the system MnO-"FeO"-SiO₂ at 1410°C.

FIGURETITLE

- 35 The density-composition relationship in MnO-"FeO"-SiO₂ melts in which $N_{\text{SiO}_2} = 0.29$ at 1410°C.
- 36 The density-composition relationship in CaF₂-"FeO"-SiO₂ melts in which $N_{\text{SiO}_2} = 0.29$ at 1410°C.
- 37 The density-composition relationship in CoO-FeO-SiO₂ melts in which $N_{\text{SiO}_2} = 0.29$ at 1410°C.
- 38 The density-composition relationship in NiO-FeO-SiO₂ melts in which $N_{\text{SiO}_2} = 0.29$ at 1410°C.
- 39 The effects of the replacement of Fe²⁺ ions by Ca²⁺, Mn²⁺, Co²⁺, and Ni²⁺ ions on the density of an iron silicate containing 29 mole per cent silica.
- 40 The oxygen density-composition relationships occurring in the system "FeO"-SiO₂ at 1410°C.
- 41 The difference in oxygen density between solutions and mechanical mixtures of iron silicates as a function of silica concentration at 1410°C.
- 42 The oxygen density-composition relationships in the system CaO-"FeO"-SiO₂ at 1410°C.
- 43 The oxygen density-composition relationship occurring in MnO-"FeO"-SiO₂ melts in which $N_{\text{SiO}_2} = 0.29$ at 1410°C.
- 44 The oxygen density-composition relationship occurring in CoO-FeO-SiO₂ melts in which $N_{\text{SiO}_2} = 0.29$ at 1410°C.
- 45 The oxygen density-composition relationship occurring in NiO-FeO-SiO₂ melts in which $N_{\text{SiO}_2} = 0.29$ at 1410°C.
- 46 The activity-composition relationships of various metal oxides in binary silicate solution.

FIGURETITLE

- 47 The theoretical distribution of anions occurring in various binary silicate systems.
- 48 The oxygen density deviation due to cation replacement in the system CaO-FeO-SiO₂ at 1410°C.
- 49 The oxygen density deviations due to the replacement of Fe²⁺ ions by Ca²⁺, Mn²⁺, Co²⁺ and Ni²⁺ ions along the N_{SiO₂} = 0.29 composition path at 1410°C.
- 50 Iso-free oxygen activity lines in the system CaO-"FeO"-SiO₂ at 1600°C.
- 51 The activity of iron oxide in CaO-"FeO"-SiO₂ melts at 1365°C.
- 52 Iso-iron oxide activity lines in the system CaO-"FeO"-SiO₂ at 1600°C and the system MnO-"FeO"-SiO₂ at 1550°C.
- 53(a) Iso-activity lines for silica in the system MnO-"FeO"-SiO₂ at 1550°C.
- 53(b) Proposed iso-degree of polymerisation lines in systems such as MnO-"FeO"-SiO₂.

CHAPTER 1

INTRODUCTION

The nature and structure of silicates has aroused interest in a wide range of disciplines ranging from pure chemistry to extraction metallurgy and ceramics, and the development of silicate science has benefitted greatly from these diverse fields of interest. The friendly rivalry which exists between ceramicists and metallurgists is summed up by the ceramicists' opinion that "slags are very imperfect glasses" and the metallurgists' reply that "glasses are cold and metallurgically useless slags".

In general, the ceramicist is interested in the physical properties of relatively simple acidic silicates and the extraction metallurgist is interested in the chemical properties of highly complex basic silicates. The models of silicate structure which have emerged as a result of ceramic interest are mainly pictorial in nature in that they are concerned with the manner in which the silica network is modified by the presence of basic metal oxides. On the other hand, the models of silicates which have emerged as a result of metallurgical interest have been mainly thermodynamic in nature in that they are concerned with the modification of the chemical properties of metal oxides by the presence of silica and other network forming oxides. The prime requirement of any model of silicate structure, from the viewpoint of the practical metallurgist, is that the model should be capable of

predicting the chemical behaviour of silicates, and, as a result of this, the veracity of the model, with respect to structure on an atomic scale, has been very much a secondary consideration. Within the last two decades, however, metallurgical interest in the atomic or ionic models of the structure of liquid silicates has increased and attempts are now being made to correlate the known chemical behaviour of slags with the models developed from a consideration of the physical properties. With this approach, an attempt is being made to explain the variation of empirical thermodynamic parameters in terms of atomistics.

Determination of the structure of liquid silicates is rendered difficult by the fact that no single parameter exists, specifically associated with structure, which can be measured. Thus deduction concerning structure has been based on the measurement of several different physical properties and the variation of the properties with temperature and composition. One such property is the density of the liquid. It would be expected that the measurement of density would be particularly applicable to structure determinations of liquids as any deviation from ideality can only be due to structural interactions.

In the present work, the density-composition relationships of multicomponent silicate melts containing iron oxide have been determined at 1410°C and the behaviour observed has allowed deductions to be made concerning the structure of these melts. These deductions are in agreement with recently developed thermodynamic models of anionic configuration in basic silicate melts.

CHAPTER 2

THE STRUCTURE OF LIQUID SILICATES - A LITERATURE REVIEW

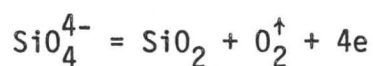
2.1 Physical Properties of Liquid Silicates2.1.1 Electrical Conductivity

Although it has been known since 1907 (1) that molten silicates conduct electricity, the development and acceptance of an ionic theory of slags has been inhibited by the fact that slag behaviour, with respect to slag-metal distribution, could be predicted by assuming that only neutral molecules existed in the slags (2,3). It was only when the molecular theories became unwieldy due to an excess of empirical assumptions that attention was turned to the concept of a completely ionised slag containing a limited number of ionic species (4).

Several early studies of the electrical conductivity of silicate melts indicated that ions were present. Farup et al (5) measured conductivities in the systems CaO-SiO_2 and $\text{CaO-Al}_2\text{O}_3\text{-SiO}_2$, Sauerwald and Neuendorff (6) successfully electrolysed iron silicate melts and Wejnarth (7), in measuring the conductivities of iron silicates, found that the conductivity increased with increasing FeO content and that a sharp change occurred in the conductivity at the temperature of primary crystallisation. He subsequently used this latter property to determine the melting point of slags.

The first systematic study of electrical conductivities of silicate melts was made by Martin and Derge (8) who studied melts in the system $\text{CaO-Al}_2\text{O}_3\text{-SiO}_2$. They obtained a straight line relationship

between the logarithm of the conductivity and the inverse temperature and noted that the temperature coefficient of the conductivity was positive. This indicated that the conduction was ionic rather than electronic. It was found that electrolysis of the melt occurred during which silicon migrated to the anode and calcium to the cathode, indicating that silicon was associated with negatively charged groups and calcium with positively charged groups. Evolution of a gas and occurrence of a white deposit at the anode suggested that the anode reaction was



It was concluded that the silicon and aluminium ions, with their small radii and high charges, attract oxygen more strongly than do magnesium, iron or calcium ions. SiO_4^{4-} was envisaged as being the simplest silicate ion but it was considered that these could polymerise with increasing silica content to form ring and chain ions. In spite of this evidence, it was still concluded that FeO , Ca_2SiO_4 and CaO could occur in the slag as neutral molecules, although it was conceded that the concentrations of these molecules would be very small.

The qualitative findings of Martin and Derge were supported by the results of the preliminary studies of Bockris et al (9) who measured conductivities in the system CaO-SiO_2 . They offered the following evidence for the predominantly ionic nature of liquid silicates,

- (a) Conductivity is of the same order of magnitude as for molten salts.
- (b) The temperature coefficient of conductance is positive.
- (c) The ratio of conductance above and below the liquidus temperature is about 100.

(d) Passage of current through the melt produces electrolysis.

The first study in which an attempt was made to interpret electrical conductivities in terms of the magnitude and nature of the inter-ionic forces was carried out by Bockris et al (10), who studied the systems $\text{Li}_2\text{O-SiO}_2$, $\text{Na}_2\text{O-SiO}_2$, $\text{K}_2\text{O-SiO}_2$, MgO-SiO_2 , CaO-SiO_2 , SrO-SiO_2 , BaO-SiO_2 , $\text{Al}_2\text{O}_3\text{-SiO}_2$, MnO-SiO_2 , $\text{Al}_2\text{O}_3\text{-SiO}_2$, and $\text{TiO}_2\text{-SiO}_2$. In these systems all the results were found to obey the Rasch-Hinrichsen law (11),

$$\kappa = A_{\kappa} \exp (-E_{\kappa}/RT)$$

where κ is the specific conductance, A_{κ} is a constant, and E_{κ} is the energy of activation for conductance. E_{κ} has a fundamental significance in that it can be identified with the energy required to raise a cation out of its potential well in the structure and move it through the melt under an applied potential.

The activation energies for conduction are shown in figure 1 for the various systems. A marked difference is observed between the systems containing alkali and alkaline earth oxides, although in each group E_{κ} is nearly independent of the cationic species. In Group I E_{κ} appears to be independent of the composition but in Group II, it increases with decreasing metal oxide content. The aluminium and titanium ions occupy quite different positions. From this it is evident that the cationic charge is an important factor in the mechanism of conduction. The explanation offered for these results was that the addition of a metal oxide to silica results in the breakdown of the three dimensional network to give different ions. An insight to the details of this breakdown is given by correlation of the free energy

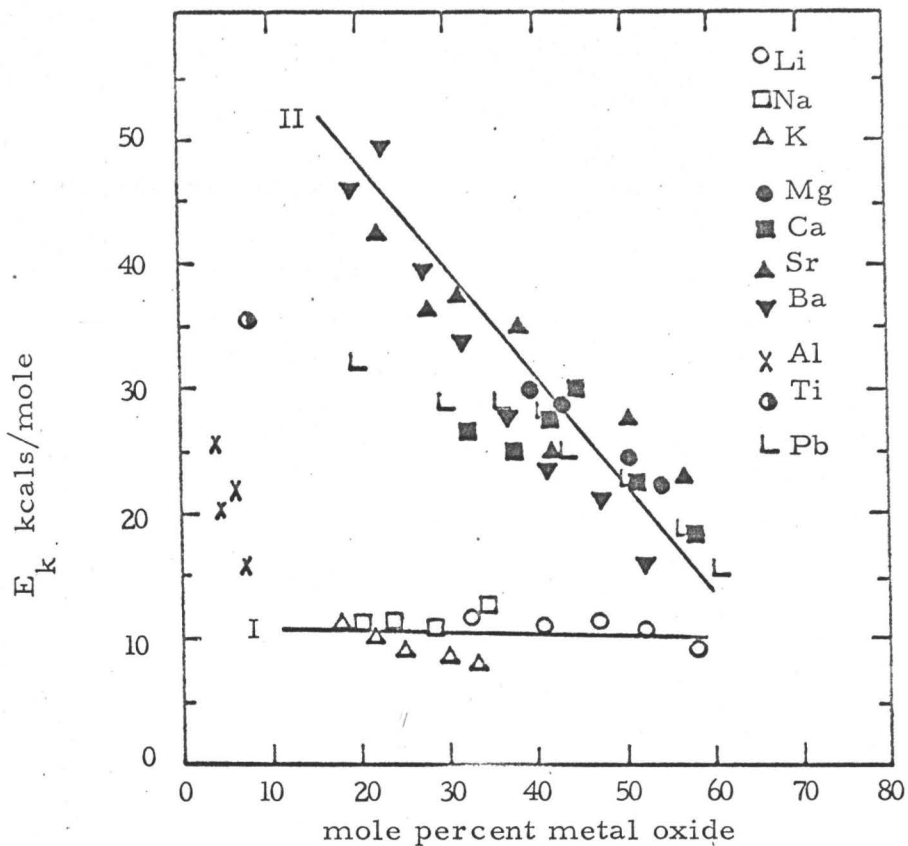


Figure 1. Activation energy for electrical conduction as a function of composition in binary silicate melts. ⁽¹⁰⁾

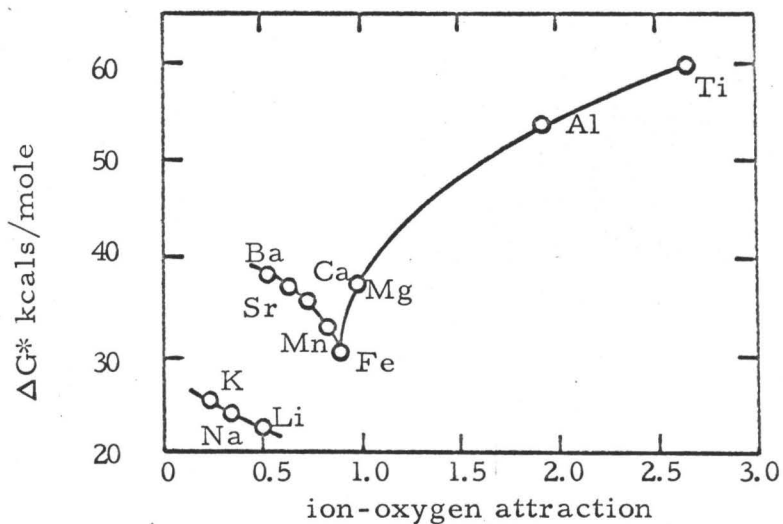


Figure 2. Free energy of electrical conduction as a function of ion-oxygen attraction in binary silicate melts. ⁽¹²⁾

for activation for the conduction process, ΔG^* , (obtained by application of the theory of absolute reaction rates to the conduction process), with a function of the coulombic interaction in the melt, the ion-oxygen attraction parameter, I , defined as:

$$I = \frac{2ze^2}{r^2}$$

where z is the valency of the cation,

e is the electronic charge,

and r is the internuclear distance between the metal and oxygen ions.

This relationship (12) is shown in figure 2. It is seen that ΔG^* affords classifications of three types.

(i) Monovalent ions $\Delta G^* \sim 20$ kcal $I = 0.24 - 0.50$

(ii) Divalent ions $\Delta G^* \sim 35$ kcal $I = 0.53 - 0.95$

(iii) Tri and tetravalent ions $\Delta G^* \sim 50$ kcal $I = 1.90 - 2.61$

The division was accounted for as follows (12). In group (i), the value of I is low and therefore the random disordered nature of the molten silica network is preserved. The potential energy of the ion does not vary greatly from one position in the network to another and the value of ΔG^* is low. In group (ii) the value of I is large enough to bring about a certain amount of local order around the cation in the structure and ΔG^* is higher as a consequence of the greater periodicity. The high values of ΔG^* for the ions in group (iii) may be attributed directly to the high values of I for these ions and also possibly to the partial covalent character of the bonds.

The variation of ΔG^* within group (i) is small presumably because I is not large enough to be significant in determining ΔG^* , which depends

mainly on the degree to which the network is broken down, and therefore, on composition. In group (ii) the value of ΔG^* decreases with increasing I for the composition $M_0.2SiO_2$ and increases with I for the composition $2M_0.SiO_2$. This is seen in Table I.

| CATION | I | ΔG^* 1750°C k.cal/mole | | |
|------------------|------|--------------------------------|---------------|----------------|
| | | $M_x 0.2SiO_2$ | $M_x 0.SiO_2$ | $2M_x 0.SiO_2$ |
| K ⁺ | 0.24 | 24.6 | 24.0 | - |
| Na ⁺ | 0.36 | 24.0 | 22.3 | - |
| Li ⁺ | 0.50 | 24.2 | 22.9 | 18.4 |
| Ba ²⁺ | 0.53 | 37.1 | 33.4 | 30.8 |
| Sr ²⁺ | 0.63 | 36.5 | 33.5 | 31.4 |
| Ca ²⁺ | 0.70 | 34.7 | 32.8 | 32.7 |
| Mn ²⁺ | 0.83 | 32.9 | 30.2 | 26.0 |
| Fe ²⁺ | 0.87 | - | 29.4 | - |
| Mg ²⁺ | 0.95 | 37.1 | 34.5 | 31.7 |
| | | 10 wt.% | | |
| Al ³⁺ | 1.90 | 52.5 | - | - |
| Ti ⁴⁺ | 2.61 | 59.3 | - | - |

TABLE I Variation of the Free Energy for Electrical Conduction ΔG^* with the ion oxygen attraction I for various cations and silicate compositions.

In group (ii) I is large enough to be significant in determining ΔG^* and the variation may be explained as follows. At the 1:2 composition the structure still retains a considerable degree of the three dimensional

character associated with the silica network. The formation of stable oxygen-ion polyhedra by cations will, therefore, help to increase the randomness of the rest of the structure and the lattice will tend towards that characteristic of the alkali metal silicates. The value of ΔG^* for some of the cations (which in this case, are of the same type) will, therefore, be reduced. These effects will be dependent on the value of I . At the 2:1 composition the network structure is completely broken down and the structure consists of cations and SiO_4^{4-} ions. The value of ΔG^* will depend on the potential energy of the ion in the initial and transition states along the reaction co-ordinate. As the value of I increases, the value of the potential energy in the initial state will become increasingly negative. In the transition state, the potential energy will be determined mainly by the repulsive interaction between the cation and the oxygen ions. As the repulsive forces arise mainly from the mutual interpenetration of the ions and the resultant repulsion on the nuclei, the potential energy will be approximately constant. Therefore, ΔG^* will tend to increase with increasing I . The ions Mg^{2+} , Mn^{2+} , and Fe^{2+} are not characteristic of any of the groups above and the anomalous results are thought to be due to the different electronic structures in the cases of Fe^{2+} and Mn^{2+} and to the influence of polarisability and tendency to covalency in Mg^{2+} .

In the above interpretation, the experimental findings have been correlated and qualitatively explained assuming all interactions to be completely ionic in nature. This assumption is inherent in the use of the ion-attraction parameter I .

2.1.2 Viscosity

The determination of the viscosity of a melt gives a figure which is related to the resistance to flow or internal shear in the liquid. Although such a figure has little fundamental significance, the variation of viscosity with temperature yields the so-called activation energy for viscous flow via the empirical relationship

$$\eta = A\eta \exp (-E\eta/RT)$$

where η is the viscosity,

$A\eta$ is a constant,

and $E\eta$ is the activation energy for viscous flow.

This activation energy has a fundamental meaning in that it can be identified with the energy necessary for one gram mole of silicate ions to form a hole, surmount the energy hill from one position and fall into the adjacent hole. Hence, from the activation energy for viscous flow, it should be possible to gain some indication of the size of the entity taking part in the flow process. It has been suggested, from measurements on simple ionic melts, that the viscosity is entirely an anionic effect (13), the cations being too small, except in the case of a few fluorides, to affect the flow properties.

The first mechanism postulated for viscous flow resulted from studies by Endell and Hellbrugge on the three alkali silicate systems (14). The observed large decrease in viscosity when metal oxides were added to liquid silica was interpreted as being the result of a progressive breakdown of the three dimensional lattice to give silicon-oxygen ions, the limit being reached at the orthosilicate composition, where the

melt consisted only of discrete SiO_4^{4-} anions and metal cations. At compositions corresponding to 50 and 33 mole per cent metal oxide infinite chains and sheets, respectively, were postulated.

Bockris and co-workers (15,16) have measured viscosities in the alkali silicate and alkaline earth silicate systems over a sufficiently wide range of temperature to permit calculation of the activation energies for viscous flow. The relationships obtained between E_η and composition are shown in Figure 3. It is seen that between 10 and 55 mole per cent metal oxide E_η is low (25 to 60 kcals) compared with the value of 134 kcals for molten silica and the variation of E_η is small over a wide range of composition. For the alkali silicate systems a sharp increase in E_η occurs at about 12 mole per cent metal oxide and for the alkaline earth silicates the increase occurs at about 20 mole per cent metal oxide. These results invalidate the earlier theory of Endell and Hellbrugge as it is known (17,18) that the formation of the infinite chain and sheet structures postulated in the earlier theory would cause considerable increases in the energy of activation. Bockris points out that the only type of structure consistent with the behaviour of the energy of activation v. composition is one containing discrete silicate ions. These are considered to be of the following form. When the O/Si ratio is 4, i.e. at the ortho-silicate composition, the silicate ions occur as SiO_4^{4-} . Reduction of the O/Si ratio to 7/2 results in the polymerisation of two of these SiO_4^{4-} ions to form an $\text{Si}_2\text{O}_7^{6-}$ ion. On further addition of silica, polymerisation continues, the flow unit being the discrete silicate chain ion, and the constitution of these ions, for a given composition, depends

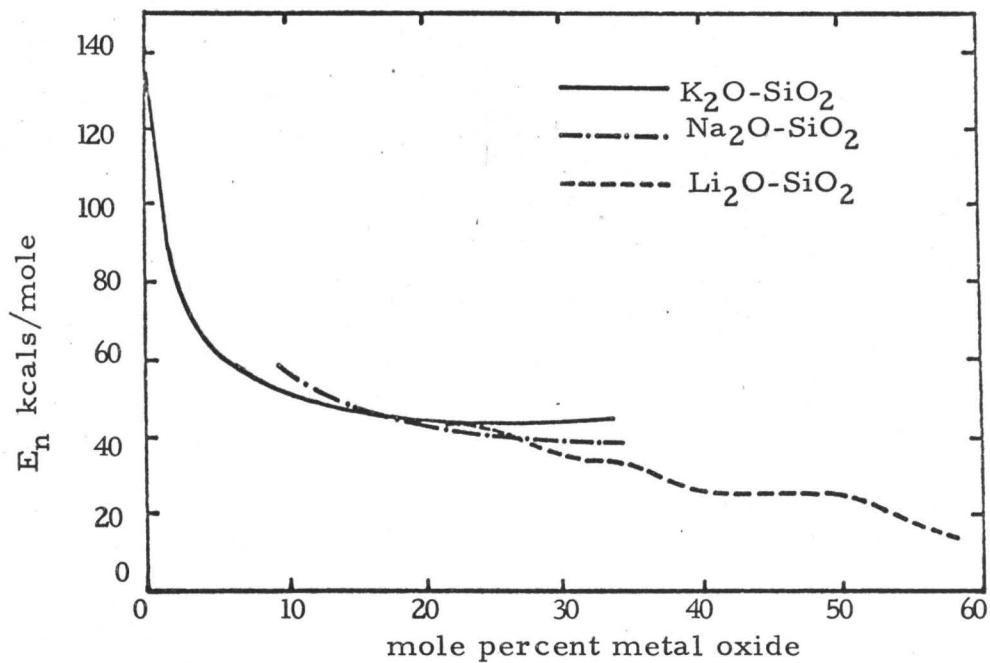
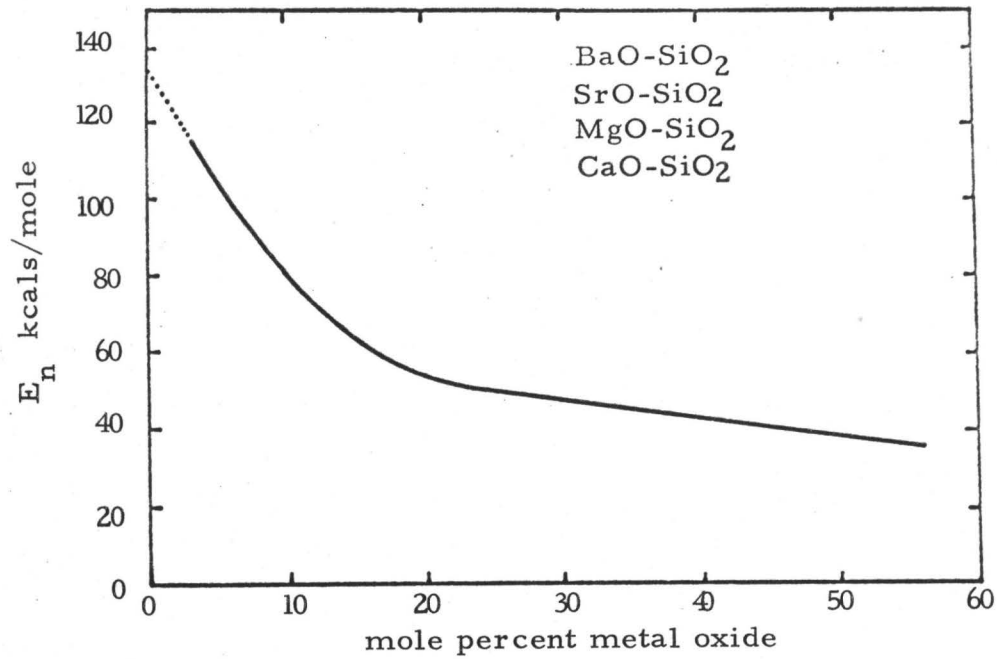


Figure 3. Energies of activation for viscous flow as a function of composition in alkali and alkaline earth silicate melts. (15, 16)

only on electro-neutrality considerations. Although the chain length rapidly approaches infinity between 50 and 52 per cent metal oxide, the activation energy observed at 50 per cent is not consistent with the presence of infinite chains. At 52 per cent metal oxide it has been postulated that a ring-type ion must be the flow unit. The ring ion $\text{Si}_3\text{O}_9^{6-}$ is suggested and this ion fulfills the requirements of stoichiometry, electroneutrality and stereochemistry. $\text{Si}_3\text{O}_9^{6-}$ is found in the mineral wollastonite (CaSiO_3) (19) and benitoite ($\text{BaTiSi}_3\text{O}_9$) (20). As an alternative, it was suggested that the ion at 50 per cent metal oxide may be $\text{Si}_4\text{O}_{12}^{8-}$, which is found in apophyllite. The oxygen angles in these ions are, respectively, 133 and 145 degrees. At the disilicate composition, the simplest ion which satisfies electroneutrality and stoichiometry requirements is the $\text{Si}_6\text{O}_{15}^{6-}$ ion, which is considered to be made up from two $\text{Si}_3\text{O}_9^{6-}$ ions. The oxygen angle is unchanged at about 135 degrees. The corresponding four member ring is $\text{Si}_8\text{O}_{20}^{8-}$.

On addition of silica to 50 per cent $\text{M}_x\text{O}_y - \text{SiO}_2$ melts, silicate anions of increasing complexity are thought to form which permit the formation of discrete flow units without severing Si-O bonds, in accordance with the small increase in activation energy up to 88 per cent silica. It was suggested that such complex ions are $\text{Si}_9\text{O}_{21}^{6-}$ and $\text{Si}_{12}\text{O}_{27}^{6-}$, being of the general formula $\text{Si}_n\text{O}_{2n+3}^{6-}$. The ions postulated between 10 and 50 per cent are listed in Table II. The simplest assumption compatible with the small change of E_n with composition over the range 10 to 50 per cent metal oxide is that at any composition, an equilibrium mixture of two or more of the discrete ions in Table II exists. The approximate proportions of each has been calculated as a function of metal oxide concentration (15).

| COMPOSITION | MOLE % METAL OXIDE | DISCRETE ION | APPROX. CHAIN LENGTH (Å) |
|-----------------------------|-----------------------|------------------------------------|--------------------------------|
| $\text{SiO}_2 + \text{MO}$ | 50 | $\text{Si}_3\text{O}_9^{6-}$ | |
| $2\text{SiO}_2 + \text{MO}$ | 33 | $\text{Si}_6\text{O}_{15}^{6-}$ | 6 |
| $3\text{SiO}_2 + \text{MO}$ | 25 | $\text{Si}_9\text{O}_{21}^{6-}$ | 9 |
| $4\text{SiO}_2 + \text{MO}$ | 20 | $\text{Si}_{12}\text{O}_{27}^{6-}$ | 12 |
| $5\text{SiO}_2 + \text{MO}$ | 16.7 | $\text{Si}_{15}\text{O}_{33}^{6-}$ | 15 |
| $6\text{SiO}_2 + \text{MO}$ | 14.3 | $\text{Si}_{18}\text{O}_{39}^{6-}$ | 18 |
| $7\text{SiO}_2 + \text{MO}$ | 12.5 | $\text{Si}_{21}\text{O}_{45}^{6-}$ | 21 |
| $8\text{SiO}_2 + \text{MO}$ | 11.1 | $\text{Si}_{24}\text{O}_{51}^{6-}$ | 23 |

TABLE II Anions present at compositions between 10 and 50 mole per cent metal oxide.

As the discrete anions become longer, a limit of chain length is reached, beyond which the ions become unstable. In Group I, E_n rises sharply at about 10 per cent metal oxide. This is taken to be the composition at which the discrete anions become unstable and rearrangement to the random three dimensional network of silica occurs. The formation of the continuous three dimensional lattice probably occurs at lower silica compositions for Group II because of the bridging tendency of the divalent cations. This would encourage joining up

between the discrete anions and thus encourage the commencement of the three dimensional bonding.

On the addition of metal oxide to silica, Si-O bonds are broken and the cations are randomly distributed throughout the lattice, their presence giving rise to two major effects, (i) weak points are introduced into the silica network by rupture of the Si-O bonds and (ii), the Si-O bonds near the metal cation are weakened, owing to the polarising effect of the cation. Thus, a general loosening effect on the lattice occurs. At equimolar compositions, the divalent cation participates in the continuous linking of the network by bridging two oxygen atoms whereas the two univalent cations do not. In this model, the effects due to the metal oxides of Groups I and II will be expected to differ because at equimolar composition, there will be twice as many univalent cations as divalent cations and the divalent cations tend to maintain the continuous bonding of the lattice by bridging oxygen atoms. Hence on the addition of Group II metal oxides the decrease in E_n will be more gradual, i.e. the collapse of the silica framework will occur only when comparatively more metal oxide has been added, in agreement with Figure 3.

Viscosity studies have been conducted in an attempt to determine the effect of the addition of calcium fluoride on the structures of liquid silicates. Kozakevitch (21) studied the effects of calcium fluoride on viscosities in the system $\text{CaO-Al}_2\text{O}_3\text{-SiO}_2$ and postulated that if CaF_2 entered the silicon-oxygen lattice by breaking Si-O bonds in a manner similar to CaO, then one mole of CaF_2 should be equivalent to two moles of CaO (Figure 4). The results did not fit this theory

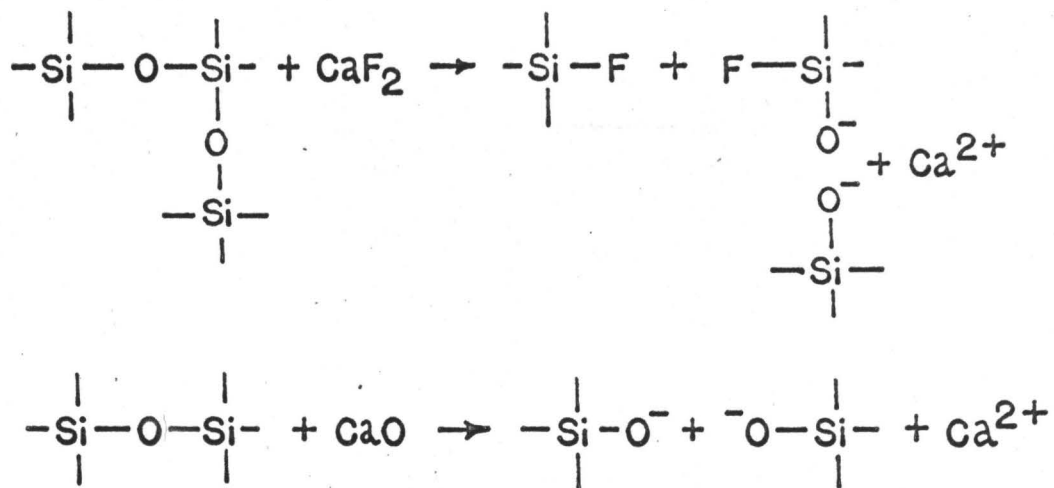


Figure 4. Comparison of the effects of CaO with the hypothetical effect of CaF_2 on the silica network. (21)

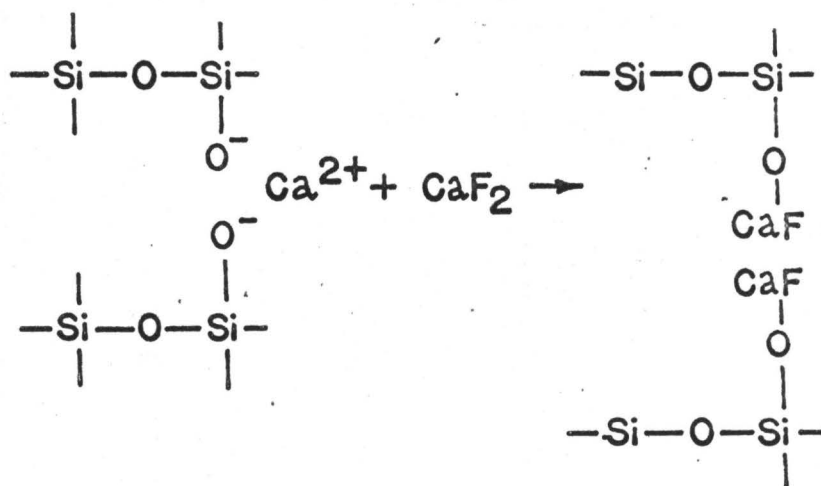


Figure 5. Hypothetical solvating effect of the addition of CaF_2 to silicate melts. (22)

as the effect of CaF_2 was found to be much greater than that predicted by the above mechanism.

Additional studies of the effect of calcium fluoride on the viscosities of melts in the system $\text{CaO-Al}_2\text{O}_3\text{-SiO}_2$ have been carried out by Bills (22). The results obtained were interpreted as indicating that CaF_2 enters the silicate network by breaking Si-O bonds with a consequent reduction in the size of the silicate flow unit. It was postulated that fluoride ions do not replace oxygen ions in the melt. This is in accordance with the theories of Baak (23), who suggests that the substitution of a fluoride ion for an oxygen ion in the silicate network would result in the appearance of a new compound in the phase diagram. It was thus suggested by Bills that the calcium fluoride ionises in such a way as to act as a solvating agent for the large silicate anions. When calcium fluoride is added the ionic forces are overcome because unstable CaF^+ ion pairs solvate the silicate anions. This is shown in Figure 5. Since this action reduces a substantial part of the resistance to flow due to electrostatic attraction between the large anionic units through the divalent cations, the viscosity is lowered. If this postulate is correct, then the magnitude of the effect of CaF_2 on the decrease in viscosity indicates that normally the flow resistance due to ionic interactions is just as important as the size of the flow units themselves. It has thus been suggested by Bills that this is the reason why viscosities in the binary alkaline earth silicates are so much higher than in the corresponding binary alkali silicates, where electrostatic binding of silicate anions cannot take place due to the presence of only univalent

cations. It should be noted that while this is qualitatively in agreement with the results of Bockris et al (16), it is not in agreement with the results of Shartsis et al (24) who measured viscosities in the alkali silicate systems in the temperature range 1000°C to 1400°C. In this study, it was found that the viscosities decreased in the order K, Na, Li, which is the reverse of the order expected on the basis of the cation-oxygen ion bond strength. This indicated that factors other than the ionic potential of the cation are important in affecting the viscosity. The size of the alkali cation was considered as a possible factor. The potassium ions may move as single units and the large cation size might cause them to meet a greater resistance than the smaller sodium or lithium cations.

From viscosity studies in the temperature range 425°C to 650°C (25, 26, 27) it has been found that in some composition ranges, the order of the effect on viscosity in the alkali silicates is the reverse of that found at high temperatures, i.e. the viscosity increases in the order Na, K. An explanation for this has been proposed from a consideration of the free volume in the structure (28). It is considered that the activation energy for viscous flow comprises two parts, (i) an energy U required to form a hole into which the flow unit may move and (ii) an additional energy ΔU required for the actual movement of the flow unit. It was suggested that at low temperatures, both U and ΔU are effective and that U for potassium silicates is less than U for sodium silicates. At high temperatures, however, there is sufficient free volume present in the structures for movement to take place without any local increase in volume. Hence, U is very small or

zero and ΔU for potassium silicates is greater than ΔU for sodium silicates. The reversal of the effect of lithium and potassium on viscosity would be expected to be even greater but no low temperature data is available for the system $\text{Li}_2\text{O-SiO}_2$.

2.1.3 Density

Although the variation of density with temperature and composition of a melt occurs as a direct result of structural interactions in the melt, and hence, would be expected to yield information on the nature of the liquid state, surprisingly few density studies have been carried out.

Heidtkamp and Endell (29) have studied the density-temperature-composition relationships in the system $\text{Na}_2\text{O-SiO}_2$ and Shartsis et al (24) have measured densities in the alkali silicate systems. However, only one investigation, that of Bockris, Tomlinson and White (30), has produced any significant interpretation as to the structure of the liquid silicates. Callow (31) has calculated molar and partial molar volumes in binary silicate glasses and has drawn some conclusions concerning the structure, but it has been pointed out (30) that these conclusions cannot be extended to liquid silicates as the density of a glass depends on its thermal history (32).

Bockris et al (30) found that an abrupt increase in the expansivities of melts in the alkali silicate systems occurred at about 12 mole per cent M_2O . This is shown in Figure 6. The significance of this value of 12 per cent was demonstrated in the following way. One mole of silicate contains $(1-N)A$ silicon atoms where N is the mole fraction of M_2O in the binary silicate and A is Avogadro's Number.

Each silicon atom has a half share in four Si-O-Si bridges. Thus, for one mole of final solution, the number of bridges before addition is $2(1-N)A$, the number of bridges broken by $M_2O = NA$ and the number of unbroken bridges remaining is $2(1-N)A - NA = (2-3N)A$. Hence, the ratio of broken to unbroken bridges is $N/(2-3N)$, which for $N \approx 0.12$ is $1/14$. Thus at 12 mole per cent, M_2O $1/14$ of the bridges are broken. By building a scale model of vitreous silica and adding M and O atoms, thereby breaking Si-O-Si bridges, it was found that when the M_2O introduced corresponded to 12 mole per cent, 14 Si-O-Si bridges were just sufficient to surround every ionic link by a cage. This cage is shown in two dimensions in Figure 7. Since the cage is made up of strong Si-O-Si bridges having negligible inherent thermal expansion the thermal expansion associated with the ionic bonds is not displayed. At M_2O contents of greater than 12 mole per cent some thermal expansion would be expected. However, for a change in composition from 11 to 13 mole per cent M_2O the change in expansivity is from 6×10^{-6} to 5×10^{-4} a factor of about 100, whereas, over the range 13 to 50 mole per cent, the expansivity increases by a factor of only 2 to 6 (Figure 6)

The rapid increase of expansivity in the range 11 to 13 mole per cent M_2O is considered to be due to the cations. If the three-dimensional bonding continued to be gradually broken down up to 33 mole per cent M_2O as was suggested by Endell and Hellbrigg (33), then no considerable increase in thermal expansivity would be expected at 12 mole per cent. Such a marked and sudden increase at 12 per cent would, however, be expected if, at compositions greater than 12 mole per cent M_2O , the continuous three dimensional Si-O-Si bonding restraining the lattice expansion no longer existed.

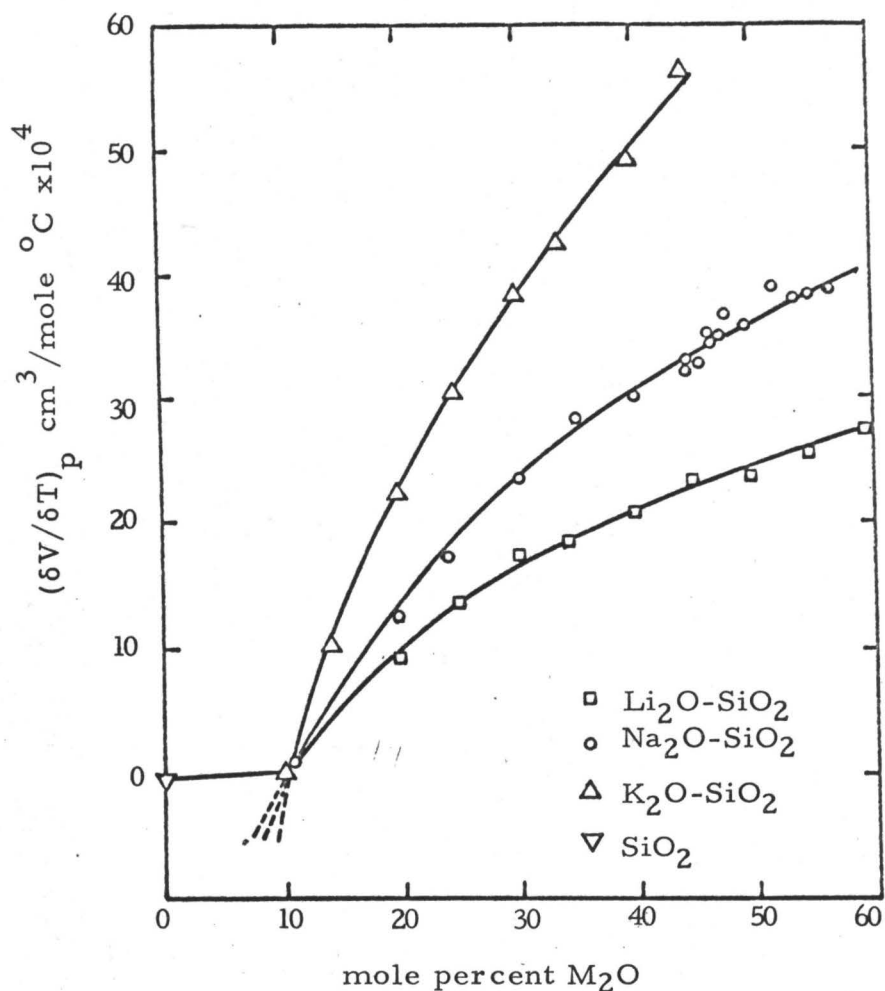


Figure 6. Thermal expansivity as a function of composition in alkali silicate melts. ⁽³⁰⁾

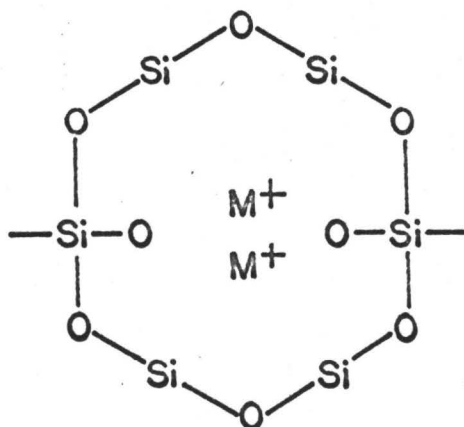


Figure 7. Two-dimensional representation of the cage occurring in alkali silicate melts at $N_{M_2O} = 0.12$ ⁽³⁰⁾

Shartsis, Spinner and Capps (24) did not attempt any detailed structural interpretation of their density results. They did, however, by consideration of the ion-oxygen attraction parameter of the cations, explain the differing thermal expansivities in the alkali silicate systems, (Figure 6). Since the ion-oxygen attraction is smaller for the K^+ ion than for the Na^+ and Li^+ ions, the electrostatic forces operating between the metal ions and the silicate anions are weaker in the case of potassium silicates. Hence, the potassium silicate lattice can expand more readily than can the sodium or lithium silicate lattices.

The model of silicate structure proposed by Bockris et al (30) from consideration of their density results was found to correspond to that derived from consideration of the viscosity data (9), and consideration of the interpretations made from both studies allowed the details of the discrete anion model to be extended. The anion structures which were proposed from consideration of the viscosity behaviour were built upon (i) the tetrahedral co-ordination of oxygen around silicon, and (ii) the angle of about 109° usually found for covalent bonds around silicon. However, calculation of the partial molar volume of the silica in the alkali silicates showed that only a very small change in \bar{V}_{SiO_2} occurs between 0 and 33 per cent M_2O . This indicated that the silicate structures over the composition range 0 to 33 per cent must have similar stereochemistry, i.e. the Si - O - Si angle must be about the same as that found in vitreous silica, namely about 140° . The discrete anion structure consistent with this angle was based upon building units of the $Si_3O_9^{6-}$

ring (16) and the general picture of liquid silicates was given as,

- | | | |
|-------|---------------------------------|--|
| (i) | 0 to 12 per cent M_2O | Continuous three dimensional lattice with gradual breakdown of the network. |
| (ii) | About 12 per cent M_2O | Breakdown of the continuous lattice to form discrete silicate anions. |
| (iii) | 12 to 33 per cent M_2O | A mixture of discrete ions of general formula $(Si_nO_{2n+3})^{6-}$. At any given composition a mixture of various anions is present and, given a definite Si-O-Si angle, the formula of the predominant ion is uniquely determined by electro-neutrality considerations. |
| (iv) | 50 to 66 per cent M_2O | A mixture of $Si_3O_9^{6-}$ rings with those of $Si_6O_{15}^{6-}$ (or $Si_4O_{12}^{8-}$ and $Si_8O_{20}^{8-}$ rings) |
| (v) | 50 to 66 per cent M_2O | Chains of general formula $Si_nO_{3n+1}^{(2n+2)-}$. |
| (vi) | Greater than 66 per cent M_2O | Uninvestigated. |

An alternative model for the range 12 to 33 per cent M_2O was suggested on the basis of the miscibility gaps in the $M_xO_y-SiO_2$ systems (34). The tendency to immiscibility increases with increasing ion-oxygen attraction of the metal cations (35). The cation attempts co-ordination with the maximum number of O^- ions and the miscibility gaps are taken as proof that a change in the randomly disordered lattice which exists below 12 per cent M_2O must occur in the immiscible region. Two structures are formed, one similar to that of vitreous silica and the other close to 33 per cent M_xO_y , (the miscibility gap

in the alkaline earth silicate systems is close to 33 per cent M_xO_y). Although no miscibility gaps exist in the phase diagrams of the alkali silicates the same tendency is considered to exist. A characteristic of the structure for compositions of M_2O slightly greater than 12 per cent is that ionic links in the silicate are, for the first time, within "co-ordinating distance" of each other, ie. no longer entirely separated into cages by directional Si-O-Si bonds. It is considered that tendency towards a miscibility gap is now expressed in the formation of a microphase M_2O-SiO_2 as a film of a few atomic layers thickness separating analogues of the SiO_2 -rich region, which may be regarded as islets of vitreous silica. These islets contain a negligible concentration of the ionic links present in the randomly broken down silicate lattice at compositions of less than 12 per cent because the ionic links are collected to form the ionic film analogue of the M_2O+SiO_2 - rich layer in the immiscible region.

This model for the 12 to 33 per cent region is found to be consistent with the almost constant partial molar volume of silica calculated over the range 0 to 33 per cent M_2O . This is because most of the silica in the structure over this range is in the form of SiO_2 islets, which have the same Si-O-Si angle as that in vitreous silica. The model is also consistent with the sudden change in thermal expansion at 12 per cent M_2O because the islets of SiO_2 are separated from each other by ionic layers in which a full ionic expansion can be displayed.

Calculation of the size of these islets shows that at 12 per cent M_2O the diameter of a spherical islet is $38\overset{\circ}{\text{A}}$ and at 33 per cent it has been reduced to $12\overset{\circ}{\text{A}}$, which is a similar value to the equivalent

radius of the silicate anions in the discrete anion model at this composition.

In the islet model, the structure can be regarded as being microheterogeneous and hence slip can occur between islets and ionic films without involving the energy of activation necessary to break Si-O bonds. The increase in the solubility of NaF (36) at compositions greater than 13 per cent M_2O in silicates is consistent because only then is there an ionic liquid ($M_2O + SiO_2$) in which the ionic NaF can dissolve. At compositions of 33 per cent M_2O , the islets are considered to become identical with the discrete anions.

2.1.4 Surface Tension

The surface tension of a liquid is a manifestation of the unsatisfied bonds present on the surface of the liquid. Its value is a measure of the concentration and nature of these bonds and hence, if it is considered that the surface constitution is the same as the bulk liquid constitution, then consideration of the surface tension of a liquid and its variation with temperature and composition would be expected to provide information on the liquid structure.

Many surface tension measurements have been made on molten silicates (37) but the results have been used principally for the interpretation of practical phenomena. Dietzel (38) found that the surface tension of silicates varied in a manner dependent on the electrostatic field strength of the ions. He showed that a relationship existed between Z/R , the ratio of the cation valency to the ionic radius, and F , the increase in surface tension produced in a liquid silicate by the addition of unit weight per cent of a given oxide.

This relationship is shown in Figure 8. For the ions K, Na, Li, Ba, Ca, Zn, and Mg, which are present as cations, the F factor increases with Z/R as would be expected. At higher values of Z/R the F factor decreases. On this part of the curve are the ions Zr, Al, Ti, and B which form complex anions in which they are firmly bonded to the oxygen. This network formation reduces the contribution of these ions to the bond density at the surface and hence to the surface tension. King (39, 40) and Kozakevitch (41) have measured the surface tensions of the binary silicates found in steelmaking slags and Shartsis and Spinner (42) have studied the alkali silicates. The relationships obtained, which are shown in Figure 9, are quite smooth, passing without inflexion through the compositions of the solid compounds. This is in agreement with viscosity and conductivity measurements and provides additional evidence that molecular compounds are not present as such in liquid silicates. This conclusion, however, cannot be drawn from surface tension results alone, since a compound does not always show a peak on the surface tension-composition curve (43). With the exception of K_2O , the almost linear increase of surface tension with increasing basic oxide content, which is much less than the corresponding change in viscosity or conductivity, is compatible with the theory of a continuous and gradual variation in the structure of the melt. It has been suggested (40) that this gradual increase is the result of the degree of association becoming less as the structure is progressively broken down. As the complex ring or chain ions are broken down, the number of smaller ionic entities increases and the resulting increase in bond density near the surface accounts

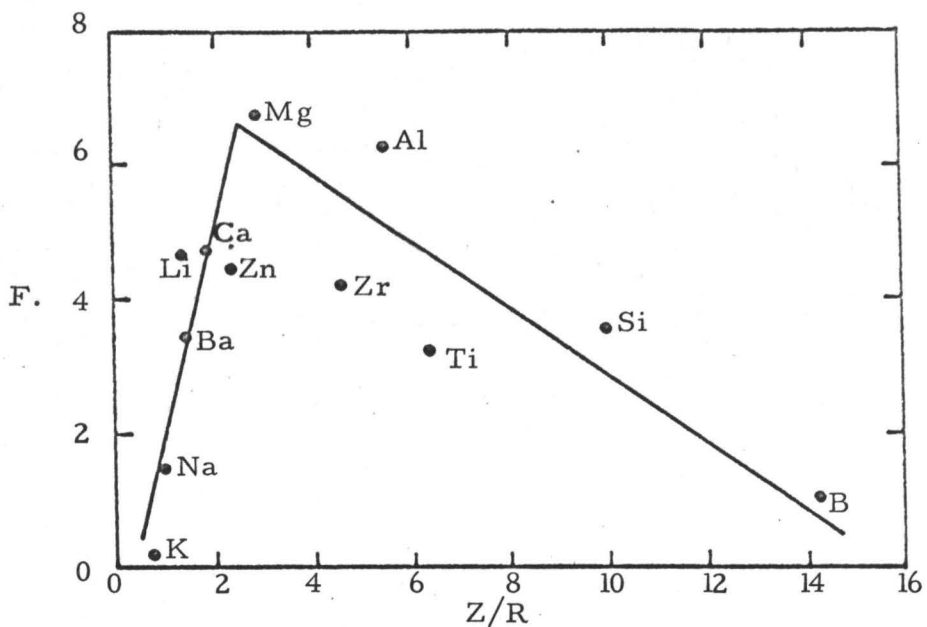


Figure 8. Relationship between F and Z/R in binary silicates (38)

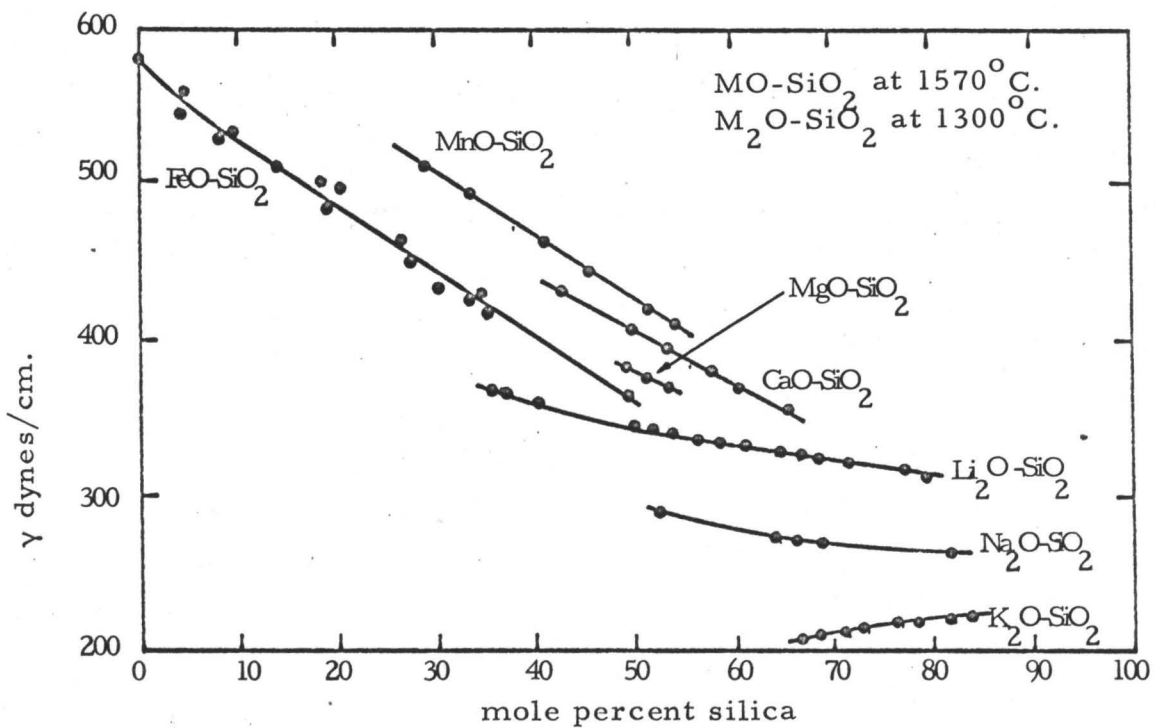


Figure 9. Surface tension as a function of composition in binary silicate melts. (40)

for the increased surface tension. It has been suggested (40) that the ion-oxygen attraction of the cation is the driving force for this breakdown and hence there is a gradual increase in the surface tension values with decreasing cation size. It must be pointed out, however, that this interpretation does not agree with the surface tension behaviour shown in Figure 9. In Figure 9, for any given silica content and temperature, the surface tension is seen to increase as the cation radius decreases, i.e. as the value of I increases. As I is a measure of the cation-oxygen bond strength, the oxygen ions bound to a cation of small radius (and of high I) are thus less available to break down the large silicate anions than are the oxygen ions bound to a cation of large radius (and of low I). Hence, according to this, the surface tension values should increase with increasing cation size.

King observed that in many silicates, the surface tension increases with temperature and that a systematic variation in the temperature coefficients of surface tension occurs. The variation of temperature coefficient with silica content and Z/R (for meta-silicate compositions) is shown in Figures 10 and 11 respectively. It is seen that the temperature coefficients tend to become abnormal, i.e. positive, as the ion-oxygen attraction increases and a similar tendency is shown at high silica contents in any one system. The silica content at which a positive temperature coefficient occurs decreases with increasing ion-oxygen attraction. For normal liquids, the surface tension decreases fairly uniformly with increase in temperature and it is probable that the real cohesion between molecules remains unchanged since the decrease in surface tension can be correlated

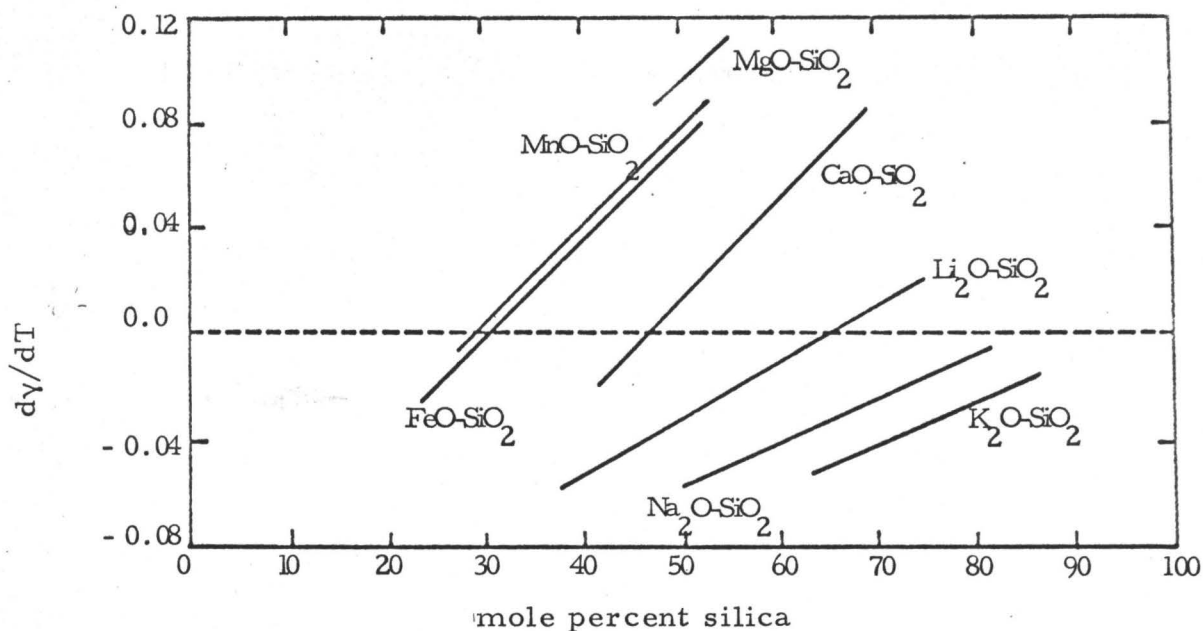


Figure 10. Temperature coefficients of surface tension as a function of composition in binary silicate melts. (40)

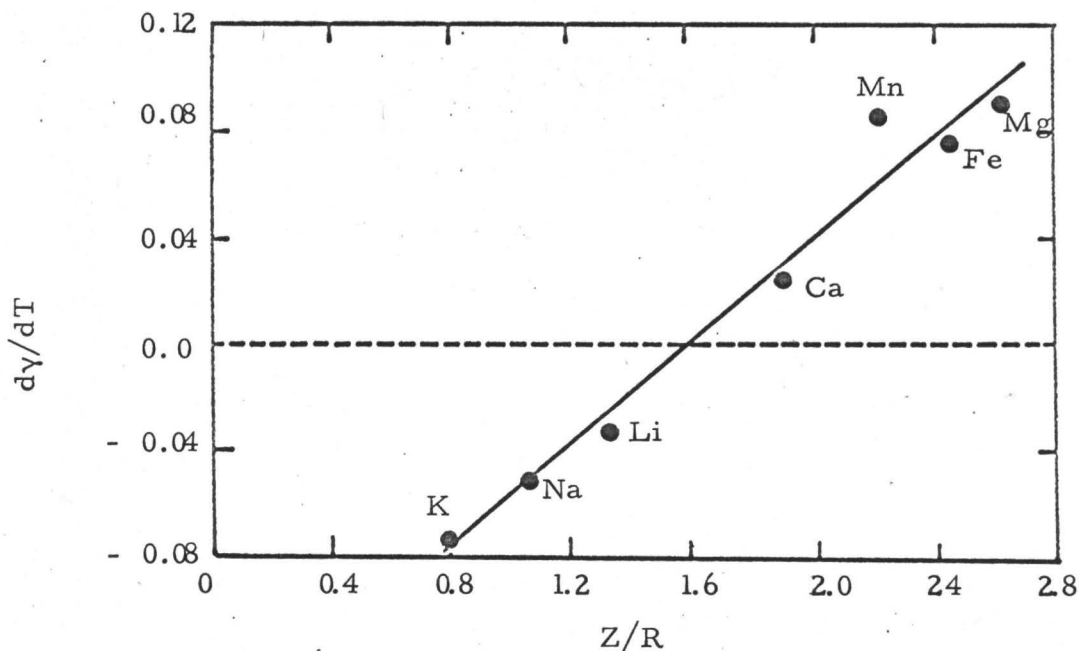


Figure 11. Temperature coefficients of surface tension as a function of Z/R in binary metasilicate melts. (40)

with the change in specific volume. As available values for liquid silicate densities show that the density decreases with increasing temperature it would appear that some process contrary to that of thermal expansion is operating to increase the surface tension.

Shartsis and Spinner suggested that the abnormal behaviour resulted from concentration of the solute at the surface. When a solute (SiO_2) lowers the surface tension of a solvent (M_xO_y), it is concentrated to some extent at the surface of the liquid, thus maintaining a minimum surface energy. Increasing the temperature tends to distribute the solute more randomly so that the surface concentration falls. The surface tension may, therefore, increase, or if $d\gamma/dT$ is still negative, its numerical value may be low. King pointed out, however, that this postulate leads to the difficulty that, in the case of the $\text{K}_2\text{O}-\text{SiO}_2$ system, where K_2O lowers the surface tension, the resulting surface excess must be assumed to become larger at higher temperatures. Entropy considerations make this unlikely and also it has been calculated that the excess surface concentrations are extremely small (40).

Dietzel has suggested that in molten borates certain asymmetrical molecular groups may be orientated parallel to the surface, thus tending to reduce the surface tension. The degree of orientation would be expected to fall off with increase in temperature possibly giving rise to abnormal values of $d\gamma/dT$ for some distance above the melting point. Adam (44) has discussed the objections to such ideas and has concluded that the degree of orientation is necessarily small.

The most plausible explanation is that due to King, who postulates

that a decrease in the degree of association in the silicates occurs with increasing temperature. The positive temperature coefficients are thus the result of a breakdown of the anion structure at higher temperatures into simpler units. The extent of this breakdown is governed by the possible complexity of the structure which depends on the ion-oxygen attraction and the silica content. The experimental results correlate well with this explanation.

2.1.5 Phase Relationships

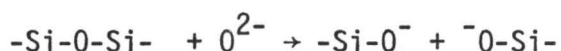
Valuable information on the nature of liquid silicates has been obtained from consideration of the phase relationships occurring in silicate systems. In this respect, examination of the regions of immiscibility occurring in silicate melts has been shown to be amenable to structure interpretation (45, 46).

In the solid state oxides can be regarded as being close-packed arrays of oxygen ions with the cations accommodated in the spaces or holes between the oxygen ions. The co-ordination number of the cation is thus determined largely by the relative sizes of the cations and the interstices within the close packed oxygen lattice. In the case of Ca^{2+} , Mg^{2+} , Mn^{2+} , and Fe^{2+} the cations are accommodated in the octahedral holes and hence have six-fold co-ordination with the resulting structures being similar to that of NaCl. However, with larger cations, which cannot be accommodated in the spaces available, the oxygen lattice is dilated and the cations have an eight-fold co-ordination. Conversely, the smaller cations Si^{4+} , Al^{3+} and P^{5+} have a tetragonal four-fold co-ordination.

For a constant electronic charge on the cation, the bond energies

between the cation and each oxygen ion increase as the co-ordination is lowered, and hence, in view of the higher cationic charges and lower co-ordination numbers of the acid cations, it would appear that the Si-O bond is stronger than, for example, the Fe-O or Ca-O bond. The differing metal ion-oxygen bond strengths have been correlated with the extents of liquid immiscibility found in many binary and multi-component phase diagrams. The liquidus traces of several binary silicate systems are shown in Figure 12. The immiscibility has been attributed (45) to the tendency of the basic oxide to retain its normal co-ordination with oxygen in preference to the high co-ordination which it must adopt if it enters a hole or cell in the silicate lattice. In the three dimensional silica structure, each cation is required to enter a hole much larger than itself in which it is co-ordinated by twelve oxygen ions. This co-ordination decreases as the silica structure is broken down but it only falls to six at the ortho-silicate composition. An increase in the co-ordination of the cation above that at which it is just in contact with the surrounding oxygen ions increases the length of the cation-oxygen ion bonds and raises the energy of the system. The structure is thus less stable than it would be if the oxygen ions and the cations of the basic oxides were free to adopt their normal shortest distances of separation. The degree of instability is raised as the cation-oxygen bond strength is increased in the pure basic oxide and as the size of the cation is decreased. A measure of the force between the cation and the oxygen ion is given by the ion-oxygen attraction parameter and this can be correlated with the extent to which the basic oxide dissolves in silica.

In these liquid solutions, competition between the silicon and the metal cations for the oxygen ions occurs and solution takes place as a result of the willingness of the basic metal cation to give up its oxygen ions to break down the silica network according to



Whether or not this will occur, and, if so, to what extent, is determined by the strength of the metal ion-oxygen bond, i.e. on the value of the ion-oxygen attraction parameter. In the case of the alkali oxides, as a result of the cation being monovalent, the M-O bond is relatively weak and thus the oxygen ions from the metal oxide are available for dissolving the silica over the entire composition range. Hence, as can be seen in Figure 12, complete miscibility occurs. In the case of the divalent basic oxides, however, the values of I are higher and they increase in the order BaO, SrO, CaO, MnO, ZnO, FeO, MgO, due to the decreasing cation size in this order. Hence the oxygen ions from these oxides are more tightly bound to the metal cation and thus are less available to dissolve the silica. The extent to which silica is dissolved consequently decreases in the above order (Figure 12). In the case of the system BaO-SiO₂, the inflexion in the liquidus curve indicates a tendency towards immiscibility, but the M-O bond strength would appear to be just less than that required for the cation to maintain its original co-ordination. Hence, the increase in the energy of the system due to the increased M-O bond length is not quite sufficient to render the solution unstable.

It has been suggested (46) that the limit of miscibility in

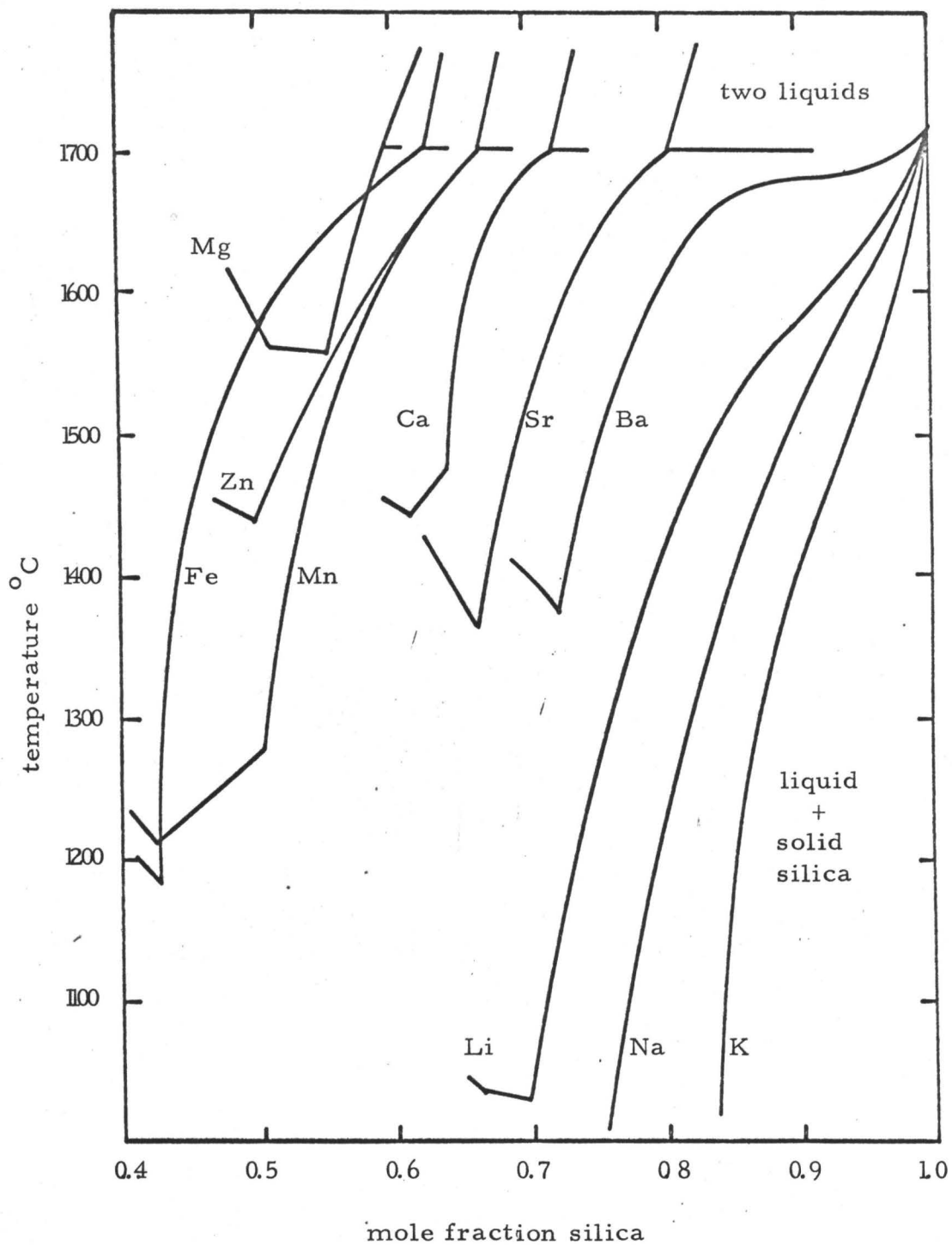


Figure 12. Silica saturation surfaces in various binary silicate systems. (47).

these systems corresponds to the composition of specific complexes, i.e. that on adding metal oxide to silica, the metal oxide-rich liquid phase does not become sufficiently stable until a composition based on one of the units described by Bockris and Lowe (15), is reached. This suggestion is somewhat idealised and it has been modified by Bodsworth (47) who suggested that the O/Si ratio at which immiscibility occurs corresponds rather to a peak in the distribution curve of one of the silicate complex ring or chain structures. Bodsworth points out that the miscibility limit of ZnO and MnO correspond closely to the composition for the transition from chain type to ring type silicate anions. This suggestion itself is perhaps somewhat idealised and the fact that similar quantitative significance cannot be attributed to the miscibility limits of other binary silicate systems suggests that either the cases of ZnO and MnO are coincidental or the anionic species transition points are variable from one system to another.

When silica is mixed with any two of the basic oxides which form immiscible liquids in their binary silicate systems a two liquid region, which joins the miscibility limits of the binary systems, is formed. Generally, the miscibility limit approximates to a straight line across the ternary system. This suggests that the change in the near co-ordination of the basic oxide cations is almost a linear function of their concentration in the liquid. When only one of the binary systems exhibits immiscibility, the immiscible region extends for only a short distance into the ternary system.

Liquid immiscibility can occur in ternary systems, the separate binaries of which show no immiscibility, e.g. in the system CaO-FeO-P₂O₅ (48).

In this respect, however, it is worth noting that the $\text{FeO-P}_2\text{O}_5$ liquidus curve indicates a tendency towards unmixing. Here the co-ordination requirements are that the smaller cations are co-ordinated by the smaller anions and the larger cations by the larger anions, i.e. Fe^{2+} with the O^{2-} and the Ca^{2+} with the PO_4^{3-} anions. It has been suggested (46) that the extent to which this type of rearrangement occurs depends on the difference between the free energies of formation of $3\text{CaO.P}_2\text{O}_5$ and $3\text{FeO.P}_2\text{O}_5$. While strong positive deviations from ideality exist in the corresponding silicate ternary system, i.e. CaO-FeO-SiO_2 (3,49) the fact that this type of immiscibility does not occur may be attributed to the very much smaller difference between the free energies of formation of 2FeO.SiO_2 and 2CaO.SiO_2 . The free energies of formation of the above mentioned phosphate and silicate compounds can be taken as indicating the relative affinities which the various ions have for one another e.g. in the system $\text{CaO-FeO-P}_2\text{O}_5$ the preferred ionic associations would appear to be $\text{Fe}^{2+}-\text{O}^{2-}$ and $\text{Ca}^{2+}-\text{PO}_4^{3-}$. The tendency for the Fe^{2+} ions to be co-ordinated by oxygen ions and Ca^{2+} to be co-ordinated by phosphate ions is sufficient to bring about immiscibility.

A third distinct type of liquid immiscibility has been observed in the systems $\text{Na}_2\text{O-MnO-SiO}_2$ and $\text{MnO-Al}_2\text{O}_3\text{-SiO}_2$ (46). No gap of this type occurs in the systems $\text{Na}_2\text{O-FeO-SiO}_2$ or $\text{FeO-Al}_2\text{O}_3\text{-SiO}_2$, i.e. when MnO is replaced by FeO in these systems. Also none is reported in systems where MnO is replaced by CaO or MgO. The explanation offered for this phenomenon is based on consideration of the states of co-ordination of the divalent Mn^{2+} cations. In MnO.SiO_2 the Mn^{2+} is in

six-fold co-ordination but the co-ordination in $2\text{MnO}\cdot\text{SiO}_2$ is less certain. Evidence shows however (50) that Mn^{2+} might be in eight-fold co-ordination in $2\text{MnO}\cdot\text{SiO}_2$ and the immiscibility may thus be due to the occurrence of Mn^{2+} in two states of co-ordination in the liquid. i.e. six-fold in liquid containing $\text{Si}_2\text{O}_7^{6-}$ anions and eight-fold in liquid containing $\text{Si}_3\text{O}_9^{6-}$ anions. It has been pointed out (46) that the oxides which favour this type of immiscibility are those which tend to eliminate the normal type of immiscibility found in binary systems.

White, Howat and Hay (51) observed thermal arrests while heating manganese silicates of composition between $\text{MnO}\cdot\text{SiO}_2$ and $2\text{MnO}\cdot\text{SiO}_2$, above the liquidus. These arrests did not fit into the accepted phase diagram and they were attributed to the breakdown of $\text{MnO}\cdot\text{SiO}_2$ and $2\text{MnO}\cdot\text{SiO}_2$ in the liquid state. They were thought to be associated with the formation of two liquids above the liquidus. It was suggested that this type of liquid immiscibility might be responsible for anomalous viscosity and surface tension effects found by Towers and Kay (52) and by King (40). These effects were attributed to the breakdown of the anion structure at higher temperatures and this explanation was thought to be not altogether unrelated to two liquid formation although anomalous surface tension values were found to varying degrees in the systems $\text{MgO}\cdot\text{SiO}_2$, $\text{FeO}\cdot\text{SiO}_2$ and $\text{CaO}\cdot\text{SiO}_2$ as well as $\text{MnO}\cdot\text{SiO}_2$.

2.1.6. Discussion of the Interpretation of the Physical Behaviour of Liquid Silicates

The preceding sections have shown how a structural model has been developed from consideration of the physical behaviour of liquid

silicates. It is particularly evident that no single physical property can provide complete information on the structure of the liquid silicates. Instead, a picture has gradually emerged as a result of consideration of a wide range of physical properties. In essence, the problem has been to determine the nature of the breakdown of the continuous three-dimensional silica lattice by addition of metal oxide from the pure silica to the orthosilicate composition. The structures of the two limiting compositions, i.e. SiO_2 and $2\text{M}_x\text{O}_y \cdot \text{SiO}_2$ have been inferred from a knowledge of the corresponding solid structures, as determined by x-ray techniques (53, 54, 55). Liquid silica is considered to be a disordered version of crystalline silica and the liquid orthosilicate is considered to be a solution comprising only cations and SiO_4^{4-} anions (56). In anticipation of later sections it is to be noted that the latter supposition has not been supported by any experimental evidence.

The studies of physical properties have been confined mainly to the alkali and alkaline earth silicates because of the complete solubility of alkali oxides and the moderate solubility of alkaline earth oxides in liquid silica. Occurrence of wide miscibility gaps in the silicate systems of the transition metal oxides appears to have discouraged parallel studies on these systems. The only physical measurements which have been made on simple basic silicates appear to be those of surface tension.

Interpretation of the physical behaviour of liquid silicates has been difficult due to the fact that almost all of the physical properties are affected by more than one factor, and it is evident that the most useful deductions have been obtained almost exclusively

from consideration of the behaviour of simple systems. In the case of viscosity studies it has been variously considered that resistance to flow in the liquid is determined by anion size, cation-oxygen bond strength and cation size, and the conflicting interpretations which are possible would appear to detract from the usefulness of viscosity as a property from which structure deductions could be made. In fact, it is reasonable to assume that all three of the factors mentioned affect the viscosity to a greater or lesser degree, and the extent to which each factor participates is both composition and temperature dependent. It is interesting to note that in the derivation of the activation energies for viscous flow no attempt has been made to obtain a correlation between the fact that the viscosity decreases with increasing temperature and the possibility that the sizes of the anionic flow units also decrease with increasing temperature. In view of the conclusions drawn from the anomalous temperature coefficients of surface tension, it is quite reasonable to assume that the effect of increasing temperature is to significantly decrease the anion size and hence to decrease the relative contribution of anion size to the viscosity. Also it is reasonable to assume that increasing temperature will result in a decrease in the contribution to the viscosity of cation-oxygen ion bond strength due to the thermally-induced reduction of the bond energy. In the case of the addition of CaF_2 to calcium alumino-silicates, it is difficult to interpret the data unambiguously as the ionic entities occurring in the initial melts are virtually unknown.

The problem of a single physical property being dependent on more than one factor occurs again in the interpretation of the density

and thermal expansivity measurements. In this case, the thermal expansivity is determined by the fraction of liquid volume occupied by unexpandable silicate anions, the fraction of liquid volume occupied by expandable ionic liquid and the expansivity of the cation oxygen bonds in this ionic liquid. Again in the interpretation of expansivity measurements, any temperature effect on these factors has been ignored, and again, as in the case of the viscosity measurements, it is reasonable to assume that the expansivity should increase with increasing temperature as a result of the decrease in silicate anion size, and hence, in the fraction of unexpandable liquid. In addition, the expansivity of the ionic liquid would be expected to increase as a result of thermal relaxation of the ionic bonds.

In the breakdown of the silica lattice by metal oxide additions, it has been suggested (40) that the driving force for this breakdown is the strength of the cation-oxygen bond relative to the strength of the silicon-oxygen bond, and the ion-oxygen attraction parameter I has been proposed as a measure of the cation-oxygen bond strength. Interpretation of experimental results in terms of the cation-oxygen bond strength has been extremely qualitative in nature due to the limited validity of this parameter. Use of the parameter I implicitly assumes that the cation-oxygen bond is completely coulombic or ionic in nature and that it only depends on the cation charge and cation radius. In fact, in a liquid silicate, it is to be expected that the bond strength between a cation and oxygen which is already bonded to a silicon atom, is dependent on the ionisation potential of the ion at the temperature of consideration and on the presence, or lack of, spherical co-ordination

of the cation in the structure, ie. on the degree of polarisation which the cation is capable of exerting and is permitted to exert on the oxygen. It must be remembered that the oxygen ion is already highly polarised towards its attached silicon. This polarisation of the oxygen ion, in itself, invalidates the use of the interionic distance, r , in the expression for I as r is the distance between the centre of a spherical cation and a spherical oxygen ion in the symmetrically co-ordinated solid oxide. It is worth noting that even in the solid oxide, the value of I is of very little use as the stability of the cation oxygen bond depends overwhelmingly on the value of the lattice energy of the particular crystalline oxide.

In spite of these reservations concerning the validity of the ion-oxygen attraction parameter, some useful correlations have been established. For example, in the surface tension studies, a smooth correlation was obtained between Z/R (a measure of I) and the temperature coefficient of surface tension. However, on the other hand, the correlation between I and the extent to which basic oxides dissolve in silica is quite unacceptable. In this correlation the limit of miscibility of basic oxide in silica was compared with the ion-oxygen attraction, which, for equivalent cations, was taken as being inversely proportional to the cation radius. It was suggested that the liquid miscibility gap widened as the cation-oxygen bond strength increased (i.e. as the cation radius decreased). This infers that the cation-oxygen bond strength increases in the order, say, Ca, Mn, Fe, but common experience shows that the order of stability of the oxides, as indicated by free energy of formation, melting point, etc., increases

in the reverse order. As the stability of the oxide is an expression of the interionic bond energies this example serves to illustrate the weakness of the ion-oxygen attraction parameter as a meaningful concept. Between the two extreme cases outlined above lies the partially successful correlation of I with parameters derived from the electrical properties of liquid silicates. In this case, successful correlation between ΔG^* , the free energy for electrical conduction, and I was obtained in systems containing relatively simple cations of low ionisation potential but correlation was impossible in systems containing complex transition metal ions of higher ionisation potential.

In the development of a more quantitative model of liquid silicates, it will be necessary to consider the homopolar character of bonding and the ionic bond deformation (12).

2.2 Thermodynamic Properties of Liquid Silicates

2.2.1 Molecular Models

The metallurgical approach to the understanding of the nature of liquid silicates has been stimulated by a need for the ability to predict the chemical behaviour of a slag of one composition from a knowledge of the chemical behaviour of a slag of a different composition. As chemical behaviour is best described in terms of thermodynamic properties, the thermodynamic method has been almost exclusively employed in this approach. The advantage of the thermodynamic method, from the extraction metallurgist's point of view, is that no knowledge of the structure of the reacting substances is required. On the other

hand, this approach has the disadvantage that structural interpretation cannot be made from knowledge of the thermodynamic behaviour alone. In view of this fact, the thermodynamic approach has been relegated by some workers (57) to the status of "a requirement for short range technological purposes".

Nevertheless, the accumulation of knowledge concerning the thermodynamic behaviour of slags has been accompanied by the postulation of structural models derived from the thermodynamic behaviour. These models were developed on the assumption that silicates are ideal solutions of molecules and molecular aggregates. The following serves as an illustration of the reasoning behind the development of these models.

Chipman and co-workers have obtained extensive activity data for iron oxide in steelmaking slags from a consideration of the oxygen contents of the metal beneath the slag phase. Feters and Chipman (58) observed that in the CaO-FeO-SiO₂ system the iso-FeO activity lines were symmetrical about a line joining the 2CaO.SiO₂ and FeO composition points. This led them to suggest that Ca₂SiO₄ might be one of the more important molecular aggregates in the slag. They also suggested that the deviation from Raoult's law in the binary system CaO-FeO was due to the formation of calcium ferrite molecules in the slag rather than to non-ideal mixing of FeO and CaO molecules. By considering that the system comprised molecules of FeO and CaO.Fe₂O₃, ideal behaviour was observed, i.e. $a_{\text{FeO}} = N_{\text{FeO}}$. Taylor and Chipman (3) applied the above reasoning to the 2CaO.SiO₂ - FeO join line in the system CaO-FeO-SiO₂ and showed that if the calcium silicate existed as a dimolecule, i.e. as Ca₄Si₂O₈, then the system Ca₄Si₂O₈ - FeO obeyed Raoult's Law. In a

similar manner, if $\text{CaO} \cdot \text{Fe}_3\text{O}_4$, rather than $\text{CaO} \cdot \text{Fe}_2\text{O}_3$, formed in the system $\text{CaO}-\text{FeO}$, then a better fit to Raoult's Law was obtained. These authors also observed that the FeO activity lines in the $\text{CaO}-\text{FeO}-\text{SiO}_2$ ternary terminated on the $\text{FeO}-\text{SiO}_2$ binary at points where $a_{\text{FeO}} = N_{\text{FeO}}$. They concluded therefore, that as the system $\text{FeO}-\text{SiO}_2$ obeyed Raoult's Law, no compound formation occurred, or more specifically, any compounds present were completely dissociated at 1600°C ., and hence, the only molecules present were FeO and SiO_2 . Winkler and Chipman (59) recognized the general uncertainty associated with these models, but justified them by the statement "even though no definite compound may form in the liquid state the assumption at least affords a logical pattern for the attraction between slag components that must exist in order to account for the slag-metal reactions in any metallurgical refining process The immediate usefulness of the assumption is not dependent on its ultimate truth".

The concept of slags comprising molecules of free oxides and molecular aggregates in ideal solution was developed to a high degree of practical usefulness by Schenck (2) and it was this practical usefulness rather than the ultimate truth of these models which accounted for their popularity among extraction metallurgists. The concept of molecular slags was shown to be entirely false by Korber and Oelsen (60), who considered the behaviour of the system $\text{FeO}-\text{CaF}_2$. This system separates into two liquids at 1450°C ., one being CaF_2 containing 2% FeO and the other being FeO containing 2% CaF_2 . The chemical reactivity of FeO must be the same in both phases as they are in equilibrium, and thus, according to Schenck's model, the percentage of free ferrous oxide

in the CaF_2 -rich phase would be required to be greater than the total percentage of ferrous oxide present.

Although the molecular models are convenient when considering the equilibrium behaviour of a slag-metal system, they are totally inadequate when considering the kinetic behaviour of slags, where a knowledge of the actual nature of the transporting and reacting species is of paramount importance. As knowledge of the equilibrium behaviour is becoming more complete, increasingly greater interest is being focussed on kinetic behaviour and this is stimulating a greater interest among metallurgists in determining the true structures of metallurgical slag melts. In approaching this problem, attempts are being made to explain the chemical behaviour of silicate slags in terms of the structure models which have been developed from observation of the physical properties.

2.2.2. Ionic models

With a few exceptions, studies of the physical properties of liquid silicates, conducted with a view to structural interpretations, have been confined to acidic silicates of composition between pure silica and the orthosilicate. The conclusion drawn from these studies is that the depolymerisation of the silicate anions, caused by the addition of metal oxide to pure silica, is complete at the orthosilicate composition. Thereafter, further additions of metal oxide are considered to simply add metal ions and free oxygen ions to the melt. A discrepancy arises between this model of basic silicates, which, if Temkin's rule can be applied, indicates that the thermodynamic

activity of the basic oxide in a liquid silicate of orthosilicate composition is zero, and the finite activity of the basic oxide generally found at this composition.

2.2.2.1. The Toop and Samis Ionic Model

From thermodynamic reasoning, Toop and Samis (61, 62) have proposed a general model of liquid silicates in which the model of basic silicates proposed above is a limiting case. They suggest that the reaction by which equilibrium polymerisation is established in a silicate melt should be the same for all compositions across the binary and that this equilibrium should be of a general form and should not involve specific silicate anions.

Oxygen in silicate melts occurs in three forms (63), singly bonded O^- , doubly bonded O^0 , and free oxygen ions O^{2-} , and the equilibrium between these three forms can be expressed as:



for which the equilibrium constant k can be written as:

$$k = \frac{(O^0)(O^{2-})}{(O^-)^2} \quad (2)$$

where (O^-) , (O^0) and (O^{2-}) are the equilibrium numbers of moles of singly bonded, doubly bonded and free oxygen ions per mole of slag. It is proposed that k is a constant at a given temperature and is characteristic of the cations present in any binary or ternary silicate melt.

Charge and mass balances allow (O^0) and (O^{2-}) to be expressed in terms of (O^-) and N_{SiO_2} , and hence, substitution of these expressions

into equation (2) allows an equation to be written in terms of k , N_{SiO_2} and (O^-) . Thus for any value of k , values of (O^-) , (O°) and (O^{2-}) can be determined as a function of N_{SiO_2} . Figure 13(a) shows these relationships when $k = 0.06$, and it is pointed out that the (O^-) curve exhibits the characteristic shape of an integral free energy of mixing curve. Figure 13(b) shows the relationship when $k = 0$ and, as can be seen, this is the limiting case corresponding to complete depolymerisation of the silicate anions between the metal oxide composition and the orthosilicate composition, i.e. in this composition range (O°) is zero.

Reaction between metal oxide and silica can be written as:



From this equation it is apparent that when one mole of oxygen ions react with one mole of doubly bonded oxygen atoms to form two moles of singly bonded oxygen atoms the standard free energy change, ΔG° , is given as:

$$\Delta G^\circ = -RT \ln \frac{1}{k} = RT \ln k$$

but as the actual number of moles of oxygen ions which have reacted in the melt is $(\text{O}^-)/2$ the free energy change due to equation (3) per mole of liquid silicate formed is:

$$\Delta G^{\text{mix}} = \frac{(\text{O}^-)}{2} RT \ln k$$

As the variation of (O^-) with melt composition is dependent on the value of k , free energy of mixing curves for various values of k can be drawn.

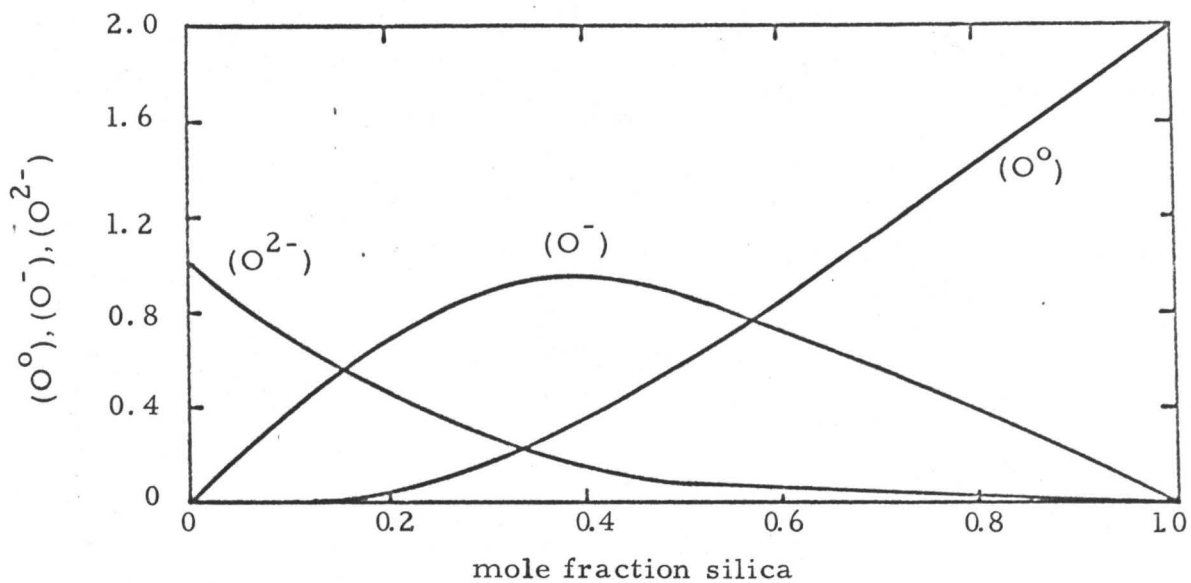


Figure 13(a) Equilibrium values of (O^0) , (O^-) and (O^{2-}) as a function of silica concentration for $k=0.06$ (Toop and Samis)⁽⁶¹⁾

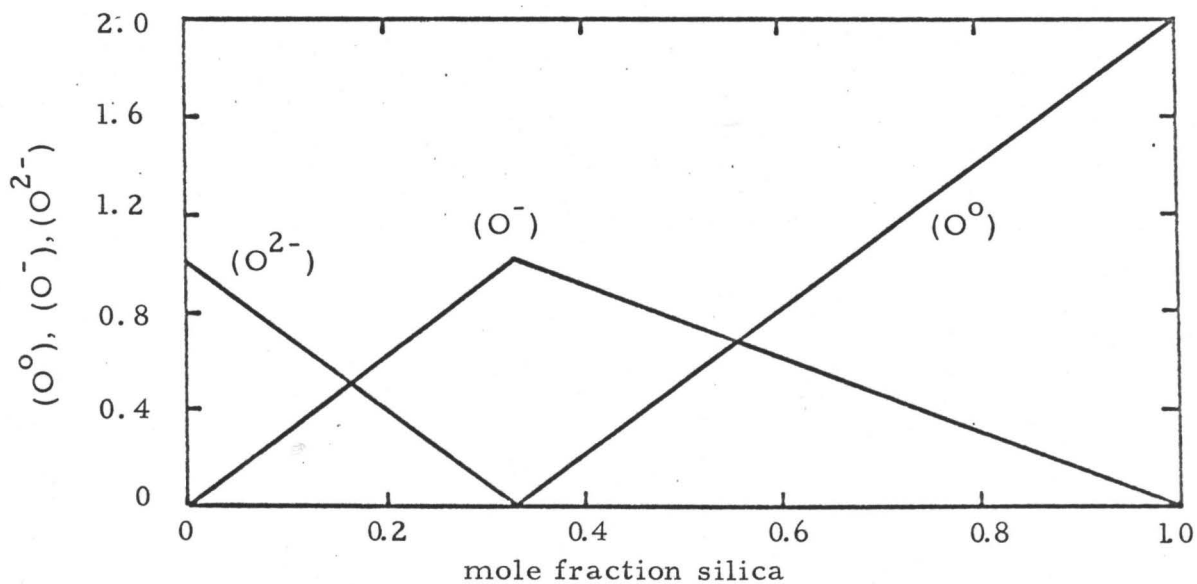


Figure 13(b) Equilibrium values of (O^0) , (O^-) and (O^{2-}) as a function of silica concentration for $k=0.0$ (Toop and Samis).

Typical curves are shown in Figure 14 where comparison is made with the measured integral free energy of mixing of liquid PbO and liquid SiO₂ at 1100°C (64) and the calculated integral free energy of mixing liquid CaO and liquid SiO₂ at 1600°C (65). The similarity between the calculated free energy curves and the characteristic free energy curves of binary silicate melts indicates that the free energy of mixing in a binary silicate melt may arise entirely from the interaction of oxygen ions and silica. Under this condition, the effect of different cations would be to allow greater or less polymerisation and hence greater or less interaction between oxygen ions and silica. Fitting of the calculated free energy curves with experimentally determined curves allows values of k to be determined for particular binary systems. This value of k then gives a measure of the extent to which polymerisation occurs in any particular system and if $k > 0$, then it is seen that depolymerisation of the silicate ions by the addition of metal oxide is not complete until the pure metal oxide composition is reached. Table III gives typical values of k for several systems.

| SYSTEM | k | TEMP. OF MELT |
|--------------------------------------|--------|---------------|
| Cu ₂ O - SiO ₂ | 0.35 | 1100°C |
| FeO - SiO ₂ | 0.17 | 1600°C |
| ZnO - SiO ₂ | 0.06 | 1300°C |
| PbO - SiO ₂ | 0.04 | 1100°C |
| CaO - SiO ₂ | 0.0017 | 1600°C |

TABLE III Values of the equilibrium polymerisation constant k for various binary silicates (61, 62).

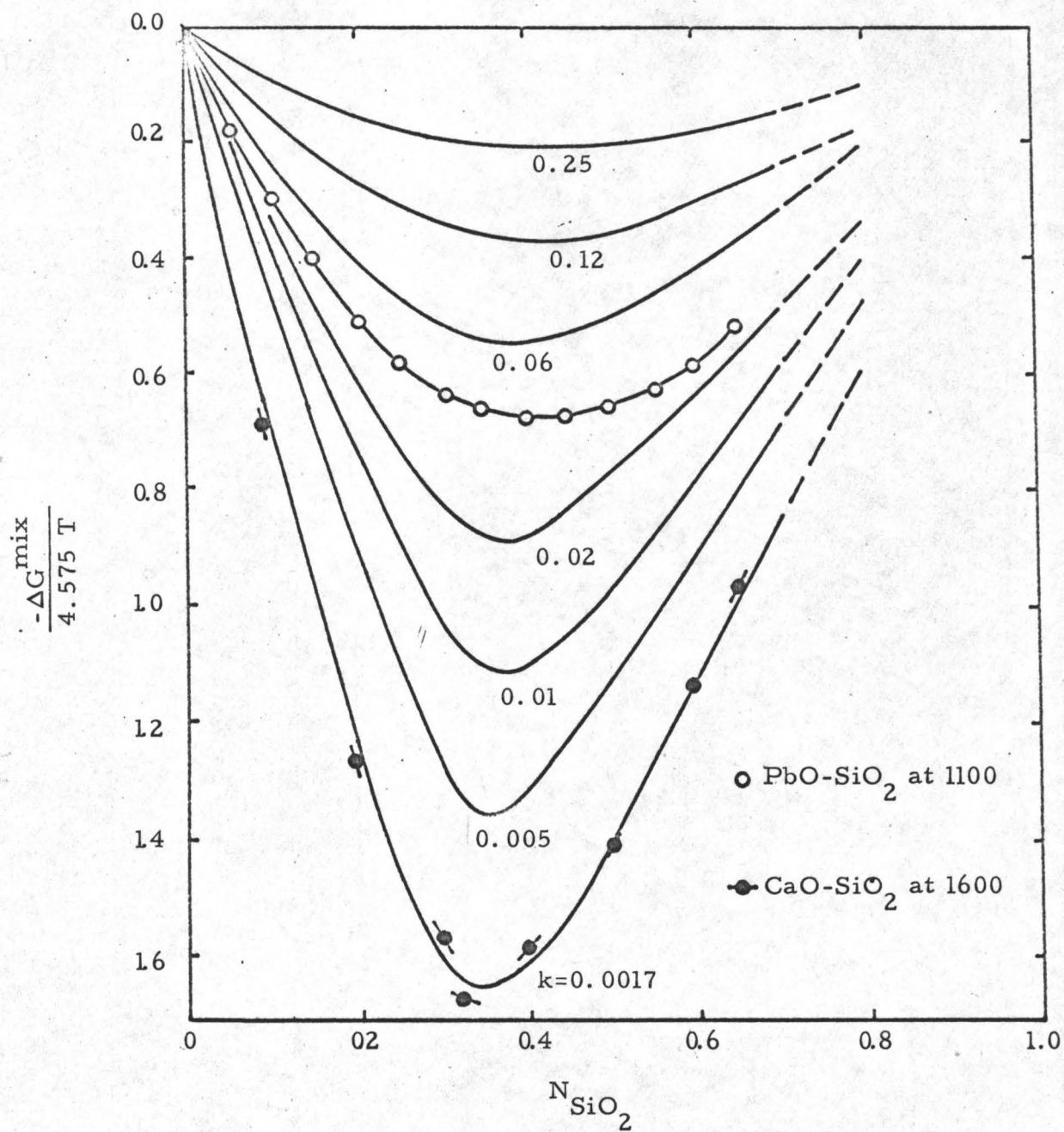


Figure 14. Calculated free energy of mixing curves for various values of k . (Toop and Samis).⁽⁶¹⁾

2.2.2.2. The Flood and Knapp Ionic Model

A more specific approach to the problem of polymerisation in silicate melts was made by Flood and Knapp (66) whose consideration of the thermodynamic activity of lead oxide in liquid lead silicates led them to suggest the form of the specific polymeric silicate anions present in these melts. In their treatment they considered the liquid lead silicates to be ideal solutions of ions and chose specific anions which forced agreement between the calculated ideal activity of PbO , i.e. N_{PbO} , and the experimentally determined activity.

Three composition ranges in the lead silicate system were considered, namely, 0 - 20 mole per cent SiO_2 , 20 - 40 mole per cent SiO_2 and 40 - 60 mole per cent SiO_2 .

(i) 0 - 20 mole per cent SiO_2

In this composition range the activity of PbO is independent of temperature, which, in indicating a partial molar heat of mixing equal to zero, suggests that the solution is behaving in a fairly ideal manner with regard to the actual ions present. It was found that, if, in this composition range, the solutions are regarded as being ideal mixtures of PbO and Pb_2SiO_4 , i.e. the anions present are O^{2-} and SiO_4^{4-} , then the calculated activity of PbO coincides with the experimental value

(ii) 20 - 40 mole per cent SiO_2

In this composition range a temperature dependence of a_{PbO} is observed and continued assumption that the solution is an ideal mixture of PbO and Pb_2SiO_4 results in the calculated activities being lower than the experimental values. This was considered to be due to an incomplete formation of SiO_4^{4-} ions by reaction of the silica

with PbO, with the resultant formation of some polymeric ion. Assumption that the polymer formed was the pyrosilicate ion $\text{Si}_2\text{O}_7^{6-}$ resulted in deviations from the simple $\text{PbO} - \text{Pb}_2\text{SiO}_4$ model occurring at a much lower silica content than was experimentally found. The required agreement with experiment was achieved by assuming that the polymeric anion is essentially larger, and of higher Si/O ratio, than the pyrosilicate ion. Such an ion is $\text{Si}_3\text{O}_9^{6-}$ and the assumption that solutions in the composition range 20 - 40 mole per cent SiO_2 contained the anions O^{2-} , SiO_4^{4-} and $\text{Si}_3\text{O}_9^{6-}$ allowed the required agreement between calculation and experiment to be obtained.

(iii) 40 - 60 mole per cent SiO_2

If the $\text{Si}_3\text{O}_9^{6-}$ ion were the only polymeric ion formed, then the calculated activity of PbO approaches zero at the metasilicate composition. As this is not the case, it appeared that the formation of a more highly polymerised ion takes place when the mole fraction of silica exceeds 0.4. The occurrence of an ion of the general formula $(\text{SiO}_{2.5})_q$ was suggested and although an oxygen ion balance suggested that q equalled 4, calculations of the activity of PbO with q equal to 4 were poor compared with calculated activity values when q equalled 6. Hence, it was suggested that the higher polymer occurring in the composition range 40 - 60 mole per cent SiO_2 is $\text{Si}_6\text{O}_{15}^{6-}$.

On the basis of these assumptions, figures 15 (a) and 15 (b) show how the composition of the liquid is changed by the addition of silica to lead oxide at 1100°C. Figure 15(a) shows the anionic fractions as a function of silica content and Figure 15(b) shows the distribution of silicon atoms present in the different species as a function of silica content

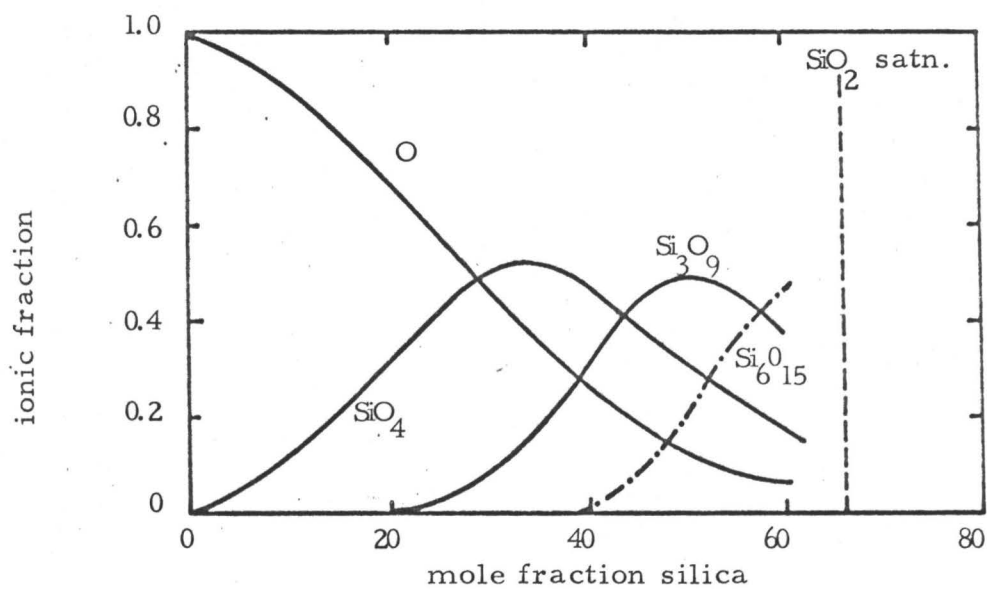


Figure 15(a). Constituent anions as a function of composition in lead silicates. ⁽⁶⁶⁾

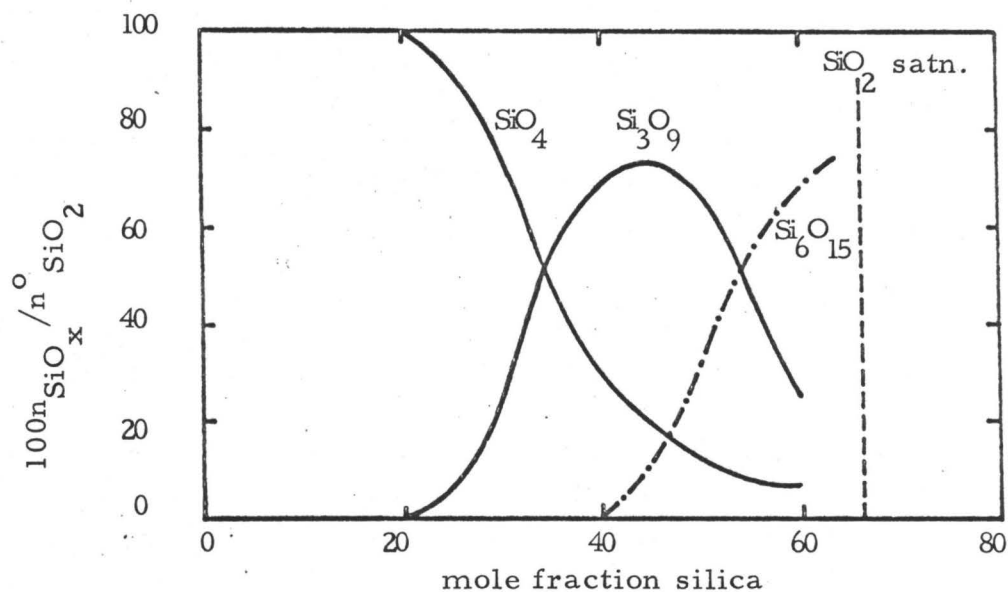
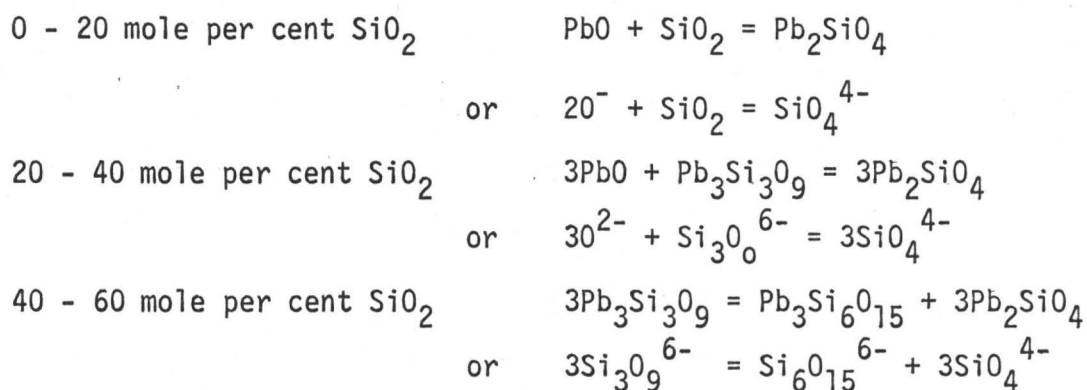


Figure 15(b). Distribution of silicon atoms present in anions as a function of composition in lead silicate melts. ⁽⁶⁶⁾

These calculations were not offered as decisive proof that SiO_4^{4-} , $\text{Si}_3\text{O}_9^{6-}$ and $\text{Si}_6\text{O}_{15}^{6-}$ are the true and only silicate ions present in the composition range 0 - 60 mole per cent silica. They were offered only as a logical indication and it was admitted that the assumption of ideal anionic mixtures might possibly conceal the true equilibrium involved.

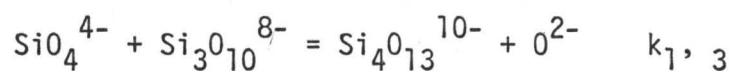
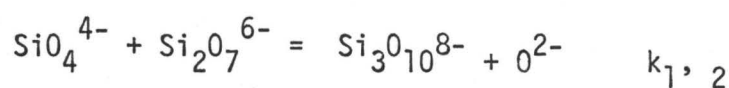
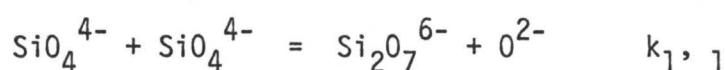
The fundamental difference between the conclusions of Toop and Samis and the conclusions of Flood and Knapp is that the former authors suggest that the equilibrium constant for polymerisation in a given binary system is a function only of temperature whereas the latter authors suggest that the equilibrium constant is also composition dependent. In essence, Flood and Knapp propose three equilibrium constants, one for each of the composition ranges considered. These equilibria are



2.2.2.3. The Masson Ionic Model

The approach of Flood and Knapp, ie. the selection of anions which force agreement between calculated and experimental activities has been developed in a more general manner by Masson (67). This more general approach also embodies the fundamental principles of the Toop

and Samis treatment. Masson considers a binary melt $MO - SiO_2$ in which the ratio of metallic oxide to silica is sufficiently high that depolymerisation may be regarded as being complete, i.e. the silica is present exclusively as tetrahedral SiO_4^{4-} ions. As the silica content of the melt is gradually increased, a series of polycondensation reactions are envisaged in which SiO_4^{4-} ions at first dimerise and then react further with higher members of the series to produce linear and branched polyionic chains. These reactions are written as:



Each reaction has an equilibrium constant, $k_{1,1}$, $k_{1,2}$, $k_{1,3}$, etc. and assuming that ion fractions may be used in place of activities, the ion fraction of each member in the series may be expressed in terms of those of the lower members.

$$N_{Si_2O_7^{6-}} = \frac{k_{1,1} \cdot N_{SiO_4^{4-}}}{N_{O^{2-}}} \cdot N_{SiO_4^{4-}} \quad (4)$$

$$N_{Si_3O_{10}^{8-}} = \frac{k_{1,2} N_{SiO_4^{4-}}}{N_{O^{2-}}} \cdot N_{Si_2O_7^{6-}} \quad (5)$$

$$N_{Si_4O_{13}^{10-}} = \frac{k_{1,3} N_{SiO_4^{4-}}}{N_{O^{2-}}} \cdot N_{Si_3O_{10}^{8-}} \quad (6)$$

etc.

The assumption is now introduced that

$$k_{1,1} = k_{1,2} = k_{1,3} = \dots = k \quad (7)$$

This is analogous to but is more limited than the assumption of Toop and Samis. The constancy of k in the Toop and Samis treatment refers to all polymerisation reactions in which an oxygen ion is eliminated whereas the above assumption refers only to the reactions of SiO_4^{4-} ions.

From equations (4), (5), (6) and (7) the sum of the ion fractions of silicate anions is obtained as

$$\begin{aligned} \Sigma N_{\text{Silicate}} &= N_{\text{SiO}_4} + N_{\text{Si}_2\text{O}_7} + N_{\text{Si}_3\text{O}_{10}} + \dots \\ &= N_{\text{SiO}_4} + \frac{k N_{\text{SiO}_4}}{N_{\text{O}}^{2-}} [N_{\text{SiO}_4} + N_{\text{Si}_2\text{O}_7} + N_{\text{Si}_3\text{O}_{10}} + \dots] \\ &= N_{\text{SiO}_4} + \frac{k N_{\text{SiO}_4}}{N_{\text{O}}^{2-}} \Sigma N_{\text{Silicate}} \end{aligned}$$

$$\text{Hence, } \Sigma N_{\text{Silicate}} = \frac{N_{\text{SiO}_4}}{1 - \frac{k N_{\text{SiO}_4}}{N_{\text{O}}^{2-}}} \quad (8)$$

If silicate and oxygen are considered to be the sole anionic species in the melt, then the Temkin equation gives

$$\Sigma N_{\text{Silicate}} = 1 - N_{\text{O}}^{2-} \quad (9)$$

Substituting for $\Sigma N_{\text{Silicate}}$ in equation (8) and rearranging gives

$$N_{\text{SiO}_4} = \frac{1 - N_{\text{O}}^{2-}}{1 + k \left(\frac{1}{N_{\text{O}}^{2-} - 1} \right)} \quad (10)$$

which gives N_{SiO_4} as a function of $N_{\text{O}^{2-}}$ if the value of k is known for the system under consideration. In Figure 16, N_{SiO_4} is plotted against $N_{\text{O}^{2-}}$ for various values of k and it is obvious that, for $k = 0$, SiO_4^{4-} is the sole species of silicate ion in the melt. For progressively higher values of k , N_{SiO_4} decreases (at constant $N_{\text{O}^{2-}}$) and the maximum in the distribution is shifted to higher values of $N_{\text{O}^{2-}}$. The maximum in each case corresponds to the orthosilicate composition. For $k = 1$, the distribution is symmetrical about $N_{\text{O}^{2-}} = 0.5$. At this composition, $N_{\text{SiO}_4} = 0.25$. i.e. half the silicate, on a molar basis, is present as SiO_4^{4-} .

Combination of equation (10) with equations (4), (5) and (6) allows the ion fractions of the higher members of the series to be calculated as a function of $N_{\text{O}^{2-}}$ if k is known. Figure 17 shows the calculated distribution of SiO_4^{4-} , $\text{Si}_2\text{O}_7^{6-}$, $\text{Si}_3\text{O}_{10}^{8-}$ and $\text{Si}_4\text{O}_{13}^{10-}$, and $\text{Si}_5\text{O}_{16}^{13-}$ corresponding to $k = 1$.

To apply the theory outlined above, it is necessary to express the mole fraction of silica in terms of the ion fractions of the individual constituents. The necessary relation is,

$$\begin{aligned}
 N_{\text{SiO}_2} &= \frac{\text{moles of SiO}_2 \text{ from silicates}}{\text{moles MO} + \text{moles of MO from silicates} + \text{moles of SiO}_2 \text{ from silicates}} \\
 &= \frac{N_{\text{SiO}_4} + 2N_{\text{Si}_2\text{O}_7} + 3N_{\text{Si}_3\text{O}_{10}} + \dots}{(N_{\text{O}^{2-}}) + (2N_{\text{SiO}_4} + 3N_{\text{Si}_2\text{O}_7} + 4N_{\text{Si}_3\text{O}_{10}} + \dots)} \\
 &\quad + (N_{\text{SiO}_4} + 2N_{\text{Si}_2\text{O}_7} + \dots) \\
 &= \frac{N_{\text{SiO}_4} + 2N_{\text{Si}_2\text{O}_7} + 3N_{\text{Si}_3\text{O}_{10}} + \dots}{N_{\text{O}^{2-}} + 3N_{\text{SiO}_4} + 5N_{\text{Si}_2\text{O}_7} + 7N_{\text{Si}_3\text{O}_{10}} + \dots} \quad (11)
 \end{aligned}$$

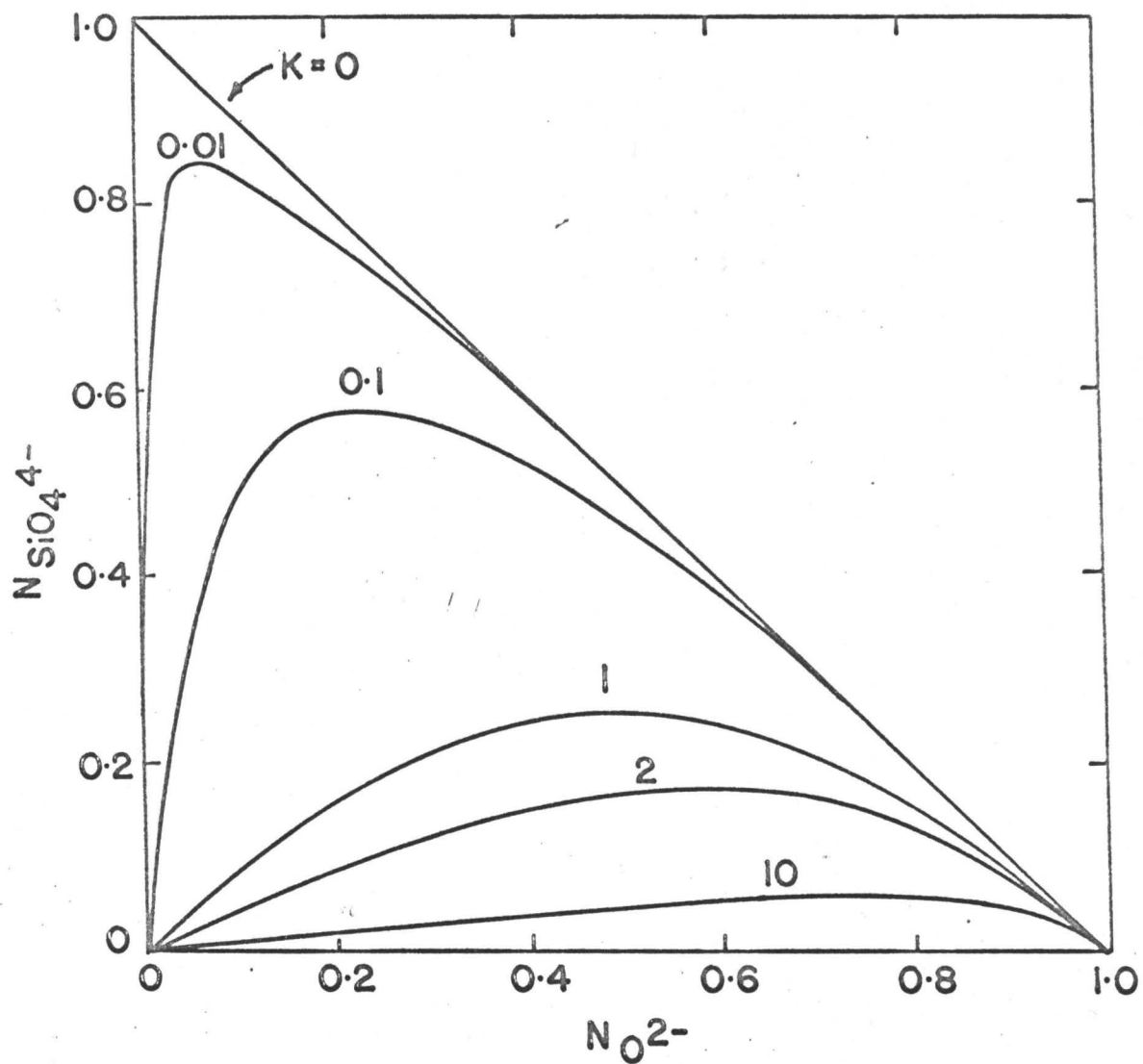


Figure 16. Theoretical curves of $N_{\text{SiO}_4}^{4-}$ against N_{O}^{2-} for various values of k . (Masson).

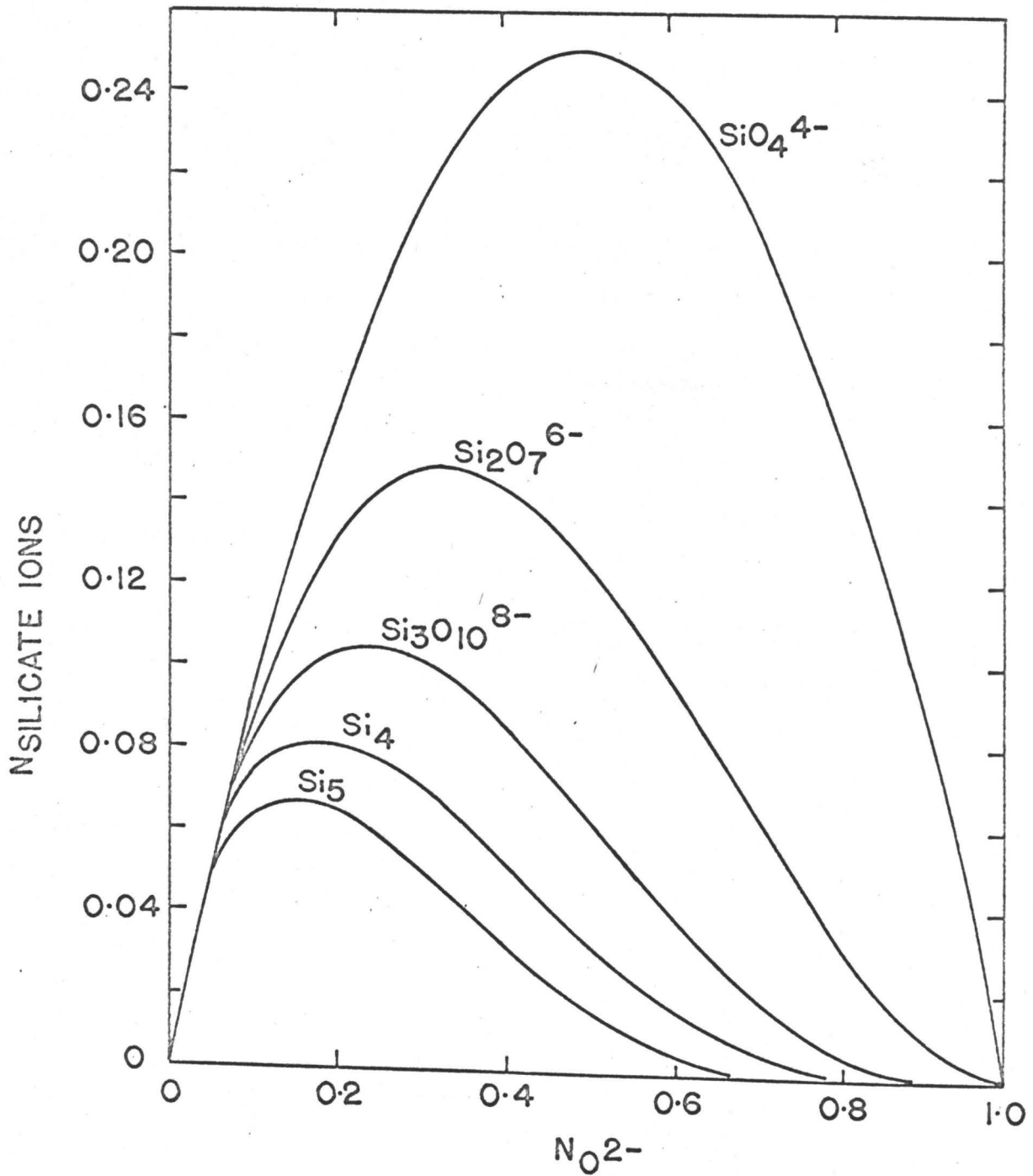


Figure 17. Theoretical curves of N_{silicate} against $N_{\text{O}^{2-}}$ for $k = 1$. (Masson) (67)

From (4), (5), (6) and (7), it follows that,

$$N_{\text{Si}_2\text{O}_7} = \left(\frac{k N_{\text{SiO}_4}}{N_{\text{O}^{2-}}} \right) N_{\text{SiO}_4}$$

$$N_{\text{Si}_3\text{O}_{10}} = \left(\frac{k N_{\text{SiO}_4}}{N_{\text{O}^{2-}}} \right)^2 N_{\text{SiO}_4}$$

$$N_{\text{Si}_4\text{O}_{13}} = \left(\frac{k N_{\text{SiO}_4}}{N_{\text{O}^{2-}}} \right)^3 N_{\text{SiO}_4}$$

etc.

Hence,

$$N_{\text{SiO}_4} + 2N_{\text{Si}_2\text{O}_7} + 3N_{\text{Si}_3\text{O}_{10}} + \dots =$$

$$N_{\text{SiO}_4} \left\{ 1 + 2 \left(\frac{k N_{\text{SiO}_4}}{N_{\text{O}^{2-}}} \right) + 3 \left(\frac{k N_{\text{SiO}_4}}{N_{\text{O}^{2-}}} \right)^2 + \dots \right\} \quad (12)$$

The summation in parenthesis may be evaluated provided $\left(\frac{k N_{\text{SiO}_4}}{N_{\text{O}^{2-}}} \right)^2$ is less than unity. Inspection of equation (8) shows that this condition is fulfilled as $1 \geq \sum N_{\text{Silicate}} \geq N_{\text{SiO}_4} \geq 0$. The numerator in equation (11)

$$\text{numerator} = \frac{N_{\text{SiO}_4}}{\left(1 - \frac{k N_{\text{SiO}_4}}{N_{\text{O}^{2-}}} \right)^2} \quad (13)$$

Similarly, it can be shown that the denominator of equation (11) reduces to

$$\text{denominator} = N_{O^{2-}} + \frac{N_{SiO_4} \left(3 - \frac{k N_{SiO_4}}{N_{O^{2-}}} \right)}{\left(1 - \frac{k N_{SiO_4}}{N_{O^{2-}}} \right)^2} \quad (14)$$

so that the mole fraction of silica is given as

$$N_{SiO_2} = 1 / \left[3 + \frac{N_{O^{2-}}}{N_{SiO_4}} + k \left\{ \frac{N_{SiO_4}}{N_{O^{2-}}} (k - 1) - 2 \right\} \right] \quad (15)$$

Combination of (10) and (15) gives N_{SiO_2} as a function of $N_{O^{2-}}$ and k .

$$N_{SiO_2} = 1 / \left[3 - k + \frac{N_{O^{2-}}}{1 - N_{O^{2-}}} + \frac{k(k-1)}{\left(\frac{N_{O^{2-}}}{1 - N_{O^{2-}}} \right) + k} \right] \quad (16)$$

Equation (16) may be expressed in terms of activities by introducing the Temkin equation in the form

$$a_{MO} = N_{M^{2+}} \cdot N_{O^{2-}} \quad (17)$$

Equation (17) is derived on the basis that anions and cations mix ideally on their separate matrices. Although there is no a priori reason to expect ideal mixing, particularly of silicate ions, in such systems these systems are examined to see how far the Temkin equation may be applicable for melts of such complexity. For a binary system where $N_{M^{2+}}$ is unity, equations (16) and (17) yield

$$N_{SiO_2} = 1 - N_{MO} = 1 / \left[3 - k + \frac{a_{MO}}{1 - a_{MO}} + \frac{k(k-1)}{\left(\frac{a_{MO}}{1 - a_{MO}} \right) + k} \right] \quad (18)$$

which gives the activity of MO as a function of composition if k is known. Theoretical plots of a_{MO} against N_{MO} for various values of k are shown in Figure 18.

Masson has applied this model to the systems FeO-SiO₂, MnO-SiO₂, PbO-SiO₂ and CaO-SiO₂ and by curve-fitting with experimentally determined activity-composition relationships has obtained values of k for these systems. These values of k are given in Table IV.

| SYSTEM | k |
|------------------------|-------|
| FeO - SiO ₂ | 1.4 |
| MnO - SiO ₂ | 0.75 |
| PbO - SiO ₂ | 0.2 |
| CaO - SiO ₂ | 0.003 |

TABLE IV Values of k for various binary silicate melts (after Masson).

Table IV shows that the tendency to polymerisation in binary silicate melts is determined by the nature of the cation and that a quantitative measure of this is provided by the magnitude of the constants $k_{1,1}$, $k_{1,2}$, $k_{1,3}$. . . This is in agreement with the conclusion of Toop and Samis. In considering the mechanism of polymerisation in such system, it is logical to expect that the average chain length will be determined by the magnitudes of both the cation-silicate ion and cation-oxygen ion attractions. It is probable that these will be roughly parallel for different cations, so that cations which have a high ion-oxygen attraction

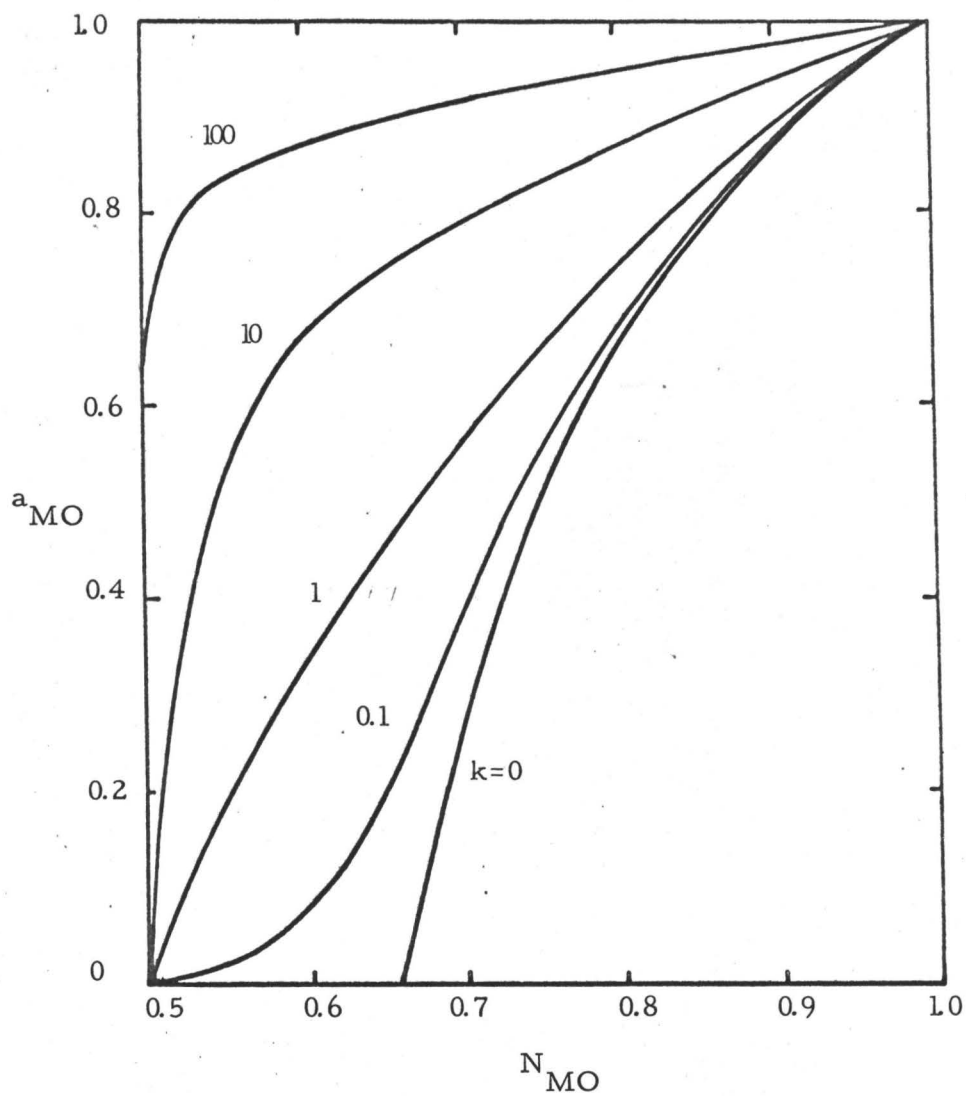


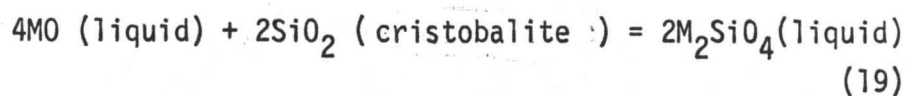
Figure 18. Theoretical curves of activity against mole fraction of metal oxide for various values of k . (Masson).⁽⁶⁷⁾

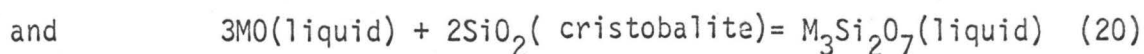
will also exhibit a high attraction for silicate ions. Cations which interact strongly with silicate ions may be expected to exert a "shielding" effect on the reactive groups of the latter and thus hinder the process of polycondensation (e.g. Ca^{2+}). For cations which are more loosely bound (e.g. Mn^{2+} , Fe^{2+}), the shielding will be less effective and polycondensation may occur. In the presence of oxygen ions, however, a competition for cations will arise so that the overall tendency towards polymerisation will be governed by the difference in magnitude between these attractions.

The ease of polymerisation in such systems is undoubtedly influenced also by the degree of polarisation of the silicate ions. For cations which are symmetrically distributed about an SiO_4^{4-} anion, the net distortion of electron density in the latter will be zero. When a cation is partially or wholly removed from the field of the silicate ion, however, leaving a negatively charged oxygen as a potential reaction site, the electron density at this site will be lowered by the polarising tendencies of the remaining cations and polycondensation will be facilitated.

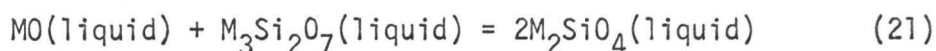
The extent of the cation-oxygen attraction will also influence the degree of ionic bonding in the silicon-oxygen linkages. These changes in bond strength due to different cations will be reflected in the standard free energies of formation of the various silicates from their constituent oxides and the individual values of $k_{1,1}$, $k_{1,2}$, $k_{1,3}$, may be calculated if the requisite free energy data are available.

The following reactions are considered.





where $M_2SiO_4(\text{liquid})$ and $M_3Si_2O_7(\text{liquid})$ are the hypothetical mono-disperse liquids in which silica is considered to be present solely as SiO_4^{4-} and $Si_2O_7^{6-}$ ions respectively. The difference between (19) and (20) gives



for which the standard free energy change may be written

$$\Delta G^\circ_{(21)} = 2\Delta G^\circ \text{ orthosilicate} - \Delta G^\circ \text{ pyrosilicate} \quad (22)$$

For the mixture of oxide, orthosilicate and pyrosilicate at equilibrium

$$\Delta G^\circ_{(21)} = RT \ln \frac{a_{MO} a_{M_3Si_2O_7}}{a_{M_2SiO_4}^2} \quad (23)$$

As the Temkin equation holds at moderate to high basicities, and as $N_{M^{2+}}$ is unity, then

$$a_{MO} = N_{O^{2-}} \quad (24)$$

$$a_{M_3Si_2O_7} = N_{Si_2O_7} \quad (25)$$

$$a_{M_2SiO_4} = N_{SiO_4} \quad (26)$$

Substituting ion fractions for activities in (23) gives

$$\Delta G^\circ_{(21)} = RT \ln \frac{N_{O^{2-}} N_{Si_2O_7}}{N_{SiO_4}^2} \quad (27)$$

$$= RT \ln k_{1,1} \quad (28)$$

Combination of (22) and (28) gives

$$RT \ln k_{1,1} = 2\Delta G^\circ \text{ orthosilicate} - \Delta G^\circ \text{ pyrosilicate} \quad (29)$$

Similarly, it can be shown that

$$RT \ln k_{1,2} = \Delta G^\circ \text{ ortho} + \Delta G^\circ \text{ pyro} - \Delta G^\circ \text{ tripoly} \quad \text{and}$$

$$RT \ln k_{1,3} = \Delta G^\circ \text{ ortho} + \Delta G^\circ \text{ tripoly} + \Delta G^\circ \text{ tetrapoly}.$$

Using equation (28) and available thermodynamic data, Masson has calculated the values of $k_{1,1}$ as a function of temperature for the system CaO-SiO_2 . These are shown in Table V.

| TEMP. °K | $k_{1,1}$ |
|----------|-----------|
| 1400 | 0.0012 |
| 1500 | 0.0018 |
| 1600 | 0.0025 |
| 1700 | 0.0033 |

TABLE V Estimated values of $k_{1,1}$ for the system CaO-SiO_2 at various temperatures.

Masson regards the above model as being of a preliminary nature and indicates the following limitations.

(a) Only binary systems have been considered. When a second cation

is introduced, the Temkin equation is no longer applicable due to the competition which arises for different cations between oxygen and silicate anions.

(b) No provision has been made for the possible formation of ring structures. Ring formation might be expected to be favoured in systems with a low value of k , where the cation-silicate interaction is high and coiling of the polyanions may occur owing to effective neutralisation of the charged groups on the polymeric chains.

(c) Predictions of the theory are not expected to be of high accuracy for the lowest members of the series nor in regions close to silica saturation.

CHAPTER 3

THE CONSTITUTION AND STRUCTURE OF IRON SILICATES

The phase relationships occurring in the Fe-O system have been determined to a high degree of precision by Darken and Gurry (68, 69) and the phase relationships in the pseudo-binary system "FeO"-SiO₂ have been determined by Bowen and Schairer (70). The phase diagram for the latter system was determined by examining and analysing melts which had been equilibrated with solid iron in atmospheres of purified "neutral" nitrogen. In the analyses of the melts all the iron present was calculated as stoichiometric FeO and hence the phase diagram produced is, in fact, a projection on the "FeO"-SiO₂ join plane of a non-planar, non-horizontal section in the phase diagram FeO-Fe₂O₃-SiO₂ (71, 72). Consequently, the "FeO"-SiO₂ pseudo-binary can only be treated as a binary insofar as equilibrium crystallisation is concerned.

By establishing equilibrium between CO-CO₂ atmospheres and liquid iron silicates contained in iron crucibles, Schuhmann and Ensio (73) have determined the activities of iron oxide in iron silicates. A second determination of this relationship has been carried out by Bodsworth (49), using H₂ - H₂O atmospheres. The relationships obtained from these two investigations are shown in Figure 19. A notable feature of the curve by Shuhmann and Ensio is the change from positive deviation from ideality at low silica concentrations to a negative deviation at 21 weight per cent silica. This type of relationship

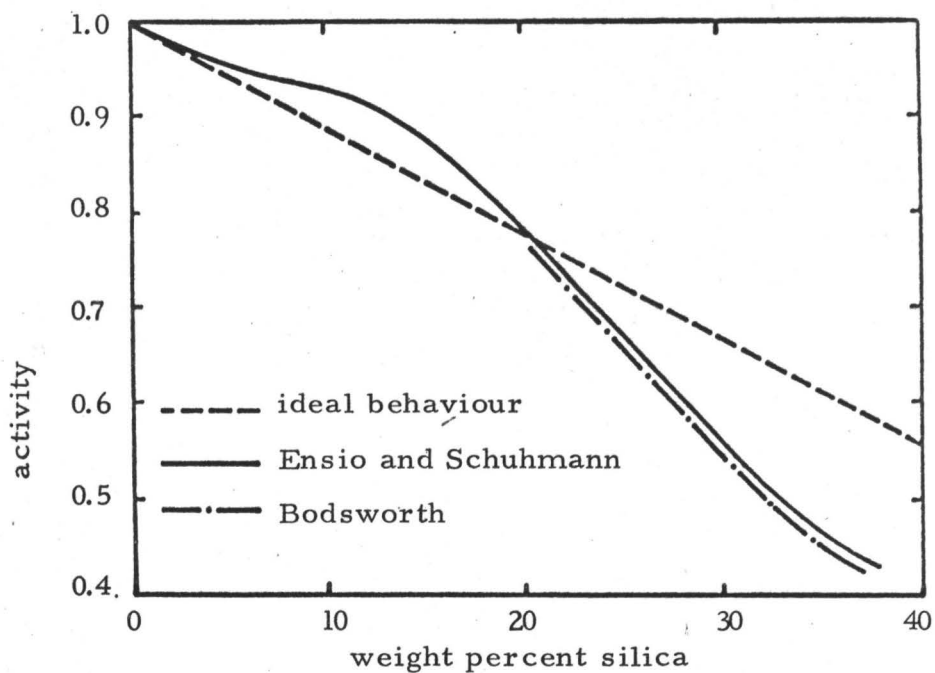


Figure 19. Experimentally determined activities of iron oxide as a function of composition in iron silicate melts. (47, 73)

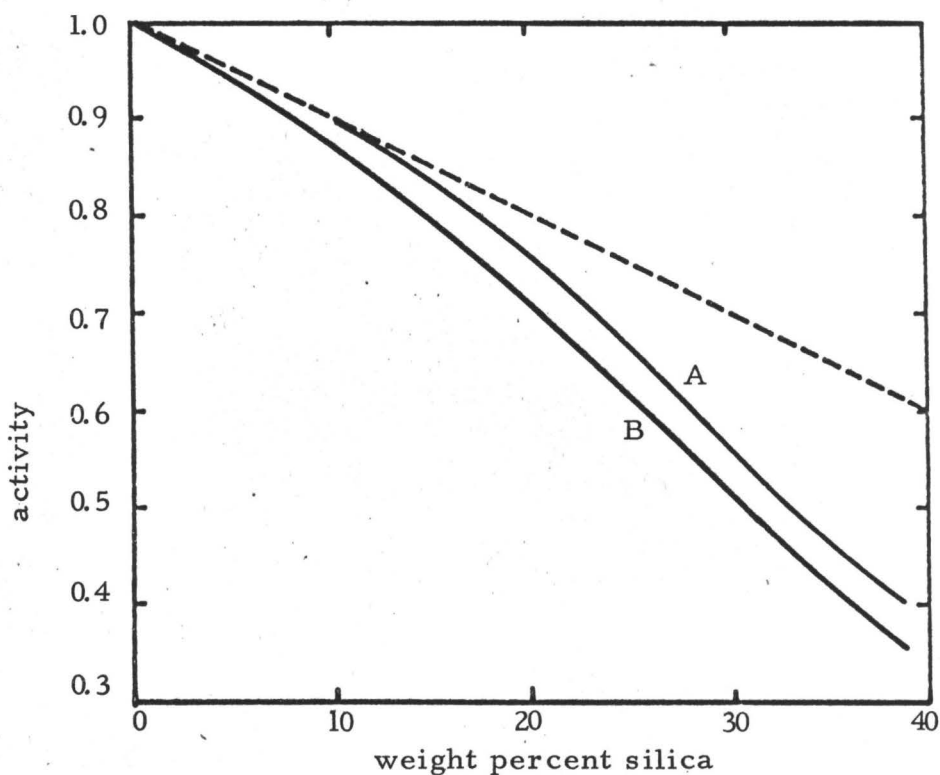


Figure 20. Calculated activities of stoichiometric iron oxide as a function of composition in iron silicate melts. (77)

is exceptional when comparison is made with the activity curves of other basic oxides in binary silicate melts (64, 74, 75, 76). Usually a negative deviation from ideality exists over the entire composition range. Interpretation of the data for the ferrous oxide - silica system is complicated by the fact that ferrous oxide is non-stoichiometric. Liquid iron oxide in equilibrium with solid iron ranges in composition from $\text{Fe}_{0.964}\text{O}$ at 1371°C to $\text{Fe}_{0.981}\text{O}$ at 1524°C , and thus the experimentally determined activities of iron oxide in iron silicates cannot be referred to the stoichiometric FeO as the standard state.

By employing a statistical model for the entropy of ideal mixing of ferrous and ferric cations, and assuming that the structures of solid and liquid iron silicates are similar, Bodsworth and Davidson (77) have attempted to subtract the effect of the presence of ferric ions from the experimental values of iron oxide activity, and so obtain the activity-composition curve of stoichiometric ferrous oxide in iron silicates. The relationships calculated are shown in Figure 20. Lines (A) and (B) are for models in which (A) the wustite phase is assumed to have an NaCl structure in which the number of cation sites available is equal to the number of oxygen ions present and (B) in which one cation site is present for each negative charge, so that all cation sites are occupied in a monovalent oxide, and half the cation sites are occupied in a divalent oxide, etc. These models are strictly justified only at infinitely low silica concentrations. The form of the derived relationships in Figure 20 led Bodsworth and Davidson to suggest that the presence of ferric ions in iron silicates accounts for the positive deviations from ideality shown in Figure 19. Lumsden (78)

has pointed out however, that as the above models have not been verified by comparing them with the experimental results of Darken and Gurry for the real binary $\text{FeO-Fe}_2\text{O}_3$, extension of the model into the ternary silicate system is meaningless.

The most striking feature of the experimentally determined activity-composition relationship is that the measured activities were found to be independent of temperature over the temperature range studied ($1250^\circ - 1365^\circ\text{C}$). This suggests that the heat of mixing is either zero or very small and implies that FeO and SiO_2 are ideally mixed in solution. This result has been questioned by Rey (79). Using the tabulated thermodynamic data for heats of formation and heat of fusion of FeO , $2\text{FeO} \cdot \text{SiO}_2$, $\text{FeO} \cdot \text{SiO}_2$ and SiO_2 (80, 81), Rey has constructed a heat of mixing diagram for iron silicates which indicates an evolution of heat on mixing in the region of the silicate compounds ($\text{FeO} \cdot \text{SiO}_2$ being regarded as a compound in this treatment) and an absorption of heat on mixing in the neighbourhood of silica. This heat of mixing diagram, along with the pseudo-binary phase diagram is shown in Figure 21. The form of this diagram led Rey to suspect the accuracy of the experiments of Schuhmann and Ensio. An explanation offered by Bodsworth and Davidson for this discrepancy is that the apparent temperature independence of the experimentally measured activities of iron oxide may be due to the occurrence of two compensating effects. It was suggested that with increasing temperature, the effect of decreasing ferric ion concentration was offset by the effect of increasing activity of stoichiometric ferrous oxide.

The marked increase in ferric ion concentration which accompanies

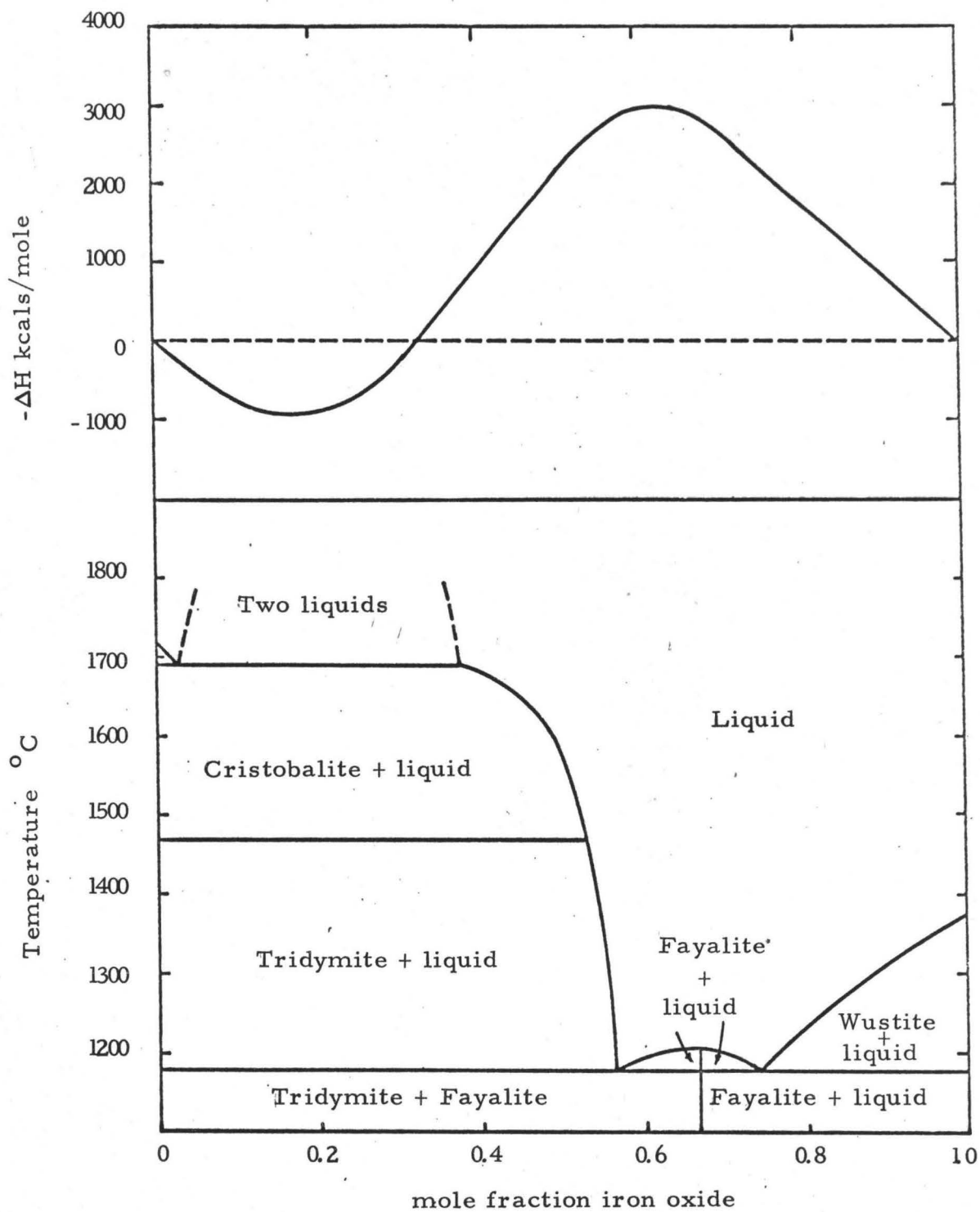
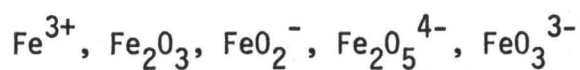
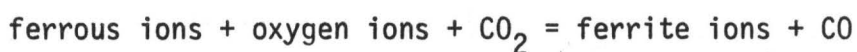


Figure 21. Heat of mixing diagram and phase diagram for iron silicates. (70, 79)

an increase in slag basicity, other factors remaining constant, led Chipman and Chang (82) to suggest that liquid iron oxide contains ferrous ions, oxygen ions and at least one other anion containing tripositive iron. Also it is difficult to imagine the Fe^{3+} cation, with its high charge and small radius, having a separate existence in the liquid state. The particular species of ferrite ion present in basic slags cannot be decided from thermodynamics alone and Chipman and Chang based their selection on the criterion of convenience. It was suggested that ferrite ions are formed from ferric ions by a series of successive neutralisations with oxide ions. e.g.



By considering the experimental data of Darken and Gurry, and choosing that ferrite ion which has an activity coefficient nearest to unity in the reaction:



the $\text{Fe}_2\text{O}_5^{4-}$ ion was suggested.

The ionic nature of iron silicate melts has been confirmed by the electrical conductivity studies of Simnad, Derge and George (83). The relationship obtained between ionic current efficiency and composition is shown in Figure 22. The conclusion drawn from this study was that liquid iron oxide consists of ferrous and ferric ions in an oxygen ion network. The break in the cell efficiency curve at 10 weight per cent silica was related to the minimum in the ferric ion concentration and the change in activity of iron oxide occurring at this composition.

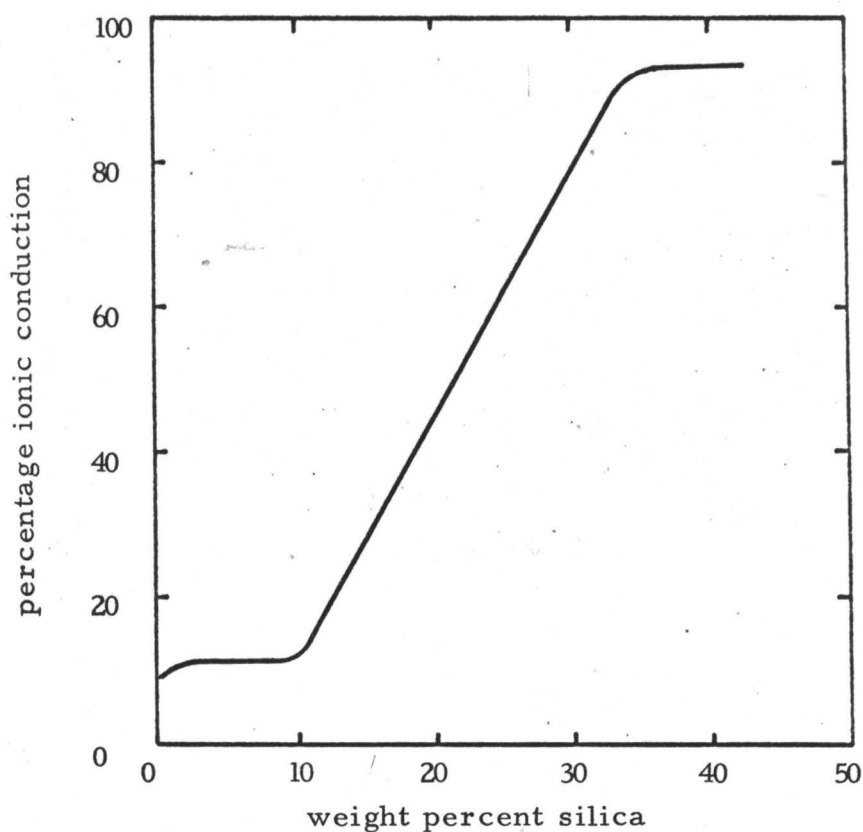


Figure 22. Percentage ionic conduction in iron silicate melts as a function of composition. (83)

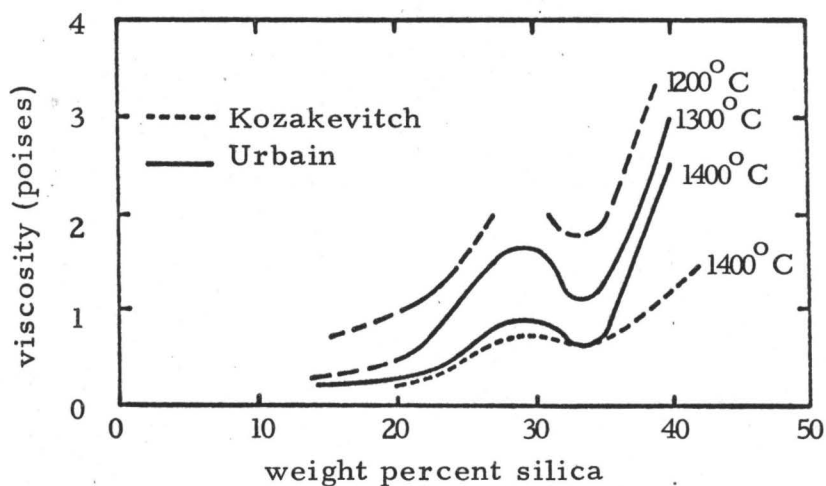


Figure 23. Viscosities of iron silicate melts as a function of composition and temperature. (84)

However, the ferric ion concentration does not in fact reach its minimum until 35 to 40 weight per cent silica is present (70). Above 10 per cent silica the ions resulting from the introduction of silica were considered to be increasingly effective in conductance and it was suggested that the break at 34 per cent silica may indicate the existence of some proportion of associated complex ion in the melt above the orthosilicate composition. It was considered that these melts consist mainly of ferrous and silicate ions with a small proportion of ferric ions. Measurement of transport numbers indicated that the ionic current is carried almost completely by ferrous ions, the electronic current being carried by a semi-conduction mechanism whereby electrons jump from ferrous to ferric ions. No temperature dependence of current efficiency was detected which is surprising in view of the fact that the total iron content of the melt increases with increasing temperature, and the ferric ion concentration decreases. Both of these factors would be expected to increase the proportion of ionic current. No information concerning the nature of the silicate anions was obtained from this investigation.

The viscosity of liquid iron oxide has been measured by Schenck et al (84) and the viscosities of iron silicates as a function of composition and temperature have been measured by Kozakevitch (85) and by Urbain (86). The relationships obtained are shown in Figure 23 and suggest that an association of ions occurs in the vicinity of the orthosilicate composition.

The advantage of being able to contain liquid iron oxide and iron silicates in iron crucibles, is attended by the disadvantage that

that the composition of these liquids is then dependent on temperature. The variation of melt composition with temperature, in accordance with the iron liquidus composition, has been sufficient, in some investigations, to prevent meaningful interpretation of the experimental data. An example of this occurs in the investigation of the variation of the density of liquid iron oxide and iron silicates with temperature (87). In this study, an increase in temperature tends to produce both an increase in density due to an increase in the iron concentration of the melt and also a decrease in density due to thermal expansion of the melt. These two effects cannot be separated in the determination of the variation of measured density with temperature.

In the measurement of temperature coefficients of surface tension (39) this problem was eliminated by containing the melts in Pt-Rh basins. The observation of abnormal temperature coefficients for the surface tensions of iron silicates when the mole fractions of silica exceeds 0.30 was taken as indicating that beyond this silica concentration the effect of the thermally induced breakdown of complex silicate anions to smaller units is sufficiently great to overcome the normal decrease in surface tension due to thermal expansion of the liquid. This is the only investigation of a physical property of basic iron silicates which has provided information on the nature of the silicate anions present. From the results obtained, which are shown in Figure 9, it was concluded that increasing silica content is accompanied by an increase in the degree of association in the melt, i.e. by an increase in the size of silicate anions present.

CHAPTER 4

THE MAXIMUM BUBBLE PRESSURE METHOD OF DENSITY DETERMINATION

4.1 Theory

Determination of the density of a liquid by the maximum bubble pressure method makes use of the fact that the pressure P at a depth h below the surface of a liquid is related to the density of the liquid ρ by the equation

$$P = h\rho g$$

where g is the gravitational constant. If a tube is immersed to a depth h in the liquid and a gas bubble is blown, then the maximum pressure required to blow the bubble is given as

$$P (\text{max}) = h\rho g + 2\gamma/r$$

where γ is the surface tension of the liquid and r is the critical minimum radius of the bubble. For a blowing tube immersed in a liquid of fixed density, the term $h\rho g$ is constant, being determined only by the depth of immersion of the tube and corresponding to the static head of liquid above this depth of immersion. The surface tension contribution $2\gamma/r$ varies inversely with the bubble radius and hence results in the occurrence of a maximum pressure during the process of blowing a bubble. Before its emergence from the blowing tube, the end of the gas column has a radius which is determined by the surface tension of the liquid and the internal diameter of the blowing tube. As the gas column emerges from the blowing tube and

begins to form a bubble, the bubble diameter decreases until, theoretically, the bubble assumes a hemispherical shape of radius equal to that of the blowing tube. Further growth of the bubble results in an increase in bubble diameter which renders the bubble unstable. At some point during this period of diameter increase, the instability introduced becomes sufficient to cause the bubble to break away. This critical minimum diameter of a stable bubble corresponds to a maximum surface tension contribution to the measured pressure and hence facilitates the measurement of the unique maximum pressure required to blow a bubble at the particular depth of immersion.

If bubbles are blown at a series of different depths of immersion in the liquid, and it is assumed that the surface tension contribution to the bubble pressure is independent of the total bubble pressure, then the density is obtained as

$$\rho = \left(\frac{\partial p}{\partial h} \right)_T \cdot \frac{1}{g}$$

4.2 Corrections required for density calculation

In the calculation of the density, three corrections are required; (1) for the variation of the manometric fluid density with variation of ambient temperature; (2) for thermal expansion of the crucible and blowing tube, and (3) for the rise in level of the melt due to displacement by the immersed tube.

Density of the manometric fluid

The manometric fluid used was dibutyl phthalate. The density temperature-relationship for this fluid is given as (88).

$$\rho (\pm 0.005) \text{ gms/cc} = 1.0619 - 0.000801 t$$

where t is in degrees centigrade.

Expansion of crucibles and blowing tube

From the x-ray data of Schmidt (89), the effective linear coefficient of thermal expansion of iron in the temperature range 25 - 1410°C is $16.9 \times 10^{-6} \text{ } ^\circ\text{C}^{-1}$. This allows the dimensions of the crucible and blowing tube at 1410°C to be calculated.

Displacement of melt surface by the blowing tube

When the blowing tube is immersed in the melt, the melt surface rises due to liquid displacement. If the external diameter of the blowing tube is $2r$, the internal diameter of the crucible is $2R$, and the depth of immersion is h , then the surface displacement Δh is given by the expression

$$\Delta h = \frac{hr^2}{R^2 - r^2}$$

For $h = 1 \text{ in.}$, $2r = 1/4 \text{ in.}$, $2R = 1 \text{ in.}$, these measurement being made at 25°C, then, after allowing for thermal expansion Δh at 1410°C = 0.066 in.

4.3 Systematic errors

The density of the liquid ρ_L can be calculated from the expression:

$$\rho_L = \frac{H \cdot \rho_M}{h}$$

where H is the manometric head

ρ_M is the density of the manometric fluid

h is the depth of immersion

The density of dibutyl phthalate is approximately unity and can be calculated to an accuracy of $\pm 5 \times 10^{-4}$ gms/cc. H is typically 14 cms. and can be measured to an accuracy of $\pm 2 \times 10^{-3}$ cm. h is typically 3 cms. and can be measured to an accuracy of $\pm 10^{-2}$ cms.

Thus from the expression

$$\rho_L = \frac{H\rho_M}{h}$$

$$\frac{\partial \rho_L}{\partial H} = \frac{\rho_M}{h} \quad \text{and} \quad \Delta \rho_L = \left| \frac{\rho_M}{h} \Delta H \right| = \frac{2}{3} \times 10^{-3} \text{ gms/cc}$$

$$\frac{\partial \rho_L}{\partial \rho_M} = \frac{H}{h} \quad \text{and} \quad \Delta \rho_L = \left| \frac{H}{h} \Delta \rho_M \right| = \frac{14 \times 5}{3} \times 10^{-4} \text{ gms/cc}$$

$$\frac{\partial \rho_L}{\partial h} = \frac{-H\rho_M}{h^2} \quad \text{and} \quad \Delta \rho_L = \left| \frac{H\rho_M \Delta h}{h^2} \right| = \frac{14}{9} \times 10^{-2} \text{ gms/cc}$$

The total uncertainty in ρ_L is then

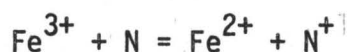
$$\begin{aligned} \therefore \Delta \rho_L &= 6.6 \times 10^{-4} + 23 \times 10^{-4} + 155 \times 10^{-4} \\ &= 0.0185 \text{ gms/cc.} \end{aligned}$$

4.4 Previous work

The determination of the density-composition relationship of iron silicate melts in equilibrium with solid iron has been the subject of several previous investigations (87, 90 - 96), all of which, except one (93), have employed the maximum bubble pressure method. The results of these investigations are shown in Figure 24 and, as can be seen, considerable disparities exist among the various relationships obtained. In the most recent investigation (95, 96), the density-

composition relationship obtained using nitrogen as the bubbling gas was different from that obtained using argon. The densities measured under nitrogen were higher than those measured under argon. The difference between the two relationships was a maximum at the iron oxide composition and decreased with increasing silica content. From these observations, the disparities occurring among the results of the previous investigations could be rationalised. It was shown that two lines, one for nitrogen and the other for argon, could be drawn to fit all the earlier data. As the density difference was a maximum at the iron oxide composition attention was focussed on liquid iron oxide.

The occurrence of a higher measured density when bubbling nitrogen suggested first that solution of nitrogen in the melt might be occurring. However chemical analysis of rapidly quenched melt samples failed to detect the presence of any nitrogen. As the analytical method of nitrogen analysis employed (the Kjeldahl method) is capable of detecting only atomically dissolved nitrogen, the results of these analyses did not preclude the possibility of nitrogen dissolving in the melt in some ionic form. This latter possibility was supported by the observation that the decrease in density difference between nitrogen blown and argon blown melts with increasing silica content paralleled the decrease in the ferric ion content of the melts (73). It was thought, therefore, that ionic nitrogen might dissolve in the melts as a result of a redox reaction of the form.



Continuous weighing measurements were made on small iron crucibles

containing liquid iron oxide, suspended in nitrogen and argon atmospheres. The magnitude of the weight increase occurring when the atmosphere was changed from argon to nitrogen and the corresponding weight decrease when the gas change was reversed, showed that this weight change corresponded only to nitrogen solution in the solid iron crucible and suspension wire.

The range of bubbling gases was extended by Ward and Henderson (97) who measured the density of liquid iron oxide bubbling He, N₂, Ne, Ar and Kr. The measured density was found to decrease smoothly with increasing atomic number of the blowing gas. This relationship is shown in Figure 25. No explanation could be offered for these observations.

CHAPTER 5

EXPERIMENTAL - THE DENSITIES OF IRON OXIDE AND IRON SILICATES

5.1 Experimental Apparatus

5.1.1. Furnace Assembly

A vertically mounted, molybdenum wound, tubular, resistance furnace was used for this investigation. The mullite furnace tube, 2 1/4 ins. O.D x 2 ins. I. D. x 27 ins. in length, was wound, over a length of 10 ins., eight turns per inch, with 0.050 ins. diameter high purity molybdenum wire. The tube was centrally located in a bricklined cylindrical steel shell of diameter 16 ins. and height 20 ins. The shell was fitted with a removable top to which was welded a 5 in. extension of 3 in. diameter stainless steel flexible bellows. The purpose of the bellows was to allow for thermal expansion of the wound tube during furnace operation. The tube was secured by means of water cooled glands and rubber gaskets, located at the base of the shell and at the upper end of the bellows. The space inside the shell, around the tube, was filled with - 8 + 72 mesh alundum grain and a protective reducing atmosphere was passed through the shell. The protective gas was supplied from a cylinder of liquid anhydrous ammonia. The ammonia was dried over magnesium perchlorate and then pre-cracked over hot iron turnings before being admitted to the shell, in order to prevent stress-corrosion cracking of the stainless steel bellows. The furnace windings were led through insulated terminals in the shell wall, to a 220 volt A.C. main supply, passing through a 3.5 Kwatt. variable transformer

an ammeter, a 25 amp. fuse and an on-off temperature controller.

A 1 3/4 in. O.D. x 1 1/2 in. I. D. x 30 ins. in length mullite working tube was placed inside and concentric with the wound tube. This working tube was fitted top and bottom with water-cooled rubber gaskets held in place by brass glands. The bottom gland was fitted with a gas inlet and a centrally located 5/16 in. diameter swagelock opening to allow gas-tight entry of a mullite thermocouple protection sheath to the working tube. The upper gland was provided with a gas outlet and a centrally-located 1/4 in. diameter swagelock opening to allow gas-tight entry of the blowing tube. The entire assembly was mounted on a metal frame.

5.1.2 Crucible assembly

Crucibles of 1 in. I. D. and 3 ins. depth were made from 4 in. x 1 1/4 in. diameter cylinders of Armco iron. Each crucible was provided with a thermocouple well of depth 1/2 in. and diameter 1/2 in. and bayonet lugs to permit its removal from the furnace. The crucibles were positioned in the furnace on a mullite stool which rested on the bottom gland of the working tube. The temperature control thermocouple sheath was introduced to the furnace through the central opening in the bottom gland and was positioned such that its upper end was located in the well in the base of the crucible.

5.1.3 Furnace atmosphere gas

The furnace atmosphere gas, He, N₂, or Ar, was dried over calcium sulphate and magnesium perchlorate and deoxidized over copper turnings at 600°C before being admitted to the base of the furnace working tube.

5.1.4 Temperature control

Furnace temperature control was effected by means of a standardized Pt/Pt-13% Rh thermocouple placed in the furnace in the mullite protection sheath and connected to an on-off temperature controller. This controller limited the temperature variation in the furnace to ± 3 centigrade degrees.

5.1.5. Blowing gas arrangement

The blowing tube was made from a 36 in. length of 1/4 in. O. D. x 0.120 in. I. D. mild steel tubing. To the end of this tube was welded a 2 in. extension of 1/4 in. diameter Armco iron rod drilled out to 5/32 in. diameter and chamfered to an angle of 45°. A 1 1/8 in. diameter by 1/8 in. thick steel disc was welded to the blowing tube three inches above its lower extremity to act as a heat shield and a guide vane. The blowing tube was admitted at the top of the furnace through the central 1/4 in. swagelock opening in the brass gland and was held in position in a vertically-mounted micrometer screw bolted to a shelf above the furnace assembly. The micrometer screw was such that one revolution transmitted a vertical movement of 2 mm. to the blowing tube. The micrometer head was capable of traversing a vertical distance of 6 cm. and could measure a vertical movement of 0.1 mm.

Before being introduced to the blowing tube, dried, deoxidised blowing gas was passed through a microneedle valve, a micro-flowmeter and an open-ended "U"-tube manometer.

5.1.6. Pressure measurement

The bubble pressure at the dibutyl phthalate manometer was measured by means of a cathetometer, which was capable of measuring a

vertical height difference of 0.001 cms.

5.1.7. Temperature profile of the furnace

The temperature profile of the furnace which was determined with a vertical travelling thermocouple is shown in Figure 26.

5.2 Preparation of Materials

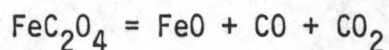
5.2.1 Preparation of wustite

Below 550°C wustite is unstable and dissociates to an iron and magnetite eutectoid. This dissociation proceeds most rapidly at 480°C but ceases below 300°C. Thus, in order to produce wustite at room temperature, extremely rapid quenching is required through the temperature range 550°C to 300°C. However, as the wustite prepared for the present investigation was to be used at 1410°C, then whether or not dissociation occurs on cooling after preparation is inconsequential as wustite reforms on reheating above 550°C.

Wustite was prepared by three methods, (i) by thermal decomposition of ferrous oxalate, (ii) by oxidation of iron, and (iii) by reduction of ferric oxide.

(i) Thermal decomposition of ferrous oxalate

The thermal decomposition of ferrous oxalate produces wustite according to the reaction



Nickel boxes containing reagent grade ferrous oxalate were placed inside a heavy steel tube which was then sealed and connected, through dibutyl phthalate bubblers, to a vacuum pump. The tube was placed in a muffle

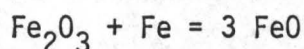
furnace and, after being evacuated, was heated gradually to 650°C over a period of four hours. On completion of the decomposition reaction, the temperature was increase to, and maintained at, 1050°C for a further two hours. The tube was then rapidly withdrawn from the muffle furnace and water-quenched.

(ii) Oxidation of iron

Iron bars were oxidised in air by inductive heating. Above 1369°C the oxide scale melted and dripped off the bar, being caught and quenched on a steel plate.

(iii) Reduction of ferric oxide

Reagent grade ferric oxide was reduced and melted in inductively heated heavy Armco iron crucibles. Wustite formed according to the reaction



and was quenched by pouring on to a steel plate. Oxidation of the iron crucible was prevented by placing it in rammed magnesia powder in the induction coil.

Of the three methods of wustite preparation employed, the method based on the reduction of ferric oxide was chosen because of its ability to allow preparation of a large quantity of wustite of uniform composition in a short time.

Wustite can also be prepared by heating stoichiometric mixtures of ferric oxide and iron powder in sealed evacuated quartz tubes. Wustite is formed after heating for three days at 900°C. (98).

5.2.2 Preparation of silica

Silica was prepared by dehydrating silicic acid at 650°C for 24 hours.

5.3 Preliminary attempts to measure the density of liquid iron oxide

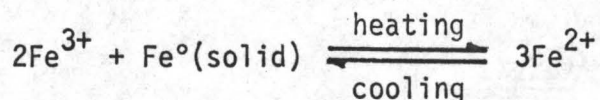
Before measurement of the density of liquid iron oxide was attempted, the density of distilled water at room temperature was measured by bubbling argon and helium. With both gases, density values of 1.00 ± 0.01 gms/cc. were obtained. This indicated that the blowing gas had no effect on the behaviour of dibutyl phthalate as a manometric fluid.

An iron crucible containing about 80 gms. of powdered wustite was placed in the furnace and heated to 1410°C under an atmosphere of dry deoxidised argon. During the eight hour period of furnace heating, deoxidised argon was also passed through the blowing tube, which was located approximately one inch above the crucible. Some twenty minutes after the furnace reached 1410°C , the blowing tube was lowered and immersed to a depth of 0.5 cms. in the melt. Contact of the blowing tube with the melt surface was indicated by a sudden rise in pressure at the manometer. The bubble rate was adjusted, by means of the micro-needle valve to 5 - 6 bubbles per minute and the furnace back pressure was released. The position of the meniscus in the lower arm of the manometer, corresponding to the maximum bubble pressure, was measured. With the depth of immersion of the blowing tube held constant it was observed that the maximum pressure required for bubble blowing increased slowly with time. After thirty minutes of bubbling the depth of immersion was increased by 0.5 cms. and the meniscus position was again measured. Again the maximum bubble pressure increased slowly with time. At thirty-minute intervals, the tube was lowered, in 0.5 cm. increments, and against each of these depths of immersion the maximum bubble pressure was observed to slowly increase with time.

The blowing tube was withdrawn from the furnace and examined. It was found that rings of dendritic iron had formed on the immersed part of the tube. This is shown in Figure 27 (a). The six "steps" correspond to the six different depths of immersion. It appeared that the formation of these rings of iron was responsible for the observed increasing bubble pressure and hence, until this iron precipitation could be eliminated a unique density value could not be obtained.

5.4 Equilibrium requirements of the system Fe(solid) - FeO(liquid) and causes of iron precipitation

(i) The composition of liquid iron oxide contained in a solid iron crucible is that of the liquidus at the temperature under consideration and can conveniently be expressed by the equilibrium



This equilibrium is temperature sensitive to the degree indicated by the slope of the liquidus line in the system Fe-O. Temperature cycling of the furnace could lead to solution and precipitation of iron up and down the liquidus and as that iron precipitated from solution on the cooling cycle is not necessarily redissolved on the heating cycle, this mechanism could lead to the production of solid iron in the melt.

If the temperature is not uniform in the crucible and the melt then, in an attempt to establish equilibrium in the system, iron will continuously dissolve from the hotter iron surface areas and deposit on the cooler iron surfaces. As immersion of the blowing tube into the melt would be expected to abstract heat from the melt, it is possible

that the temperature of the immersed surface of the blowing tube is lower than that of the crucible wall. Hence, iron could be transferred through the melt from the crucible walls to the blowing tube surface.

If the melt surface is cooled by heat losses into the gas atmosphere, then surface precipitation of iron could occur according to the reaction given above.

(ii) In addition to the temperature dependent $\text{Fe}^{3+} - \text{Fe}^{2+} - \text{Fe}^{\circ}$ equilibrium an equilibrium occurs between the oxygen ions in the melt and the oxygen in the gas phase. If, at any temperature, the partial pressure of oxygen in the gas phase is less than the value for equilibrium with iron oxide, then reduction of the iron oxide, and hence iron precipitation, will occur. This reaction has been found to be very rapid (73). As the partial pressure of oxygen in equilibrium with copper and copper oxide at 600°C is less than that for equilibrium with iron and iron oxide at 1410°C , the gas atmosphere and blowing gases used in the previous investigations and in the preliminary experiment of the present study are reducing with respect to iron oxide. In addition to this fact, the oxygen content of the blowing gas is lowered as a result of its subsequent slow passage (approx. 0.02 cm/sec.) down the mild steel blowing tube, which ranges in temperature from room temperature at its upper end to 1410°C at its lower end.

5.5 The effect of the occurrence of iron precipitation on the measured density

The effect of iron precipitation on the measured density is dependent on the extent to which the iron precipitation alters the geometry of the crucible-melt system.

(i) If iron precipitates on to the blowing tube in such a manner as to

effectively lengthen the blowing tube, then the depth of immersion of the blowing tube in the melt is increased. In such a case, the measured bubble pressure will increase and as the depth of immersion is underestimated the calculated density will be high. As has been stated, it is possible that the precipitation of iron can occur as a result of two processes (i) by lack of thermal equilibrium and (ii) by chemical reduction. In the former case, the total volume of liquid iron oxide will remain constant, the iron precipitating onto the blowing tube being transferred from the crucible walls. The effect of this will be to increase the inside diameter of the crucible and the outside diameter of the blowing tube. In the absence of other effects, the position of the surface level of the melt will not be affected by this transfer. If chemical reduction of the iron oxide occurs, however, the volume of the crucible contents will be decreased. (Reduction of 1 cc. of liquid iron oxide of density 4.55 gms./cc. and iron content of 77 wt% produces only 0.47 ccs. of solid iron at 1410°C). Thus the surface level of the melt will fall and the depth of immersion of the blowing tube will decrease. Whether or not the measured bubble pressure will increase or decrease will depend on the relative extents of surface lowering and blowing tube extension by iron precipitation. If the iron precipitation occurs entirely above the lower extremity of the blowing tube, then the measured bubble pressure will decrease and the calculated density will be low.

(ii) If iron precipitation occurs at the surface of the melt as a result of surface cooling by heat losses to the furnace atmosphere, then this heterogeneously nucleated iron will form a ring of dendritic iron

around the inside of the crucible. The formation of this ring decreases the effective diameter of the crucible at the melt surface and thus the level of the surface will rise. In such a case, the depth of immersion of the blowing tube is effectively increased and hence the measured density will be high. A typical surface ring of dendritic iron is shown in Figure 28.

In a previous study (97) the blowing gases (He, N₂, Ne, Ar and Kr) differed considerably in thermal conductivity and hence for a given gas flow rate the rate of heat removal from the melt surface by the furnace atmosphere would be proportional to the thermal conductivity of the gas. This effect of differing gas thermal conductivities was suggested by Dancy and Derge (99) as a result of studies on the electrical conductivities of melts in the system CaO - Fe_xO. They found that the measured electrical conductivity increased with decreasing atomic weight of the gas atmosphere, i.e. with increasing thermal conductivity of the gas atmosphere and attributed this effect to the presence of surface precipitated iron in their melts. The rings of iron formed at the melt surface would also account for the variation in density which occurs with different blowing gases.

If the gas atmosphere to which heat is being conducted is also reducing with respect to iron oxide, then, in addition to thermally-induced precipitation at the surface, solid iron can also be formed as a result of chemical reduction. In this case, the volume of the liquid is decreased and thus the surface level is raised to a lesser extent than would be the case in the absence of chemical reduction.

(iii) It has been suggested (91) that the measured density of iron oxide can be increased as a result of the presence of solid iron in free suspension in the melt. It was considered that this free suspension was maintained by the bubbling action. In such a case, the measured density would be that of a heterogeneous mixture of solid iron of density 7.4 gms/cc and liquid iron oxide of density 4.55 gms/cc. It is difficult to imagine, however, that small particles of solid iron could be kept in free suspension in the melt by the low gas bubbling rates employed in this and previous investigations. If such iron were present, it would fall under gravity and collect at the base of this crucible; where, being below the extremity of the blowing tube, it would only affect the measured density in that the level of the melt surface would be lowered. This would have the effect of producing a low density value rather than the high value found in that particular investigation (97). It is considered that freely suspended iron in the melt can only result from homogeneous nucleation and the requirements for such a process are more extreme than occur in these experiments. It must be assumed, therefore, that any iron precipitating is nucleated heterogeneously.

From the above arguments it is seen that the effect of iron precipitation on the crucible-melt geometry can be both considerable and variable and consequently the measured density of the melt could range in value between quite wide limits.

5.6 Modifications to the apparatus

No attempt was made to evaluate the relative magnitudes of the various possible causes of iron precipitation in the melt. Instead,

the apparatus was modified in such a manner as to eliminate, or at least minimise, all of the causes. The modifications were as follows.

(i) In an attempt to obtain a more uniform hot zone in the furnace, the furnace tube was wound differentially. This comprised winding the centre 3 ins. at a rate of 8 turns per inch, the two 1 1/2 in. end zones with 11 turns per inch and the two 2 in. intermediate zones with 9 turns per inch.

(ii) The on-off temperature controller was replaced by a saturable core reactor temperature controller which limited temperature cycling of the furnace to less than one centigrade degree.

(iii) The temperature of the copper turnings in the de-oxidising furnaces was increased to 801°C. This is the calculated temperature at which the partial pressure of oxygen in equilibrium with Cu and Cu₂O (100) is the same as that in equilibrium with Fe and FeO at 1410°C (69).

(iv) A 3 mm. O. D. x 2 mm. I. D. silica tube was placed inside the blowing tube as a liner to prevent deoxidation of the blowing gas by contact with the hot steel during its passage down the blowing tube. To accommodate the silica liner, the blowing tube inside diameter was increased from 0.120 ins. (16 gauge tubing) to 0.194 ins. (22 gauge tubing.)

(v) A molybdenum wound heating element was placed in the furnace some two inches above the crucible. This produced an asymmetric temperature profile in the furnace such that the temperature just above the melt surface was slightly higher than that of the melt surface. Thus, in addition to the direction of heat flow being from the gas to the melt, heat is also conducted down the blowing tube into the melt rather than up the tube and out of the melt. The temperature profile produced is

shown in comparison with the original in Figure 26 and the construction and positioning of the heating element is shown in Figure 29.

5.7 Determination of the density of liquid iron oxide and liquid iron silicates with the modified apparatus

Using the modified apparatus and bubbling argon, constant maximum bubble pressure measurements were obtained at each of ten depths of immersion, 0.3 cms. apart. This allowed calculation of a unique density value. Inspection of the blowing tube after removal from the furnace showed that iron precipitation on the blowing tube had been eliminated. The tip of the blowing tube is shown in Figure 27(b). Unique values of the density of liquid iron oxide were also obtained bubbling helium and nitrogen, but an attempt to measure the density bubbling krypton was unsuccessful because of surging in the blowing gas line. The results of these experiments are tabulated in table V. During a second run bubbling nitrogen, after a density value had been obtained with the modified apparatus, the silica liner tube was removed, the temperature of the copper turnings lowered to 600°C and the heating element turned off. The pressure readings became erratic and the 2σ error limits of the calculated density increased from ± 0.03 gms/cc to ± 0.17 gms/cc. The tip of this blowing tube is shown in Figure 27(c) and as can be seen, iron precipitation has again occurred.

Dehydrated silicic acid was added to iron oxide and the density-composition relationship of the iron silicate system was determined bubbling helium, nitrogen and argon in the range 0 - 34 wt. per cent SiO_2 . The equilibrium partial pressure of oxygen was calculated (73)

for each run and the temperature of the deoxidising copper turnings was adjusted accordingly. The results are listed in Table VI and are shown graphically in Figure 30. Also included in Figure 30 is the calculated density - composition relationship for mechanical mixtures of iron oxide and silica.

5.7.1 Sampling of the melt

During determination of the density of liquid iron oxide two melt samples were obtained for chemical analysis. One was obtained by lowering an iron-tipped tube, fitted with an aspirator bulb, into the melt and sucking up a small sample. The other was obtained by withdrawing the crucible from the furnace immediately after blowing, quenching it rapidly in water and sectioning it horizontally. The "middle inch" of melt, some 40 to 50 gms., was crushed and sampled for analysis. The total iron content was estimated by the potassium dichromate method of analysis for iron. The analyses of the two samples obtained from the argon and helium - blown melts are shown in Table VII. The fact that the crucible samples contained a higher total iron content at first suggested that iron had precipitated in the melt during the cooling of the crucible, but microexamination of the sample showed that this was not the case. It was considered therefore, that the oxygen contents of the small aspirator samples had increased as a result of contact of the sample with the air present in the sampling tube and the aspirator bulb. This was, in part, confirmed by the fact that the total iron contents of the crucible samples are very close to the values obtained by Darken and Gurry (69) at 1410°C. In addition, it was considered that iron oxide in contact with solid iron cannot be expected to contain

less than the equilibrium amount of iron. For these reasons, during subsequent density determinations in which iron crucibles were used, only crucible samples were analysed.

CHAPTER 6

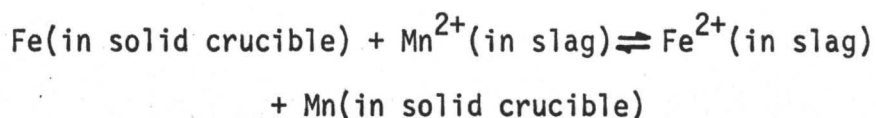
EXPERIMENTAL - THE DENSITIES OF TERNARY SILICATE MELTS CONTAINING IRON OXIDE

6.1 The Replacement of iron oxide in iron silicates by oxides more stable than "FeO".

6.1.1. Introduction

In order to contain a silicate melt in an iron crucible, it is necessary that the equilibrium oxygen pressure of the silicate melt be less than or equal to the partial pressure of oxygen in equilibrium with iron and iron oxide at the temperature of operation. For practical purposes this means that in order to contain liquid silicates of the system MO - "FeO" - SiO₂ in an iron crucible, it is required that MO be more stable than "FeO". As CaO and MnO are more stable, i.e. have a lower equilibrium oxygen pressure, than "FeO", studies of the effects of the replacement of Fe²⁺ ions in iron silicates by Ca²⁺ and Mn²⁺ ions, can be carried out in iron crucibles.

In the case of calcium iron silicates the ionisation potential of the Ca²⁺ ion is low enough to prohibit the occurrence of a detectable exchange reaction between Ca²⁺ ions in the silicate and the iron crucible, but in the case of manganese iron silicates the ionisation potentials of Mn²⁺ and Fe²⁺ are close enough to permit the exchange reaction to occur to an appreciable extent. Thus when a manganese iron silicate is melted in an iron crucible the exchange reaction



proceeds to equilibrium at which point

$$a_{\text{Mn(Fe)}} = a_{\text{Mn(slag)}}$$

and

$$a_{\text{Fe(Fe)}} = a_{\text{Fe(slag)}}$$

However, in view of the short time elapse between density determination and melt sampling, this exchange reaction need not be considered as it can safely be assumed that the density measured is that of the sampled analysed melt.

6.1.2 The System CaO - "FeO" - SiO₂

The liquid phase field occurring in the system CaO-"FeO"-SiO₂, at 1410°C, is shown in Figure 31. In order to check the reproducibility of densities obtained by the maximum bubble pressure method, the density composition relationships along three intersecting composition paths were determined. These paths, shown in Figure 32, were as follows:

- (i) CaO added to an iron silicate containing 27.90 wt.% silica (0.316 mole fraction silica)
- (ii) melts containing 0.29 mole fraction silica
- (iii) melts containing 0.23 mole fraction silica

6.1.2.1. Materials preparation

Iron silicate stock solutions of various silica contents were prepared by dissolving dehydrated silicic acid in liquid wustite contained in inductively heated Armco iron crucibles. The liquid iron silicate produced was quenched onto an iron plate, ground and analysed for silica.

Reagent grade calcium oxide was dried at 120°C for 12 hours and was stored in capped glass bottles. Silica was used in the form of crushed high purity quartz glass.

6.1.2.2. Experimental procedure

The slags for composition path (i) were made up by mixing calcium oxide with a 27.90 weight per cent silica iron silicate and the slags for composition paths (ii) and (iii) were made up by mixing an appropriate iron silicate stock, calcium oxide and crushed quartz in the desired proportions. For each experiment, the slag solution was prepared by melting the constituent mixture in situ prior to its density determination. Homogeneity of the solution was ensured by bubbling the melt at a rate of 60 - 80 bubbles per minute overnight (for a period of 10 hours) before determining the density. The equilibrium partial pressure of oxygen for each slag composition was determined from the data of Bodsworth (49) and the temperature of the de-oxidising copper turnings adjusted accordingly.

The densities obtained for the three composition paths are tabulated in Table VIII and are shown graphically as a function of composition in Figure 33. The calcium oxide contents of the melts were estimated by the ammonium oxalate method of analysis.

6.1.3. The system MnO-"FeO"-SiO₂

The manganese silicate phase diagram has been determined by White, Howat and Hay (51) and more recently by Glasser (101). According to the latter, the field of liquid manganese silicate solutions at 1410°C

extends from 24 weight per cent to 45 weight per cent silica. The liquidus surface of the system $\text{MnO}-\text{FeO}-\text{SiO}_2$ has been determined by von Wentrup (102) and by Maddocks (103). The liquid phase fields at 1410°C , according to these two phase diagrams are shown in Figure 34.

The 0.29 mole fraction composition path was chosen in order to provide direct comparison with the results of the $\text{CaO}-\text{FeO}-\text{SiO}_2$ system. According to Glasser's phase diagram, a manganese silica containing 0.29 mole fraction silica is in the liquid phase field at 1410°C . It must be pointed out, however, that according to the two ternary phase diagrams, this composition lies in the solid manganosite + liquid region at 1410°C . As a result of composition requirements for comparison with calcium iron silicate densities, the 0.29 mole fraction silica composition path was chosen in spite of the ternary phase diagram indications.

6.1.3.1. Preparation of manganous oxide

Manganous oxide was prepared by reducing reagent grade manganese dioxide contained in a nickel boat and placed in a mullite tube with hydrogen at 1000°C for 12 hours. The green MnO so produced was stored in capped glass bottles.

6.1.3.2 Experimental procedure

The experimental procedure was identical with that followed in the determination of the densities of calcium iron silicates. The equilibrium partial pressures of the melt compositions studied were determined from the data of Abraham et al (76) and Bell (104).

The densities obtained are tabulated in Table IX and the density-composition relationship is shown in Figure 35. The manganous oxide

contents of the melts were estimated by the Volhard method of manganese determination.

6.1.4 The system CaF_2 - FeO - SiO_2

The liquid phase field in the system CaF_2 - FeO - SiO_2 at 1410°C is unknown. Thus FeO was replaced in iron silicate by CaF_2 along a constant silica mole fraction composition path until the observation of erratic bubble pressures indicated the existence of two phases in the melt. The composition path with $N_{\text{SiO}_2} = 0.23$ was chosen to allow comparison with the results for the system CaO - FeO - SiO_2 . The reagent grade calcium fluoride used in making up the slag mixtures, was dried at 120°C for 12 hours prior to use.

The results are tabulated in Table X and are shown graphically, in comparison with the results of the calcium iron silicate melts of $N_{\text{SiO}_2} = 0.23$ in Figure 36.

6.2 Replacement of iron oxide in iron silicates by oxides less stable than FeO .

6.2.1. Introduction

Melts in the system MO - FeO - SiO_2 , where MO has a higher oxygen potential than FeO , cannot be contained in an iron crucible. The requirements of a metal for use as a crucible material for such melts are

- (i) that oxide of the metal is less stable than MO
- (ii) that the metal is solid at the temperature of operation.

Pure platinum satisfies these two requirements and hence platinum crucibles and blowing tips were used initially.

6.2.2 Crucibles

The platinum crucibles were 1 in. I. D. x 2 1/2 ins. in depth x 0.025 in. wall thickness and were fitted with platinum wire handles to facilitate their removal from the furnace. Considerable difficulties were encountered with these crucibles due to

- (i) rapid and extensive grain growth of the platinum at 1410°C
- (ii) solution in the platinum of metal from the metal silicates.

In order to re-use the platinum crucibles, at the conclusion of each experiment the crucible was rapidly withdrawn from the furnace by means of a hook, and the slag poured into a heavy brass mould and water-quenched. Residual silicate in the crucible was removed by treatment with hydrofluoric acid and boiling hydrochloric acid. During the first three experiments recrystallisation and considerable grain growth of the platinum was observed and during the fourth experiment, the crucible failed in service. This failure was caused by coarse metal grains (about 1/16 in. in diameter) simply falling out of the base of the crucible. It was considered that the strength of the crucible had been seriously impaired by the hydrochloric acid treatment, which, in addition to dissolving the residual slag, may have caused galvanic corrosion of the crucible at positions which differed in dissolved iron and cobalt content. As a result of this consideration the next crucible was not subjected to hydrochloric acid washing. Instead, each successive silicate composition was made up such that the known weight of the residual slag from the previous run was included in the next slag composition. In spite of this precaution, failure of the second crucible again occurred after four experiments. The problems of grain growth

and solution of iron and cobalt in platinum can be minimised in the following way.

Grain Growth

A dispersion of finely-divided alumina in platinum, by interfering with dislocation and grain boundary movement would be expected to inhibit recrystallisation and grain growth. However, alumina-dispersed platinum could only be produced by powder metallurgy techniques and hence the fabrication of crucibles from this material would be extremely difficult.

Solution of iron and cobalt

The solution of iron and cobalt (and also nickel) in platinum can be minimised by alloying the platinum with a metal, the presence of which increases the activity coefficient of iron and cobalt in the platinum. The alloying element must be such that the oxygen potential corresponding to equilibrium between the alloying element dissolved in the platinum alloy and its oxide is greater than the oxygen potential of the silicate to be contained in the alloy crucible. A suitable alloying element for this purpose is rhodium.

A third crucible of composition 80%Pt - 20%Rh was purchased. This crucible performed satisfactorily and it was found that, in addition to metal solution being eliminated, grain growth was not excessive. It was observed however, that some surface deterioration of the crucible occurred, but this was probably due to the low oxygen potential of the crucible environment.

6.2.3 Blowing tubes

It was intended initially that the blowing tubes for work with

silicates of oxygen potentials greater than that of "FeO" would be constructed from nickel tubes with platinum blowing tips. However, since at that time nickel tubing was in short supply, several tests were made using steel tubes with mild steel welded platinum tips, although it was realised that, at the oxygen partial pressures employed, the atmosphere would be oxidising with respect to the steel. These tubes were found to be serviceable for the duration of one experiment but failed during the second. Failure was due to the formation of a small hole in the weld. The presence of a hole was indicated by the fact that an increased flow rate was required in order to maintain passage of the gas through the melt.

As a first modification, the weld between the steel tube and the platinum tip was made with Hastelloy filler rod. However, this produced no significant improvement as failure now occurred by the formation of a small hole in the steel tubing adjacent to the Hastelloy weld.

As a second modification, the Hastelloy-welded steel tube was sprayed with a "protective metal coating". Three coatings were tested.*

- (i) "BoroTec No. 10009", a nickel-boron-chromium-silicon alloy
- (ii) "CobalTec No. 10091" a cobalt-base alloy, and
- (iii) "TungTec No. 10112" a nickel-base alloy with tungsten carbide particles.

Of the three coatings tests, the "CobalTec No. 10091" appeared to be the most suitable. However, even these coated tubes failed after two experiments.

Eventually, some nickel tubing was obtained⁺ 11/32 in. O.D. x 9/32 in.

* These "protective coating" materials were obtained from Eutectic Welding of Canada Ltd.

⁺ Grateful acknowledgement is made to Dr. L. A. Morris of Falconbridge, Nickel Co. Ltd., who supplied the nickel tubing.

A steel blowing tube containing a silica liner was placed inside a 5-inch length of this nickel tubing, which was then welded top and bottom to the steel tube with Hastelloy filler metal. A Pt-Rh tip was welded to the end of this composite tube using Hastelloy filler rod. This "nickel-coated" steel tube performed satisfactorily for the duration of the investigation.

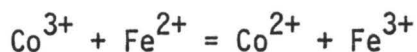
6.2.4 The system CoO-"FeO"-SiO₂

At 1410°C a liquid phase field exists in the CoO-SiO₂ system between 25 and 30 mole per cent silica. The form of the binary phase diagram (105) suggests that the liquidus surface of the ternary system CoO-"FeO"-SiO₂ should be similar to that of the system MnO-"FeO"-SiO₂.

6.2.4.1 Preparation of cobaltous oxide

Cobaltous oxide was prepared by heating reagent grade CoCO₃ in vacuum. The decomposition is complete at 200°C and the oxide produced is bright green in color. After decomposition at 200°C the oxide produced is extremely unstable and rapidly oxidises to black Co₃O₄ when exposed to the atmosphere at room temperature. This oxidation occurs as soon as air is admitted to the vacuum chamber. Relatively stable cobaltous oxide was produced by decomposing the carbonate in vacuum at 200°C and then heating the oxide produced for several hours at 900°C. This treatment produces an oxide which is brownish-cream in colour at room temperature. Analysis of this oxide indicated that it contained 21.7 - 21.8 weight per cent oxygen, which, on a molar basis, corresponds to the presence of 2.1 - 2.8 per cent Co₃O₄. Stoichiometric CoO contains 21.35 weight per cent oxygen. It is desirable to have the cobaltic

ion content as low as possible in order to minimise the occurrence of the reaction.



in the iron cobalt silicate.

6.2.4.2 Experimental procedure

"FeO" in iron silicates was replaced by CoO along the 29 mole per cent silica composition path. The equilibrium oxygen partial pressure for the silicates were calculated by assuming that the constituent binary silicates containing 29 mole per cent silica mix ideally. The activity-composition relationship for CoO in cobalt silicates has been calculated from the phase diagram (106) and the thermodynamic behaviour of the system Co-CoO has been determined by Richardson and Jeffes (100).

The densities obtained for the cobalt iron silicates are tabulated in Table XII and are shown graphically as a function of composition in Figure 37. The cobalt oxide contents of the melts were estimated using the α -nitroso- β -naphthol method of cobalt determination.

6.2.5 The system NiO-"FeO"-SiO₂

Stoichiometric NiO is yellow in colour and contains 21.42 weight per cent oxygen. Commercially available reagent grade NiO is yellowish-green in colour and contains 21.7 - 21.8 weight per cent oxygen, which corresponds, on a molar basis, to the presence of 1.7 - 2.6 per cent Ni₂O₃. Again, as with cobalt oxide, the presence of cations of higher valence is undesirable because of the possible oxidation of

ferrous ions in the nickel iron silicate.

6.2.5.1 Experimental procedure

"FeO" was replaced by NiO along the 29 mole per cent silica composition path. Again, as in the case of cobalt iron silicates, the equilibrium partial pressures of the silicates were calculated assuming ideal mixing of the constituent binary silicates. The activity-composition relationship of NiO in nickel silicates has been calculated from the phase diagram (106) and the thermodynamic behaviour of the system Ni/NiO has been determined by Richardson and Jeffes (100).

The densities obtained for the nickel-iron silicates are tabulated in Table XIII and are shown graphically as a function of composition in Figure 38. The nickel oxide contents of these melts was estimated using the dimethylglyoxime method of nickel determination.

CHAPTER 7
EXPERIMENTAL RESULTS

All densities were measured at 1410°C.

7.1 "FeO"

The values of the density of liquid iron oxide in contact with solid iron, obtained by bubbling helium, nitrogen and argon, and the analysed total iron contents of the melts are listed in Table VI.

7.2 The system "FeO"-SiO₂

The densities of twelve iron silicates were measured, nine of these by bubbling argon, two by bubbling nitrogen and one by bubbling helium. The composition range covered extended from zero weight per cent silica to 33.62 weight per cent silica. Silica saturation at 1410°C occurs at 40.5 weight per cent silica. The densities obtained are listed in Table VII and the density-composition relationship is shown graphically in Figure 30.

7.3 The system CaO-"FeO"-SiO₂

Because of the limited extent of the liquid phase field in the system CaO-"FeO"-SiO₂ at 1410°C, the replacement of "FeO" in iron silicates by CaO was restricted to less than 30 mole per cent. The densities of fifteen compositions in the ternary system were measured. These compositions were located on the three intersecting composition paths shown in Figure 32. The results obtained are listed in Table IX and

the three density-composition relationships are shown graphically in Figure 33.

Comparison of Figures 32 and 33 shows that the composition cross-over points of the three composition paths occur at 9 and 28 mole per cent CaO whereas the corresponding density-composition curves intersect at 12 and 25 mole per cent CaO respectively. However, in view of the low rate of change of density with CaO concentration these differences are considered to be insignificant.

7.4 The system MnO-"FeO"-SiO₂

Eight melts in the system MnO-"FeO"-SiO₂ were investigated. Each of these melts contained 29 mole per cent silica. It was found that a mixture of 73 weight per cent MnO and 27 weight per cent SiO₂ (29 mole per cent SiO₂) failed to liquify completely at 1410°C. 48 hours were allowed for solution to occur, after which time the crucible was withdrawn from the furnace and quenched. Inspection showed that partial melting had occurred but it appeared that this composition was in the solid + liquid region at 1410°C, in accordance with the ternary phase diagrams of von Wentrup (102) and Maddocks (103). The results obtained are listed in Table X and the density-composition relationship is shown graphically in Figure 35.

7.5 The system CaF₂-"FeO"-SiO₂

The densities of two melts, containing nominally 5 and 10 mole per cent CaF₂ and 23 mole per cent SiO₂ were measured. A third melt containing 15 mole per cent CaF₂ failed to form a single liquid. The densities obtained and the nominal compositions are listed in Table XI.

The density-composition relationship, together with the data for the corresponding concentration path in the $\text{CaO}-\text{FeO}-\text{SiO}_2$ system are shown in Figure 36.

7.6 The system $\text{CoO}-\text{FeO}-\text{SiO}_2$

Seven melts in the system $\text{CoO}-\text{FeO}-\text{SiO}_2$ were investigated. Each of these melts contained 29 mole per cent silica and CoO in the range 0 - 40 mole per cent. An eighth melt containing 50 mole per cent CoO failed to liquify completely. The fact that this composition was in the solid + liquid phase region at 1410°C was verified by visual observation of a solid phase at the bottom of the crucible when the crucible contents were quenched in the brass mould. The results are tabulated in Table XII and are shown graphically in Figure 37.

7.7 The system $\text{NiO}-\text{FeO}-\text{SiO}_2$

Density measurements were made on two melts containing 9.5 and 18.7 mole per cent nickel oxide and 29 mole per cent silica. A third melt containing 30 mole per cent NiO and 29 mole per cent silica failed to liquify completely. Again, as in the case of the 50 mole per cent CoO composition, a solid phase was observed at the bottom of the crucible. The results are listed in Table XIII and are shown graphically in Figure 38.

Figure 39 shows how the density of an iron silicate melt containing 29 mole per cent silica is changed as the iron oxide is gradually replaced by CaO, MnO, CoO and NiO.

| Bubbling gas | Density gms/cc. | Error limite 2σ | Total Iron wt% (analysed) |
|--|--------------------|---------------------------|------------------------------|
| He | 4.57 | ± 0.03 | 77.6 |
| Ar | 4.55 | ± 0.02 | 77.7 |
| N ₂ (1) | 4.61 | ± 0.03 | 77.2 |
| N ₂ (2) | 4.60 | ± 0.03 | - |
| Calculated total iron content of iron oxide in equilibrium with solid iron at 1410°C is 77.18 wt. per cent (69). | | | |
| Iron analyses are estimated to be accurate to ± 0.07 wt. per cent. | | | |

TABLE VI Density of Liquid Iron oxide in contact with solid iron at 1410°C Bubbling Helium, Argon and Nitrogen

| Bubbling Gas | Density gms/cc | Error Limit 2σ | SiO ₂ wt. pct. (analysed) | Oxygen Density $\times 10^{-20}$ |
|----------------|----------------|-----------------------|--------------------------------------|----------------------------------|
| Ar | 4.55 | ± 0.02 | nil | 381 |
| Ar | 4.37 | ± 0.03 | 4.83 | 391 |
| N ₂ | 4.20 | ± 0.03 | 9.94 | 401 |
| He | 4.20 | ± 0.03 | 9.94 | 401 |
| Ar | 4.19 | ± 0.04 | 10.67 | 404 |
| Ar | 4.09 | ± 0.03 | 13.95 | 410 |
| N ₂ | 4.04 | ± 0.04 | 14.48 | 407 |
| Ar | 3.95 | ± 0.03 | 18.83 | 418 |
| Ar | 3.84 | ± 0.04 | 23.08 | 426 |
| Ar | 3.78 | ± 0.03 | 25.46 | 430 |
| Ar | 3.75 | ± 0.02 | 26.97 | 433 |
| Ar | 3.73 | ± 0.02 | 27.90 | 435 |
| Ar | 3.62 | ± 0.02 | 33.62 | 446 |

Silica analyses are estimated to be accurate to ± 0.05 wt. pct.

TABLE VII Densities of Iron Silicates in contact with Solid Iron at 1410°C

| Blowing gas | Total iron wt.% Crucible sample | Total iron wt.% Aspirator Sample | Density, gms/cc |
|-------------|------------------------------------|-------------------------------------|--------------------|
| Ar | 77.69 | 76.47 | 4.55 |
| He | 77.63 | 71.88 | 4.57 |

TABLE VIII Analyses of iron oxide melt samples

TABLE IX Densities of calcium-iron-silicates in contact with solid iron at 1410°C

(i) CaO added to iron silicate containing initially 31.6 mole per cent silica

| Density gms/cc | Error 2σ | Weight Per Cent | | | Mole Fraction | | | Oxygen Density $\times 10^{-20}$ |
|-------------------|--------------------|------------------|-------|-------|------------------|--------|--------|-------------------------------------|
| | | SiO ₂ | CaO | "FeO" | SiO ₂ | CaO | "FeO" | |
| 3.73 | ± 0.02 | 27.90 | nil | 72.10 | 0.3163 | nil | 0.6837 | 434 |
| 3.63 | ± 0.02 | 26.45 | 4.91 | 68.64 | 0.2968 | 0.0591 | 0.6441 | 420 |
| 3.55 | ± 0.01 | 25.94 | 10.30 | 63.76 | 0.2873 | 0.1222 | 0.5905 | 414 |
| 3.52 | ± 0.02 | 24.88 | 14.30 | 60.82 | 0.2732 | 0.1683 | 0.5586 | 409 |
| 3.49 | ± 0.02 | 23.20 | 19.05 | 57.75 | 0.2524 | 0.2221 | 0.5255 | 403 |
| 3.46 | ± 0.02 | 22.08 | 23.95 | 53.97 | 0.2377 | 0.2763 | 0.4860 | 399 |

(ii) 29 mole per cent silica

| Density gms/cc | Error 2σ | Weight per cent | | | Mole Fraction | | | Oxygen Density $\times 10^{-20}$ |
|-------------------|--------------------|------------------|-------|-------|------------------|--------|--------|-------------------------------------|
| | | SiO ₂ | CaO | "FeO" | SiO ₂ | CaO | "FeO" | |
| 3.78 | ± 0.03 | 25.46 | nil | 74.54 | 0.29 | nil | 0.71 | 429 |
| 3.67 | ± 0.03 | 26.50 | 4.33 | 69.17 | 0.2978 | 0.0521 | 0.6501 | 425 |
| 3.58 | ± 0.02 | 26.51 | 8.62 | 64.87 | 0.2945 | 0.1026 | 0.6028 | 418 |
| 3.51 | ± 0.03 | 27.64 | 12.55 | 49.81 | 0.3034 | 0.1476 | 0.5491 | 418 |
| 3.44 | ± 0.02 | 28.13 | 16.64 | 55.23 | 0.3053 | 0.1935 | 0.5012 | 415 |
| 3.36 | ± 0.02 | 27.29 | 21.56 | 51.13 | 0.2929 | 0.2480 | 0.4591 | 406 |

(iii) 23 mole per cent silica

| Density gms/cc | Error 2σ | Weight per cent | | | Mole Fraction | | | Oxygen Density $\times 10^{-20}$ |
|-------------------|--------------------|------------------|-------|-------|------------------|--------|--------|-------------------------------------|
| | | SiO ₂ | CaO | "FeO" | SiO ₂ | CaO | "FeO" | |
| 3.92 | ± 0.02 | 19.96 | nil | 80.04 | 0.2297 | nil | 0.7703 | 420 |
| 3.80 | ± 0.02 | 19.68 | 4.95 | 73.37 | 0.2236 | 0.0603 | 0.7161 | 410 |
| 3.72 | ± 0.02 | 20.23 | 8.61 | 71.16 | 0.2274 | 0.1037 | 0.6689 | 407 |
| 3.64 | ± 0.02 | 20.86 | 12.78 | 66.36 | 0.2316 | 0.1521 | 0.6163 | 405 |
| 3.56 | ± 0.02 | 21.12 | 16.72 | 62.16 | 0.2321 | 0.1968 | 0.5711 | 400 |
| 3.47 | ± 0.02 | 22.15 | 21.42 | 56.43 | 0.2400 | 0.2487 | 0.5113 | 398 |

SiO₂ gravimetric analyses are accurate to ± 0.05 weight per cent.CaO volumetric analyses are accurate to ± 0.15 weight per cent.

"FeO" was obtained by difference.

TABLE X Densities of manganese iron silicate in contact with solid iron at 1410°C

| Density gms/cc | Error 2σ | Weight Per Cent | | | Mole Fraction | | | Oxygen Density $\times 10^{-20}$ |
|------------------------------|--------------------|------------------|-------|-------|------------------|--------|--------|-------------------------------------|
| | | SiO ₂ | MnO | "FeO" | SiO ₂ | MnO | "FeO" | |
| 3.76 | ± 0.02 | 26.15 | nil | 73.85 | 0.2975 | nil | 0.7025 | 427 |
| 3.72 | ± 0.02 | 25.63 | 5.06 | 79.31 | 0.2916 | 0.0488 | 0.6596 | 423 |
| 3.69 | ± 0.01 | 26.93 | 10.31 | 62.76 | 0.3055 | 0.0991 | 0.5954 | 420 |
| 3.68 | ± 0.02 | 26.85 | 14.56 | 58.59 | 0.3045 | 0.1399 | 0.5556 | 419 |
| 3.67 | ± 0.02 | 25.17 | 19.10 | 55.73 | 0.2862 | 0.1840 | 0.5298 | 418 |
| 3.69 | ± 0.03 | 24.62 | 29.23 | 46.15 | 0.2798 | 0.2815 | 0.4387 | - |
| 3.67 | ± 0.02 | 24.89 | 39.24 | 35.87 | 0.2824 | 0.3772 | 0.3404 | 419 |
| 3.65 | ± 0.02 | 24.98 | 50.11 | 24.91 | 0.2830 | 0.4810 | 0.2360 | 417 |
| 3.65 | ± 0.02 | 25.47 | 59.29 | 15.24 | 0.2880 | 0.5679 | 0.1441 | 418 |
| Would not liquify completely | | | | | 0.29 | 0.71 | nil | - |

| DENSITY gms/cc | ERROR 2σ | Nominal Mole Fraction | | |
|----------------------------------|--------------------|-----------------------|------------------|--------|
| | | SiO ₂ | CaF ₂ | "FeO" |
| 3.92 | ± 0.02 | 0.2297 | nil | 0.7703 |
| 3.80 | ± 0.02 | 0.23 | 0.05 | 0.72 |
| 3.67 | ± 0.02 | 0.23 | 0.10 | 0.67 |
| would not liquidfy completely | | 0.23 | 0.15 | 0.62 |

TABLE XI Densities of calcium iron fluorosilicates in contact with solid iron at 1410°C.

| Density gms/cc | Error 2σ | Weight Per Cent | | | Mole Fraction | | | Oxygen Density x 10 ⁻²⁰ |
|------------------------------|--------------------|------------------|-------|-------|------------------|--------|--------|---------------------------------------|
| | | SiO ₂ | CoO | "FeO" | SiO ₂ | CoO | "FeO" | |
| 3.75 | ± 0.02 | 26.10 | nil | 73.90 | 0.2969 | nil | 0.7031 | 426 |
| 3.74 | ± 0.02 | 25.57 | 4.43 | 70.00 | 0.2917 | 0.0405 | 0.6678 | 425 |
| 3.75 | ± 0.02 | 25.09 | 10.13 | 64.78 | 0.2871 | 0.0930 | 0.6200 | 423 |
| 3.77 | ± 0.02 | 24.11 | 13.11 | 61.78 | 0.2877 | 0.1204 | 0.5919 | 425 |
| 3.76 | ± 0.02 | 25.20 | 17.11 | 57.69 | 0.2891 | 0.1574 | 0.5535 | 424 |
| 3.80 | ± 0.02 | 24.98 | 26.52 | 48.50 | 0.2878 | 0.2450 | 0.4673 | 426 |
| 3.78 | ± 0.03 | 24.14 | 29.71 | 46.15 | 0.2788 | 0.2755 | 0.4458 | 420 |
| 3.84 | ± 0.02 | 24.68 | 42.37 | 32.95 | 0.2863 | 0.3941 | 0.3196 | 428 |
| would not liquify completely | | | | | 0.29 | 0.50 | 0.21 | |

SiO₂ gravimetric analysis are accurate to ± 0.05 weight per cent.

CoO gravimetric analyses are accurate to ± 0.05 weight per cent.

"FeO" was obtained by difference.

TABLE XII Densities of cobalt iron silicates at 1410°C.

| Density gms/cc | Error 2σ | Weight Per Cent | | | Mole Fraction | | | Oxygen Density $\times 10^{-20}$ |
|------------------------------|--------------------|------------------|-------|-------|------------------|--------|--------|-------------------------------------|
| | | SiO ₂ | NiO | "FeO" | SiO ₂ | NiO | "FeO" | |
| 3.75 | ± 0.02 | 26.10 | nil | 73.90 | 0.2969 | nil | 0.7031 | 426 |
| 3.74 | ± 0.02 | 25.10 | 10.34 | 64.56 | 0.2872 | 0.0951 | 0.6177 | 422 |
| 3.77 | ± 0.04 | 25.38 | 20.29 | 54.33 | 0.2913 | 0.1873 | 0.5214 | 425 |
| would not liquify completely | | | | | 0.29 | 0.30 | 0.41 | - |

SiO₂ gravimetric analyses are accurate to ± 0.05 weight per cent.

NiO gravimetric analyses are accurate to ± 0.05 weight per cent.

"FeO" was obtained by difference.

TABLE XIII Densities of nickel iron silicates at 1410°C.

CHAPTER 8
DISCUSSIONS

8.1 The systems "FeO" and "FeO"-SiO₂

In the present work it has been shown that (i) by ensuring equilibrium between iron and the iron oxide or iron silicate melt with respect to the oxygen content of the gas phase, (ii) by minimising temperature variation in the melt-crucible system, and (iii) by preventing surface cooling of the melt, the previously reported effect of blowing gas composition on the measured densities of liquid iron oxide and liquid iron silicates has been eliminated (97). The elimination of this effect is attributed directly to the prevention of iron precipitation in the melt. Henderson (107) has calculated the magnitude of the effect of the formation of a ring of dendritic iron at the melt surface on the location of the melt surface (i.e. on the depth of immersion of the blowing tube) for helium blown iron oxide melts. These calculations were made from observations of the meniscus position in sectioned, quenched crucibles. It was found that the ratio of the rate of change of measured bubble pressure with depth of immersion to the rate of change of measured bubble pressure with corrected depth of immersion was 5.05/4.55. The value for the density of a helium-blown iron oxide melt at 1410°C, previously reported as 5.05 gms/cc, was thus 4.55 gms/cc. This is in exact agreement with the value obtained experimentally in the present investigation and while this is perhaps fortuitous, the calculation nevertheless demonstrates the magnitude of the effect of an alteration in the crucible-

melt geometry, brought about by iron precipitation, on the measured density of the melt.

The density-composition relationship obtained for the iron silicate system is shown in Figure 30, together with a calculated density-composition relationship for mechanical mixtures of iron oxide (density 4.55 gms/cc) and silica (density 2.20 gms/cc). In this calculation, the composition of "FeO", and hence the density of "FeO", in the mixture is assumed to be independent of the silica content of the mixture. In the actual silicate solution, however, the ratio of $\text{Fe}^{3+}/\text{Fe}^{2+}$ in the "FeO" decreases with increasing silica content. In the density-composition curve for the actual solutions, distinction cannot be made between the possible effect of the decreasing ferric ion content and the effect of the increasing silica content on the measured density, and hence the two density-composition relationships shown in Figure 30 are not strictly comparable. Comparison can only be made if it is assumed that the effect of the varying ferric ion content on the actual density of the silicate melt is negligible in comparison with the effect of the varying silica content.

8.2 The Oxygen Density

The difference between the behaviour of the actual solution and the behaviour of the mechanical mixtures is seen in more fundamental terms when the oxygen density is considered. The oxygen-density is the number of oxygen atoms, present as doubly-bonded, singly-bonded or free oxygen ions, in one cubic centimeter of melt, and is given as (108)

$$\text{oxygen density} = \frac{\rho \cdot A \cdot N_{\text{O}}}{\text{M.W.}}$$

where ρ is the density of the melt in gms/cc

A is Avogadro's Number

N_o is the mole fraction of oxygen atoms in the melt

and MW is the molecular weight of the melt

In the case of iron silicate, $N_o = (N_{FeO} \times 1) + (N_{SiO_2} \times 2)$

and $M.W. = (N_{FeO} \times MW_{FeO}) + (N_{SiO_2} \times M.W. SiO_2)$

The oxygen density of a melt of given composition is a measure of the efficiency with which the oxygen atoms are packed in the structure. Hence, the variation of oxygen density with composition would be expected to provide an indication of the changes in structural configuration accompanying composition change. The oxygen density-composition relationships occurring in iron silicate melts and in the mechanical mixtures are shown in Figure 40 and the difference between these two relationships is shown as a function of silica concentration in Figure 41. For the purpose of calculating the oxygen densities plotted in Figure 40, the solutions were considered to be in the pseudo-binary system "FeO"- SiO_2 . In fact the form of the difference curve in Figure 41 is independent of whether the solutions are regarded as being in the pseudo-binary system "FeO"- SiO_2 or whether they are regarded as being in the ternary system $FeO-Fe_2O_3-SiO_2$.

Figure 41 indicates that a gradual increase in the efficiency of packing of oxygen atoms occurs in the melt with increasing silica content. However, consideration of the oxygen density difference-composition relationship alone does not allow differentiation to be made between this increasing efficiency being due to better packing of small anionic entities in the melt or to an increase in the average anion size,

i.e. an increase in the degree of polymerisation. Consideration of the models of Toop and Samis (61) and Masson (67) suggests that the latter is the case, i.e. that the increasing efficiency of oxygen packing with increasing silica content is the result of an increasing degree of polymerisation in the melt.

According to the models of Toop and Samis and Masson, the degree of polymerisation occurring in a binary silicate melt is dependent on (i) the silica concentration and (ii) the cationic species and (iii) the temperature. In the present investigation, measurement was made of the densities of ternary silicate melts in which the mole fraction of silica and the temperature were maintained constant. In effect this constitutes iso-thermal replacement of the Fe^{2+} ions in an iron silicate by other cations.

In the system $\text{CaO}-\text{FeO}-\text{SiO}_2$ three intersecting composition paths were studied, principally to provide a check on the reproducibility of the experimental data. The oxygen density-composition relationships of these three composition paths are shown in Figure 42, and the oxygen density-composition relationships resulting from the replacement of Fe^{2+} ions in an iron silicate by Mn^{2+} , Co^{2+} and Ni^{2+} ions along the $N_{\text{SiO}_2} = 0.29$ composition path are shown in Figures 43, 44 and 45 respectively.

In the interpretation of the variation of oxygen density with cation replacement, it is desirable to compare the oxygen densities of the actual solutions with the oxygen densities of the corresponding

mechanical mixtures. However, in order to calculate the density, and hence the oxygen density, of the mechanical mixtures, a knowledge is required of (i) the density-composition relationship of iron silicate melts across the entire binary and (ii) the density of the pure metal oxide which is replacing "FeO", when in the hypothetical liquid state at 1410°C. (the oxides CaO, MnO, CoO and NiO are solid at 1410°C). As the density-composition relationship of iron silicate melts is known only up to silica saturation (44.9 mole per cent SiO₂ at 1410°C) the densities of mechanical mixtures along the ternary composition path between 35 and 70 mole per cent MO cannot be calculated directly. They would require extrapolation of the data obtained in the concentration-range .0 to 36 mole per cent MO. The density-temperature relationships of liquid CaO, MnO, CoO and NiO are not known, nor are the volume changes which accompany melting of these oxides. Indeed, of the four oxides, only the thermal expansivity of CaO has been accurately determined in the solid state (110). Tabulated values of the densities of these oxides even in the solid state vary considerably (109 - 112).

In view of the difficulty of calculating the oxygen densities of mechanical mixtures a different approach must be adopted in order to facilitate interpretation of the variation of the oxygen density of the actual solutions with change in composition. The approach adopted is based on the concept of oxygen density deviation.

8.3 Oxygen Density Deviation

The oxygen density deviation is simply the difference between the oxygen density of the ternary silicate and the oxygen density of the

corresponding iron silicate. In using the concept of oxygen density deviation, the assumption is made that the oxygen density of a silicate melt is a function only of the anionic configuration of the melt, i.e. is determined only by the degree of polymerisation occurring in the melt. It is evident that this assumption is not strictly valid as the replacement of ferrous ions by larger or smaller cations would be expected to produce a decrease or increase in the oxygen density due to dilation or contraction of the structure. The extent of this dilation or contraction, however, is considered to be negligible as the difference between the volumes of the ferrous ion and the replacing cations in the melt is extremely small in comparison with the volume occupied by the silicate anions.

Thus, the oxygen density deviation is considered to be due entirely to the effect of the cation replacement on the anionic configuration of the melt, i.e. on the degree of polymerisation of the melt. The direction of the oxygen density deviation indicates the direction in which the polymerisation reaction is proceeding as a result of cation replacement. A decrease in oxygen density (corresponding to a negative oxygen density deviation) indicates a decrease in the packing efficiency of oxygen atoms and implies that depolymerisation is occurring. Conversely an increase in oxygen density (corresponding to a positive oxygen density deviation) indicates an increase in the packing efficiency of oxygen atoms and hence an increase in the degree of polymerisation.

8.4 The Masson Model

Before examining the oxygen density deviations occurring in the systems studied in the present investigation it is of interest to

examine the constituent binary silicate systems in terms of the Masson model. Figure 46 shows the activity-composition relationships of metal oxides in the systems CaO-SiO_2 , MnO-SiO_2 , FeO-SiO_2 , CoO-SiO_2 and NiO-SiO_2 . From the Masson model, k values of 0.003, 0.75, 1.4, 3.33 and 46 respectively are obtained for these systems. The k values allow the theoretical anionic distributions to be calculated and these are shown as plots of N_{Silicate} against $N_{\text{O}^{2-}}$, for each of the five binary systems in Figure 47. In each plot the distribution of anions occurring at $N_{\text{SiO}_2} = 0.29$ is indicated and the mole fractions of each of these anions are listed in Table XIV.

As can be seen from Figure 47 and Table XIV, the value of k for a particular binary system gives a comparative measure of the degree of polymerisation occurring at any composition. Hence, in a ternary silicate system comprising any two of these binaries, comparison of the k values for the binary systems give an indication of the direction in which the polymerisation reaction will proceed as the composition moves from one binary along a path of constant silica content across the ternary to the other binary system. Specifically, on the replacement of Fe^{2+} ions in an iron silicate by Ca^{2+} and Mn^{2+} ions a depolymerisation of the constituent anions is predicted, Ca^{2+} ions effecting a greater depolymerisation than Mn^{2+} ions. On the other hand, when Fe^{2+} ions are replaced by Co^{2+} and Ni^{2+} ions an increase in the degree of polymerisation is predicted and the effect of Ni^{2+} in this respect will be greater than the effect of Co^{2+} .

| System | k | $N_{O^{2-}}$ | $N_{SiO_4^{4-}}$ | $N_{Si_2O_7^{6-}}$ | $N_{Si_3O_{10}^{8-}}$ | $N_{Si_4O_{13}^{10-}}$ | $N_{Si_5O_{16}^{12-}}$ | $\Sigma N_{\text{higher than } Si_5}$ |
|----------------------|-------|--------------|------------------|--------------------|-----------------------|------------------------|------------------------|---------------------------------------|
| CaO-SiO ₂ | 0.003 | 0.3141 | 0.6814 | 0.0045 | - | - | - | - |
| MnO-SiO ₂ | 0.75 | 0.5633 | 0.2761 | 0.1015 | 0.0373 | 0.0137 | 0.0050 | 0.0031 |
| FeO-SiO ₂ | 1.4 | 0.6241 | 0.2039 | 0.0932 | 0.0426 | 0.0195 | 0.0089 | 0.0078 |
| CoO-SiO ₂ | 3.33 | 0.7085 | 0.1230 | 0.1230 | 0.0711 | 0.0411 | 0.0238 | 0.0187 |
| NiO-SiO ₂ | 46 | 0.8935 | 0.0164 | 0.0138 | 0.0117 | 0.0099 | 0.0084 | 0.0463 |

FIGURE XIV Mole fraction of anions theoretically present in various binary silicate systems when $N_{SiO_2} = 0.29$

8.5 Comparison between actual and predicted behaviour

Figure 42 shows that the replacement of Fe^{2+} ions by Ca^{2+} ions along the composition paths shown in Figure 32, effects a decrease in oxygen density. This indicates that the replacement of Fe^{2+} ions by Ca^{2+} ions produces depolymerisation. In the case of the composition path obtained by adding CaO to iron silicate containing initially 31.6 mole per cent silica, in addition to Ca^{2+} ions replacing Fe^{2+} ions, the silica content of the melts is decreasing. Both of these factors effect a depolymerisation. From a consideration of the oxygen density-composition relationship in iron silicates, shown in Figure 40, it is possible to subtract from the oxygen densities of melts on the above ternary composition path, that contribution which is due to the decreasing silica content. This allows the contribution to the oxygen density deviation due to the replacement of Fe^{2+} ions by Ca^{2+} ions to be isolated. In this calculation it is assumed that the effect of the $\text{Ca}^{2+}/\text{Fe}^{2+}$ ratio and the effects of the silica content on the degree of polymerisation occurring in the melt are independent of one another, i.e. that there is no interaction effect between these two factors. The oxygen density deviations due to replacement of Fe^{2+} ions by Ca^{2+} ions along the three composition paths are shown in Figure 48.

In the case of the $N_{\text{SiO}_2} = 0.29$ composition path in the system MnO-"FeO"- SiO_2 it is seen from Figure 43 that the oxygen density decreases smoothly with cation replacement until 0.18 mole fraction MnO is present. Thereafter, the oxygen density remains constant. The oxygen density deviations due to Ca^{2+} and Mn^{2+} replacement along the $N_{\text{SiO}_2} = 0.29$ composition path are shown in Figure 49, and it is evident that the

direction and relative magnitudes of the oxygen-density deviations are in agreement with the predictions of the Masson model. The constant oxygen density deviation in the system MnO-"FeO"-SiO₂ when $N_{\text{MnO}} > 0.18$ is surprising as a priori reasoning would suggest that the oxygen density should decrease across the entire ternary. Whether or not the oxygen density deviation in the system CaO-"FeO"-SiO₂ would eventually become constant cannot be determined because of the limited extent of the liquid phase field along the $N_{\text{SiO}_2} = 0.29$ composition path.

The limited extents of the liquid phase field along the $N_{\text{SiO}_2} = 0.29$ composition paths in the systems CoO-FeO-SiO₂ and NiO-FeO-SiO₂ prevent determination of whether or not the oxygen density deviation after remaining constant over an initial composition range of cation replacement, becomes positive, in accordance with prediction, and in agreement with the observed effect of the replacement of Mn²⁺ ions by Fe²⁺ ions in manganese-iron silicates.

It thus appears that polymerisation-depolymerisation is not symmetrical along iso- N_{SiO_2} composition paths. Although an immediate depolymerisation occurs when a cation of higher ionisation potential is replaced in its binary silicate system by a cation of lower ionisation potential, immediate increase in the degree of polymerisation does not occur when a cation of lower ionisation potential is replaced in its binary silicate system by a cation of higher ionisation potential.

8.6 The activity of free oxygen ions and the oxygen density

Using experimentally determined data for the activity of iron oxide in the system CaO-FeO-SiO₂ (113) and the values of $a_{\text{Fe}^{2+}}$ in this

system calculated from their model, Toop and Samis have determined the iso-oxygen ion activity lines in the system CaO-FeO-SiO_2 at 1600°C by means of the relationship

$$a_{\text{O}^{2-}} = \frac{a_{\text{FeO}}}{a_{\text{Fe}^{2+}}}$$

These iso- $a_{\text{O}^{2-}}$ lines are shown in Figure 50, and, as can be seen, along iso- N_{SiO_2} composition paths, from the iron silicate binary to the calcium silicate binary, the value of $a_{\text{O}^{2-}}$ decreases smoothly over an initial composition range and then becomes constant. The value of N_{CaO} at which $a_{\text{O}^{2-}}$ becomes constant along iso- N_{SiO_2} composition paths increases with increasing N_{SiO_2} . If it can be assumed that $a_{\text{O}^{2-}}$ is a measure of the actual numbers of free oxygen ions present in the melt, then this behaviour indicates that, in the initial composition range of cation replacement, the number of free oxygen ions present decreases, and that, at some point along the iso- N_{SiO_2} path, the number of free oxygen ions present becomes constant. Hence, as the number of free oxygen ions in the melt is determined by the degree of polymerisation occurring, this behaviour is in agreement with the trend of the oxygen density deviations.

8.7 The activities of metal oxides in ternary silicate melts

The positive deviations from ideality of a_{FeO} in the system CaO-FeO-SiO_2 are well known. Figure 51(a) shows the experimentally determined iso-activity lines for "FeO" in this system at 1365°C due to Bodsworth (49), and Figure 51(b) shows the variation of a_{FeO} with N_{FeO} along the $N_{\text{SiO}_2} = 0.29$ composition path. The replacement of Fe^{2+} ions in an iron silicate by Ca^{2+} ions results in a depolymerisation of

the silicate anions and this is accompanied by a decrease in the number of free oxygen ions present in the melt. Consideration of Temkins' Rule suggests that if all the ions present are behaving ideally, i.e. are considered to be ideally mixed on their respective quasi-lattices, then since the ionic fractions of both Fe^{2+} and O^{2-} are decreasing, the former due to Ca^{2+} ion replacement and the latter due to depolymerisation, a_{FeO} , as given by the product $N_{\text{Fe}^{2+}} \cdot N_{\text{O}^{2-}}$ would follow line A shown in Figure 51(b). Line B in Figure 51(b) represents the ideal decrease in a_{FeO} due to Ca^{2+} replacement if no change in the degree of polymerisation occurs, i.e. if $N_{\text{O}^{2-}}$ remains constant across the ternary. The deviation of these melts from ideality indicates the existence of appreciable ionic interaction. In view of the decrease in the degree of polymerisation, it is evident that the magnitude of this interaction is considerably greater than has been considered hitherto, i.e. than apparently occurs if the change in degree of polymerisation is not considered.

The magnitude of the deviation from ideality of a_{FeO} can be correlated with the relative degrees of polymerisation occurring in the constituent binary silicate systems. Figure 52 shows the iso- a_{FeO} lines in the system CaO-FeO-SiO_2 at 1600°C due to Elliot (113) and the iso- a_{FeO} lines in the system MnO-FeO-SiO_2 at 1550°C due to Bell (104). As can be seen the magnitude of the deviation from ideality in the system CaO-FeO-SiO_2 is greater than in the system MnO-FeO-SiO_2 . This is related to the postulate that for any given silica content, the degree of polymerisation occurring in the binary system decreases in the order FeO-SiO_2 , MnO-SiO_2 , CaO-SiO_2 . From a consideration of these differing degrees of

polymerisation in the binary systems, it would be expected that the magnitude of the deviation from ideality of a_{MnO} in the system CaO-MnO-SiO₂ would lie between the magnitude of the deviation from ideality of a_{FeO} in the system CaO-FeO-SiO₂ and the magnitude of the deviation from ideality of a_{FeO} in the system MnO-FeO-SiO₂. Calculations by Carter (114) have shown this to be the case.

8.8 Ionic interactions in binary and ternary silicate melts

If no polymerisation occurred in basic binary silicate melts, i.e. if the only anionic species present were O^{2-} and SiO_4^{4-} , then at any composition, the ratio of free oxygen ions to oxygen atoms singly bonded to silica (O^{2-}/O^-) would be a minimum. The suggestion that this ratio should be a minimum originally resulted from a consideration of the coulombic energies of the bonds Si-O and M-O, i.e. as the coulombic energy of the bond Si-O is greater than that of the M-O bond, where M^{2+} is a basic cation, then the only free oxygen ions present in the melt were those occurring in excess of the requirement of complete SiO_4^{4-} formation. If polymerisation does occur in a basic binary silicate melt, then the ratio O^{2-}/O^- increases and the occurrence of a ratio of O^{2-}/O^- greater than its minimum value cannot be explained solely in terms of the relative coulombic energies of the bonds Si-O and M-O. A criterion of interest is the difference between the "bond strength" of the cation and a free oxygen ion and the "bond strength" of the cation and a singly bonded oxygen. For polymerisation to occur the strength of the $\text{M}^{2+}-\text{O}^{2-}$ bond must be greater than that of the $\text{M}^{2+}-\text{O}^-$ bond, and in terms of the coulombic energy of these bonds, which is proportional to the product of the ionic charges, this is seen to be the case. If, however, the relative bonds strength of $\text{M}^{2+} - \text{O}^{2-}$ and $\text{M}^{2+} - \text{O}^-$

were the only criterion then the basic oxide and silica would be mutually insoluble, corresponding to a maximum (infinite) value of O^{2-}/O^- in the co-ordination shell of the cation. It is suggested that the completely depolymerised state represents the state of maximum configurational entropy and thus the degree of polymerisation occurring in the binary melt occurs as the result of a balance between the co-ordination requirements of the cation for the possible anions, which is determined by the relative energies of the bonds $M^{2+}-O^{2-}$ and $M^{2+}-O^-$ and the decrease in entropy of the system due to the polymerisation. For example, when an Fe^{2+} ion in an iron silicate is replaced by a Ca^{2+} ion, the above-mentioned balance occurring in the iron silicate is upset and depolymerisation occurs. It is suggested that this depolymerisation proceeds in accordance with the following scheme. As the degree of polymerisation occurring in a calcium silicate is less than that occurring in the corresponding iron silicate the O^{2-}/O^- ratio is correspondingly less in the calcium silicate and thus when an Fe^{2+} ion in an iron silicate is replaced by a Ca^{2+} ion, the Ca^{2+} attempts to effect a decrease in the ratio O^{2-}/O^- in its vicinity. The bond strength between Ca^{2+} and either O^{2-} or O^- is greater than the strengths of either the $Fe^{2+}-O^{2-}$ or $Fe^{2+}-O^-$ bonds (due to the difference in ionisation potential of the cations) and hence the Ca^{2+} ion is dominant in determining the ionic configuration in its vicinity or co-ordination shell. The decrease in the O^{2-}/O^- ratio in the vicinity of the Ca^{2+} ion is effected by means of the Ca^{2+} being co-ordinated mainly by silicate ions. Thus when an appreciable number of Ca^{2+} ions are present, each of which is co-ordinated by a preponderance of silicate anions, the Fe^{2+} ions are co-ordinated by

a preponderance of free oxygen ions in an attempt to maintain the O^{2-}/O^- ratio occurring in the iron silicate. The replacement of Fe^{2+} ions by Ca^{2+} ions increases this Ca^{2+} - silicate ion/ $Fe^{2+}-O^{2-}$ preferred association to such an extent that the activity of iron oxide actually increases initially (Figure 51(b)) and only begins to decrease when the effect of the overall decreased concentration of Fe^{2+} and O^{2-} ions in the melt outweighs the effects of the preferred ionic association. The replacement of Fe^{2+} ions by Ca^{2+} will be accompanied by a tendency towards two liquid formations in the ternary silicate. In the corresponding phosphate ternary system, liquid separation actually occurs, forming an iron oxide-rich liquid and a calcium phosphate-rich liquid (46).

The above scheme of preferred ionic associations is general to all ternary silicate systems which contain cations of differing ionisation potentials, i.e. which are made up from binary silicate systems exhibiting different degrees of polymerisation.

On the basis of the Masson model, it is suggested that the following rule is operative - "The more stable the metal cation with respect to the metal atom, i.e. the lower the ionisation potential of the metal ion, then the greater is the cations' preference for association with, and co-ordination by, O^- ions rather than for association with, and co-ordination by O^{2-} ions". According to this rule, the Ca^{2+} ion, which has a lower ionisation potential than the Fe^{2+} ion, is associated with a lower O^{2-}/O^- ratio in silicates than is the Fe^{2+} ion. Hence, polymerisation occurs to a lesser extent in calcium silicates than in the corresponding iron silicates.

If the relative stabilities of the metal oxides and metal orthosilicate

in the order Ca, Mn, Fe, Co, Ni, are considered it is seen that both the stabilities of the oxides and the stabilities of the orthosilicates decrease in the above order. This is simply a consequence of the fact that the ionisation potential of the metal atom increases in this order. On the basis of the above discussion on the relative bond strengths between the cation and an O^{2-} ion and the cation and an O^- ion, it is suggested that the rate of decrease of stability of the oxides (in which the cation is co-ordinated only by O^{2-} ions) in the order Ca, Mn, Fe, Co, Ni is less than the rate of decrease of the stability of the solid orthosilicates (in which the cation is co-ordinated only by O^- ions), i.e. in the order Ca, Mn, Fe, Co, Ni the silicate is becoming less stable relative to the oxide. Additional evidence of this behaviour is obtained from a consideration of Cu^+ where it is found that copper orthosilicate does not even exist (115). It is suggested, therefore, that the greater rate of decrease in stability of the solid orthosilicate compound is a direct result of the fact that the lattice requirements of the solid orthosilicate permit only SiO_4^{4-} anions, i.e. only cation- O^- bonds, whereas in the order Ca, Mn, Fe, Co, Ni the cation has an increasingly greater preference for co-ordination by O^{2-} ions than by O^- ions. The fact that copper orthosilicate does not exist suggests that, in this case, the requirement of the copper cation for continued preferred association with O^{2-} ions rather than with O^- ions overwhelms the lattice requirements of the solid orthosilicate compound. In addition, copper oxide and silica are insoluble in the solid phase which again indicates the overwhelming preference for the Cu^+-O^{2-} association.

8.9 The activity of silica in ternary silicate melts

Bell (104) has calculated the iso-silica activity lines in the system MnO-FeO-SiO_2 . These are shown in Figure 53(a) and as can be seen, they are of the same form as would be expected of iso-degree of polymerisation lines if polymerisation-depolymerisation were symmetrical across the ternary. As polymerisation-depolymerisation does not appear to be symmetrical across the ternary it is suggested that the iso-degree of polymerisation locii would be of the form shown schematically in Figure 53(b). In view of the observation that the degree of polymerisation, i.e. the anionic configuration, changes across iso- N_{SiO_2} composition paths in the ternary system it is seen that ideal mixing of cations along the iso- N_{SiO_2} paths does not occur. Instead ideal mixing of cations only occurs along the iso-degree of polymerisation lines. In the case of the system MnO-FeO-SiO_2 , as a result of the degrees of polymerisation occurring in the constituent binary silicate systems being similar, the iso-degree of polymerisation lines do not differ greatly from the iso- N_{SiO_2} lines and hence the assumption that ideal mixing of Fe^{2+} and Mn^{2+} ions occurs along iso- N_{SiO_2} paths is a reasonable first approximation.

8.10 The Effect of Temperature on Polymerisation

The effect of temperature on the degree of polymerisation occurring in basic silicate melts is uncertain as the evidence available is conflicting. For example, it has been suggested that the abnormal temperature coefficients of surface tension (40) are due to a decrease in the degree of association of silicate ions with increasing temperature, i.e. with increasing temperature there is a decrease in the degree of polymerisation. On the other hand calculation by Masson (67) of the temperature variation

of the value of k for calcium silicate indicated that k , and hence the degree of polymerisation, increases with increasing temperature. In view of the fact that polymerisation in the melt disappears on freezing, the temperature criterion might be expected to be the degree of superheat of the melt above its liquidus temperature. If this is the case, then the present investigation has not been carried out "iso-thermally" with respect to the effect of temperature on polymerisation. This question of what temperature should be used to compare physical properties of melts of differing composition has been a source of uncertainty in the past (116).

8.11 The Constancy of Oxygen Density

The constancy of the oxygen density, along iso-silica concentration paths, as shown in Figures 43, 44, 45, has been interpreted as indicating a constancy in the degree of polymerisation. It is difficult to explain this effect in terms of the scheme of ionic associations suggested previously. Although this behaviour is consistent and is in agreement with the change in activity of free oxygen ions, it cannot be explained in terms of the model in its present state. It is significant to note, however, that constancy of the oxygen density occurs only towards that side of the ternary which contains the cation of lower ionisation potential, i.e. the cation which plays the dominant role in determining the preferred ionic associations in the ternary melt.

8.12 The Effect of CaF_2 additions to Iron Silicates

Figure 36 indicates that the replacement of "FeO" by CaF_2 produces a greater decrease in density than does replacement by CaO. However, a knowledge of the density behaviour alone is not sufficient to allow a

prediction to be made of the structural rearrangements occurring as a result of the introduction of CaF_2 . The limited solubility of CaF_2 , as compared with the solubility of CaO , together with the observed large density decrease suggest that a considerable degree of ionic rearrangement is occurring.

CHAPTER 9

SUMMARY

The density-composition relationship of iron silicates in contact with iron at 1410°C has been determined. From this relationship the oxygen densities of iron silicate melts have been calculated, and comparison of these oxygen densities with the oxygen densities of mechanical mixtures of iron oxide and silica have indicated that the degree of polymerisation of the silicate anions occurring in these melts increases with increasing silica content. This is in agreement with recently-developed thermodynamic models of basic binary silicate melts.

The "FeO" in an iron silicate containing 29 mole per cent silica has been replaced to varying degrees by CaO, MnO, CoO and NiO. The density behaviour resulting from this cation replacement indicated that small additions of CaO and MnO produce a depolymerisation of the silicate anions, the extent of this depolymerisation being greater in the case of replacement by Ca^{2+} ions than in the case of replacement by Mn^{2+} ions. This behaviour is in agreement with the prediction that the degree of polymerisation occurring in the binary silicate systems increases in the order CaO-SiO_2 , MnO-SiO_2 , FeO-SiO_2 . In the case of MnO replacement it was found that continued depolymerisation, with cation replacement, does not occur across the entire iso-silica composition path in the ternary system. The degree of polymerisation of the silicate anions remains constant over a wide range of composition at the MnO rich side of the composition path. Constancy of the oxygen density was also observed

when "FeO" was replaced by CoO and NiO. This behaviour is in agreement with the behaviour of the activity of free oxygen ions present in ternary melts.

"FeO" in an iron silicate containing 23 mole per cent silica has been replaced by CaO and CaF₂ and the density decrease resulting from CaF₂ replacement was found to be greater than that resulting from CaO replacement. This behaviour, together with the observed low solubility of CaF₂ in the iron silicate indicated that considerable ionic interaction and structural rearrangement occur as a result of the presence of CaF₂.

From consideration of the differing degrees of polymerisation which can occur in ternary silicate melts a general scheme of ionic associations has been developed which has been correlated with the activities of metal oxides and silica in these melts.

17. W. Kauzmann and H. Eyring, *J. Amer. Chem. Soc.* 62, 3113 (1940).
18. G. Kimble, *Treatise on Physical Chemistry*, New York. 1951, p.354.
19. B. E. Warren and W. L. Bragg. *Z. Krist.* 68, 168 (1929).
20. W. H. Zachariasen. *Z. Krist.* 74, 139 (1930).
21. P. Kozakevitch. *Rev. Met.* 51, 569 (1954).
22. P. M. Bills. *J. Iron and Steel Inst.* 201, 133 (1963).
23. T. Baak. *Proc. Conf. Phys. Chem. Iron and Steelmaking.* Dedham, Massachusetts. 1956 Wiley. New York 1958.
24. L. Shartsis, S. Spinner and W. Capps. *J. Amer. Ceram. Soc.* 35, 155 (1952).
25. N. W. Taylor and P. S. Dear. *J. Amer. Ceram. Soc.* 20, 296 (1937).
26. N. W. Taylor and R. F. Doran. *J. Amer. Ceram. Soc.* 24, 103 (1941).
27. J. P. Poole. *J. Amer. Ceram. Soc.* 32, 230 (1949).
28. J. E. Stanworth. *Physical Properties of Glass.* Oxford Univ. Press London 1950.
29. G. Keidkamp and K. Endell. *Glastech. Ber.* 14, 89 (1936).
30. J. O'M. Bockris, J. W. Tomlinson and J. L. White. *Trans. Farad. Soc.* 52, 299 (1956).
31. R. J. Callow. *J. Soc. Glass. Technology.* 36, 137 (1952).
32. R. W. Douglas and J. D. Izard. *J. Soc. Glass Tech.* 35, 206 (1951).
33. K. Endell and J. Hellbrugge. *Naturwiss.* 30, 421 (1942).
34. M. Rey. *Farad. Soc. Disc.* 4, 257 (1948).
35. J. O'M. Bockris. *Farad. Soc. Disc.* 4, 320 (1948).
36. T. F. W. Barth. *Amer. J. Science.* 224, 102 (1932).
37. C. L. Babcock. *J. Amer. Ceram. Soc.* 23, 12 (1940).
38. A. Dietzel. *Kolloidzshr.* 100, 368 (1942).
39. T. B. King. *Trans. Soc. Glass Tech.* 35, 241 (1951).

40. T. B. King. The Physical Chemistry of Melts. Inst. of Mining and Metallurgy. London 1953 p. 35.
41. P. Kozakevitch. Rev. de Met. 8, 505 (1949).
42. L. Shartis and S. Spinner. J. Res. Nat. Bur. Stand. 46, 385 (1951).
43. J. J. Bikerman. Surface Chemistry. Academic Press. New York (1947).
44. N. K. Adam. Physics and Chemistry of Surfaces. London (1940).
45. B. E. Warren and A. G. Pincus. J. Amer. Ceram. Soc. 23, 301 (1940).
46. R. Hay, P. T. Carter and S. K. Kabi. J. Soc. Glass Tech. 40, 429 (1956).
47. C. Bodsworth. Physical Chemistry of Iron and Steel Manufacture, Longman 1963 p. 87.
48. W. Oelsen and H. Maetz. Mitt. Kaiser Wilhelm Inst. fur Eisenforschung 23, 195 (1941).
49. C. Bodsworth. J.I.S.I. 193, 13 (1959).
50. E. Brandenberger. Schweizer Archiv fur Angen Wissenschaft und Technik 2, 52 (1936).
51. J. White, D. D. Howat and R. Hay. J. Roy. Tech. College. Glasgow. 3, 231 (1933-36).
52. H. Towers and J. Kay. Trans. Brit. Ceram. Soc. 49, 341 (1950).
53. W. H. Zachariasen. J. Amer. Chem. Soc. 54, 3841 (1932).
54. W. L. Bragg. The Structure of Silicates. Akad. Verlag. Leipzig 1930.
55. J. Biscoe and B. E. Warren. J. Amer. Ceram. Soc. 21, 287 (1938).
56. F. D. Richardson. Proc. Conf. Phys. Chem. of Iron and Steelmaking Dedham, Massachusetts 1956. Wiley N. Y. 1958, p. 55.
57. J. O'M. Bockris. The Physical Chemistry of Melts. Inst. of Mining and Metallurgy. London 1953, p. 9.
58. K. L. Fetters and J. Chipman. Trans. A.I.M.E. 145, 95 (1941).

59. T. B. Winkler and J. Chipman. *Trans. A.I.M.E.* 167, 111 (1946).
60. F. Korber and W. Oelsen. *Mitt. Kaiser-Wilhelm Inst. Eisenforsch.* 15, 272 (1933).
61. G. W. Toop and C. S. Samis. *Trans. Met. Soc. A.I.M.E.* 224, 878 (1962).
62. G. W. Toop and C. S. Samis. *Canadian Met. Quart.* 1, 129 (1962).
63. C. J. B. Fincham and F. D. Richardson. *Proc. Roy. Soc.* A223, 40 (1954).
64. F. D. Richardson and L. E. Webb. *Trans. Inst. Min. Metallurgy* 64, 529 (1954-55).
65. L. S. Darken and R. W. Gurry. *Physical Chemistry of Metals.* McGraw-Hill N. Y. 1953, p. 340.
66. H. Flood and W. J. Knapp. *J. Amer. Ceram. Soc.* 46, 61 (1963).
67. C. R. Masson. *Proc. Roy. Soc.* A287, 201, no. 1409 (1965).
68. L. S. Darken and R. W. Gurry. *J. Amer. Chem. Soc.* 67, 1398 (1945).
69. L. S. Darken and R. W. Gurry. *J. Amer. Chem. Soc.* 68, 798 (1946).
70. N. L. Bowen and J. F. Schairer. *Amer. J. Science* 24, 177 (1932).
71. A. Muan and E. F. Osborn. *Phase Equilibria among Oxides in Steelmaking.* Addison Weseley 1965, p. 53.
72. A. Muan. *Trans. A.I.M.E.* 203, 965 (1955).
73. R. Schuhmann, Jr. and P. J. Ensio. *Trans. A.I.M.E.* 191, 401 (1951).
74. H. B. Bell, A. B. Murad and P. T. Carter. *J. Metals.* 4, 718 (1952).
75. T. Rosenquist. *Trans. A.I.M.E.* 191, 535 (1951).
76. K. P. Abraham. M. W. Davies and F. D. Richardson. *J.I.S.I.* 196, 82 (1960)
77. C. Bodsworth and I. M. Davidson. *Phys. Chem. of Process Metallurgy, Part 1, Metallurgical Society Conferences, Vol. 7, Interscience* N. Y. p. 233.
78. J. Lumsden. *ibid.* p. 243.

79. M. Rey. Phys. Chem. of Melts. Inst. of Min. and Metallurgy.
London 1953, p. 63.
80. O. Kubaschewski and E. L. Evans. Metallurgical Thermochemistry.
London. Butterworth Springer, 1951.
81. F. D. Richardson, J. H. E. Jeffes and G. Withers. J.I.S.I. 166, 213 (1950).
82. J. Chipman and L. Chang. Trans. A.I.M.E. 185, 191 (1949).
83. M. T. Simnad, G. Derge and I. George. Trans. A.I.M.E. 200, 1386 (1954).
84. H. Schenck, M. G. Froberg and W. Rodhe. Arch. Eisenhuttenw. 32, 521 (1961).
85. P. Kozakevitch. Rev. Met. 47, 201 (1950).
86. G. Urbain. J. Chim. Phys. 49, 316 (1952).
87. J. Henderson. Trans. A.I.M.E. 230, 501 (1964).
88. A. I. Kemppinen and N. A. Gokcen. J. Phys. Chem. 60, 126 (1956).
89. V. W. Schmidt. Ergeb. Tech. Rontegenkunde 3, 194 (1933).
90. S. I. Popel and O. A. Esin. Zh. Prikl. Khim 29, 651 (1956).
91. J. Henderson, R. G. Hudson, R. G. Ward and G. Derge. Trans. Met.
Soc. A.I.M.E. 221, 807 (1961).
92. H. Schenck, M. G. Froberg and K. Hoffman. Arch. Eisenhuttenw. 33, 369 (1962).
93. M. G. Froberg and H. H. Brandi. Arch. Eisenhuttenw. 34, 591 (1963).
94. A. Adachi and K. Ogino. Technol. Rept. Osaka Univ. 12, 147 (1962).
95. R. G. Ward and P. L. Sachdev. Trans. Met. Soc. A.I.M.E. 233, 1496 (1965).
96. P. L. Sachdev. M. Eng. Thesis. McMaster University 1964.
97. R. G. Ward and J. Henderson. Trans. Met. Soc. A.I.M.E. 233, 1795 (1965).
98. G. Brauer. Handbook of Preparative Inorganic Chemistry, Vol. 2.
Academic Press N. Y., London 1965, p. 1498.
99. E. A. Dancy and G. Derge. Trans. Met. Soc. A.I.M.E. 236, 1642 (1966).
100. F. D. Richardson and J. H. E. Jeffes. J.I.S.I. 160, 261 (1948).

101. F. P. Glasser. *Am. J. Science* 256, 405 (1958).
102. H. von Wentrup. *Tech. Mitt. Krupp.* 5, 131 (1937).
103. W. R. Maddocks. *Iron and Steel Inst. (London) Carnegie Schol. Memoirs* 24, 64 (1935).
104. H. B. Bell. *J.I.S.I.* 201, 116 (1963).
105. P. Asanti and E. J. Kohlmeier. *Z. Anorg. Chem.* 265, 96 (1951).
106. C. R. Masson. Private communication.
107. J. Henderson. Private communication.
108. E. D. Lacy. *The Vitreous State*. p. 23. Glass Delegacy of the University of Sheffield 1955.
109. J. W. Mellor. *A Comprehensive Treatise on Inorganic and Theoretical Chemistry*. Longmann, Green and Co. 1922, vols. 3, 12, 14 and 15.
110. P. T. B. Shaffer. *High Temperature Materials*, Vol. 1.
111. *International Critical Tables of Numerical Data, Physics, Chemistry, and Technology*. McGraw-Hill.
112. *Handbook of Chemistry and Physics*. Chemical Rubber Publishing Co., Cleveland. 43rd edition 1962.
113. J. F. Elliot. *J. Metals* 7, 485 (1955).
114. P. T. Carter. *J. Met. Club Roy Tech. Coll. (Glasgow)* 8, 43 (1955-56).
115. E. M. Levin, C. R. Robbins and H. F. McMurdie. *Phase Diagrams for Ceramists*. Amer. Ceram. Soc. Ohio 1946, p. 86.
116. R. G. Ward. *An Introduction to the Physical Chemistry of Iron and Steelmaking*. Arnold, London p. 18.

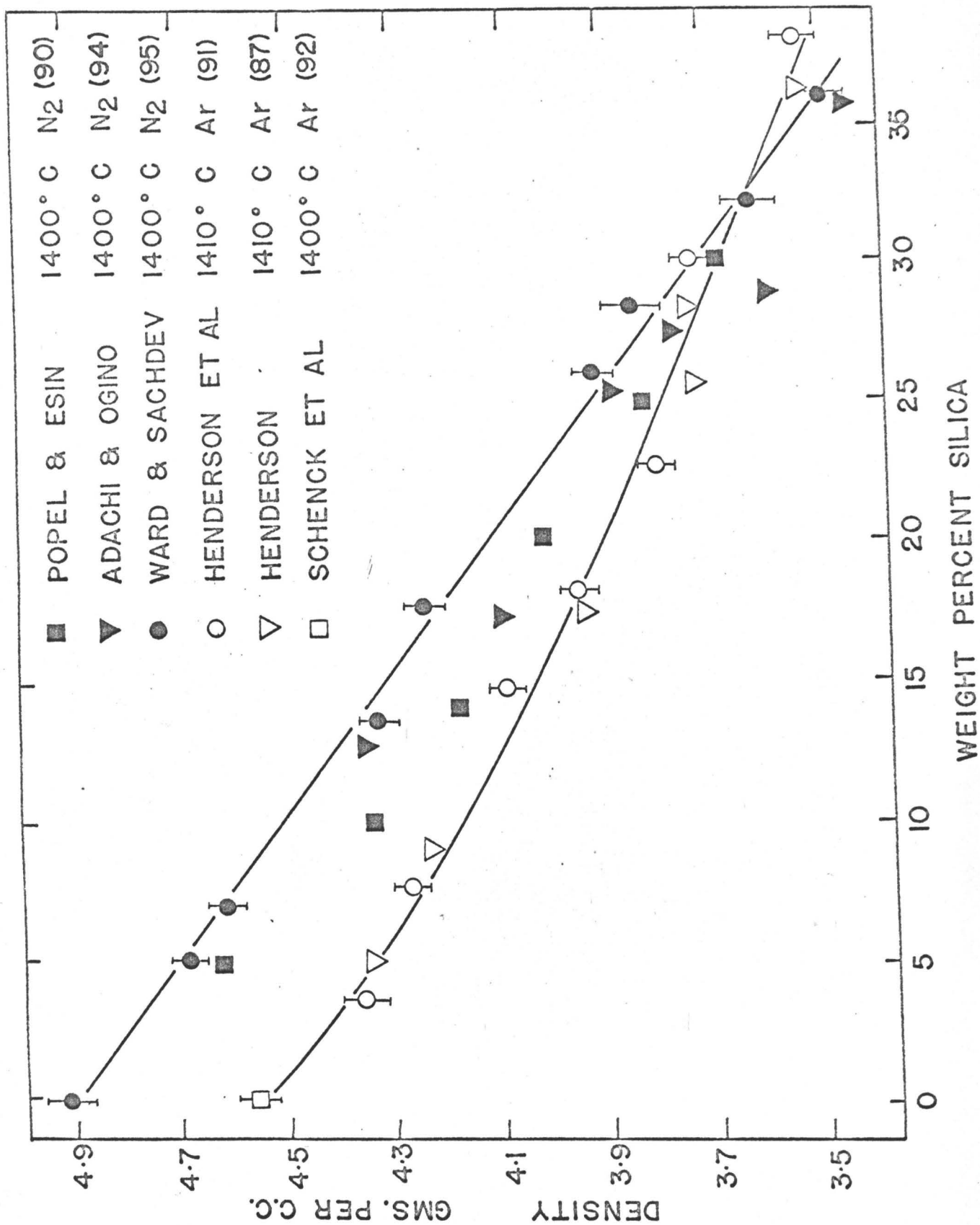


Figure 24. Previous determinations of the density-composition relationship of iron silicate melts in contact with solid iron.

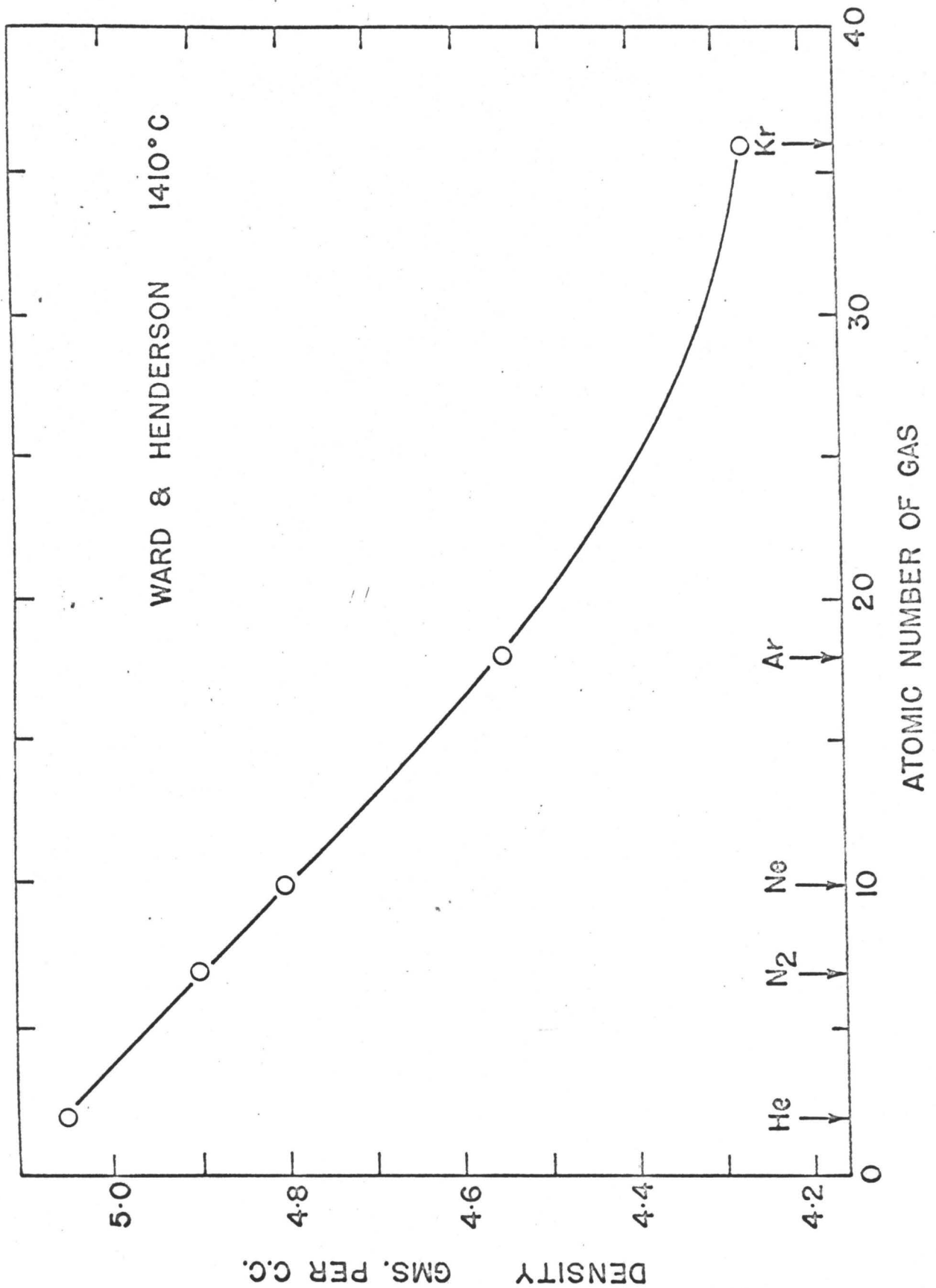


Figure 25. Measured density of liquid iron oxide as a function of the atomic number of the blowing gas.

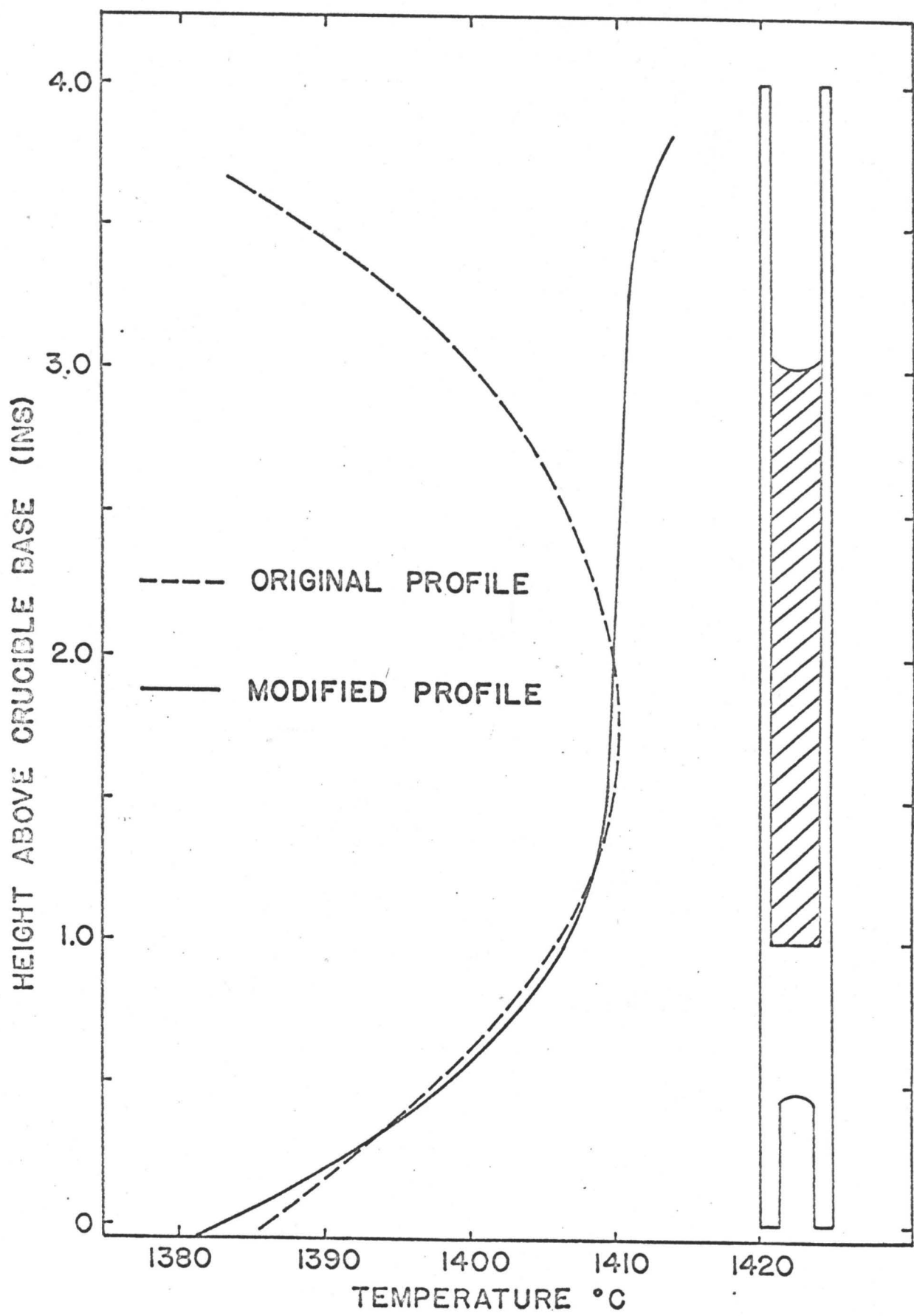


Figure 26. Temperature profiles and crucible location in the furnace.



(a)

(b)

(c)

Figure 27.

The tips of blowing tubes after,

- (a) bubbling liquid iron oxide with highly deoxidised gas.
- (b) bubbling liquid iron oxide with gas containing the equilibrium partial pressure of oxygen for contact with liquid iron oxide and solid iron at 1410°C .
- (c) bubbling liquid iron oxide with gas containing the equilibrium partial pressure of oxygen for contact with liquid iron oxide and solid iron at 1410°C followed by bubbling with highly deoxidised gas.



Figure 28. Typical ring of iron formed at the melt surface due to heat abstraction.

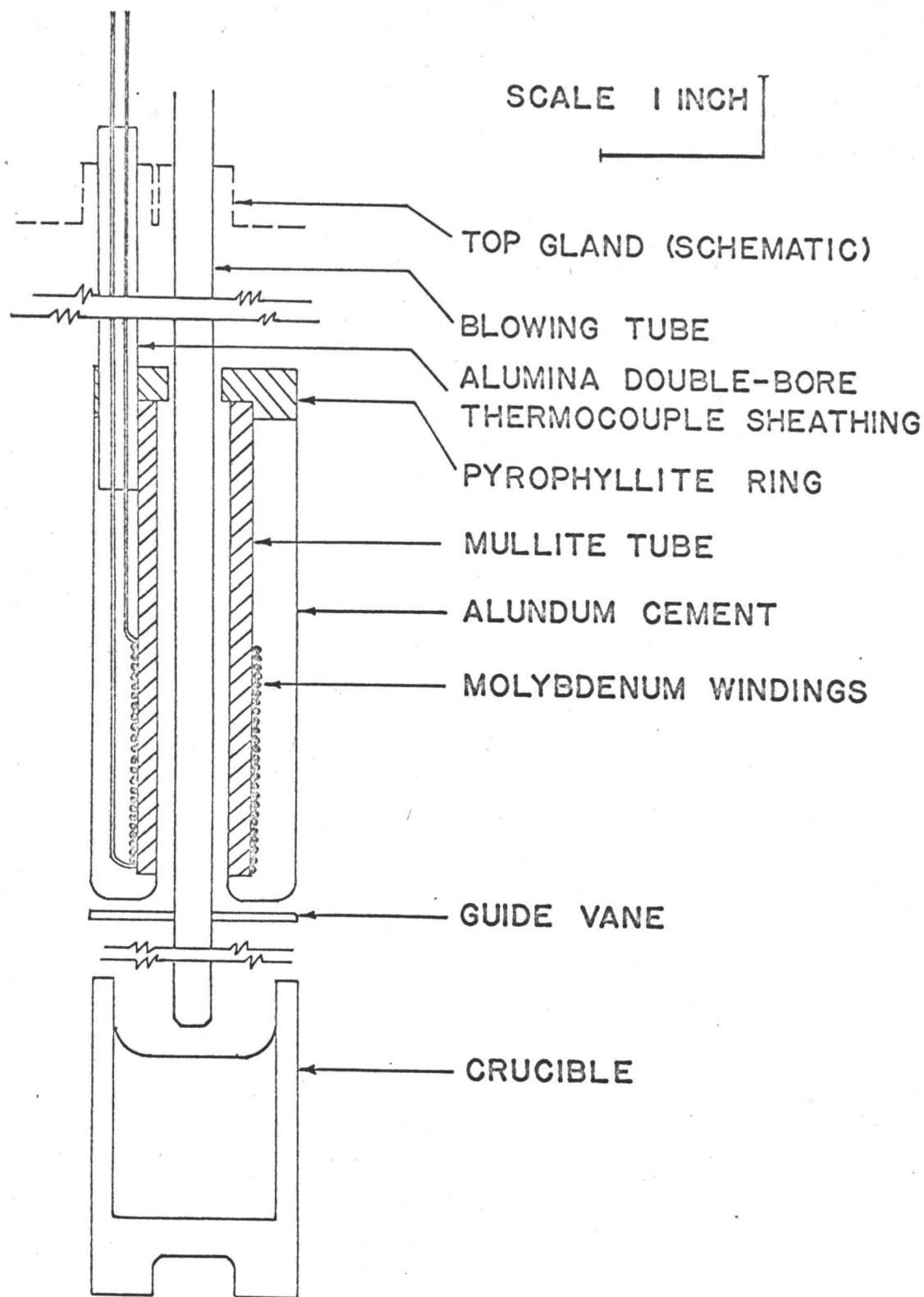


Figure 29. Construction of the heating element.

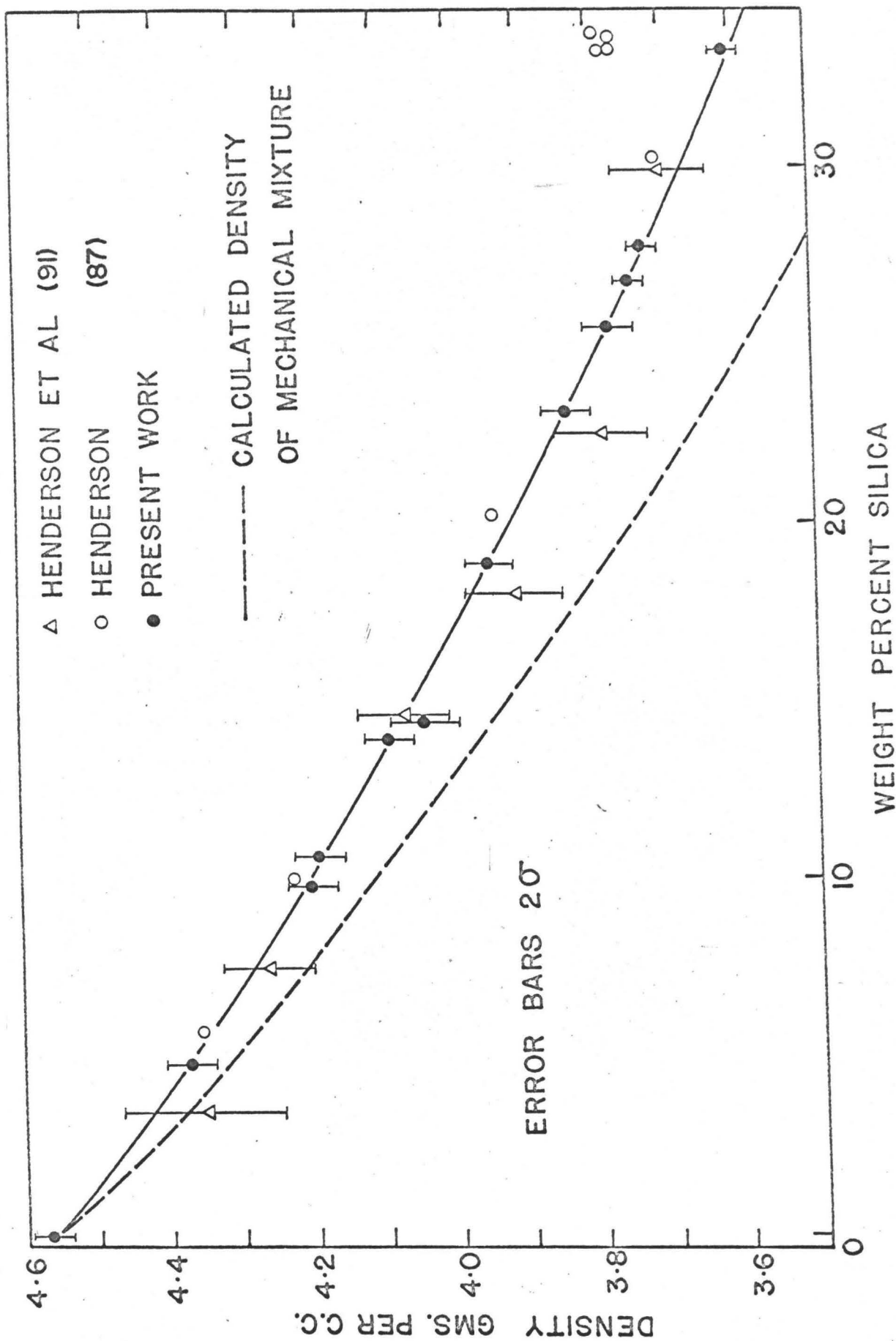


Figure 30. The density-composition relationship of iron silicates in contact with iron at 1410°C.

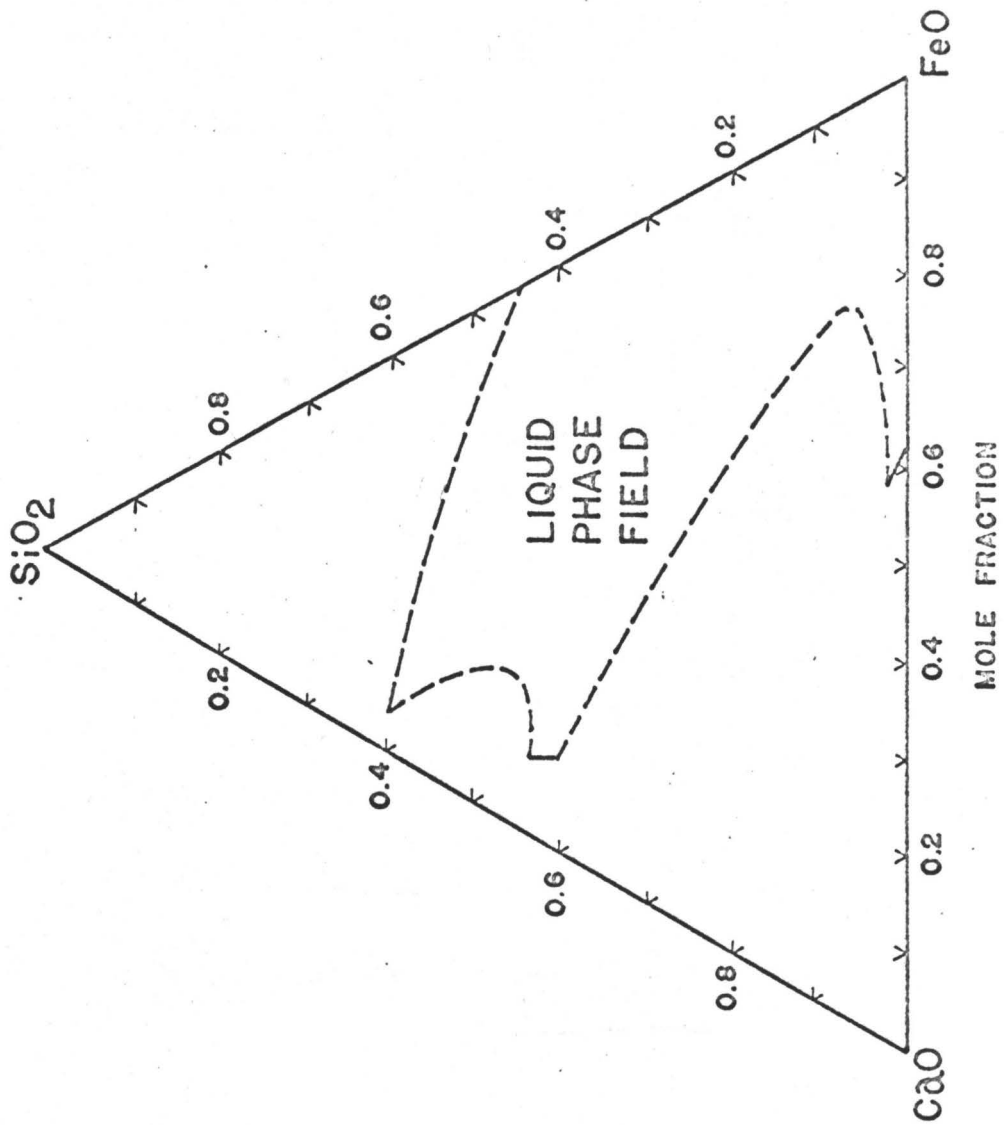


Figure 31. The liquid phase field in the system CaO-'FeO'-SiO₂ at 1410°C.

○ CaO ADDED TO AN IRON SILICATE CONTAINING 27.90 WT %

SILICA (MOLE FRACTION 0.316)

△ 0.29 MOLE FRACTION SILICA

▽ 0.23 MOLE FRACTION SILICA

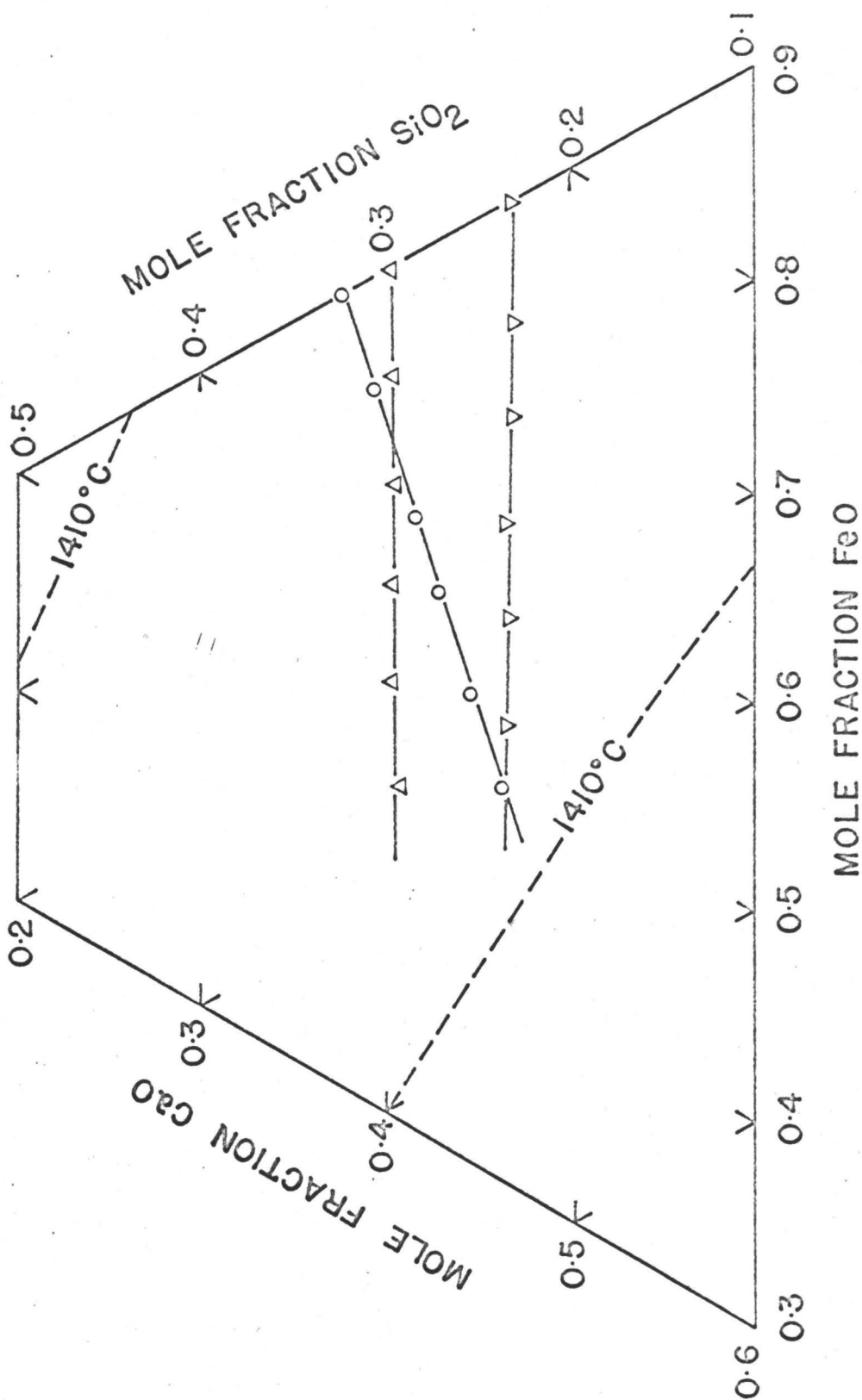


Figure 32. Composition paths studied in the system CaO-FeO-SiO₂

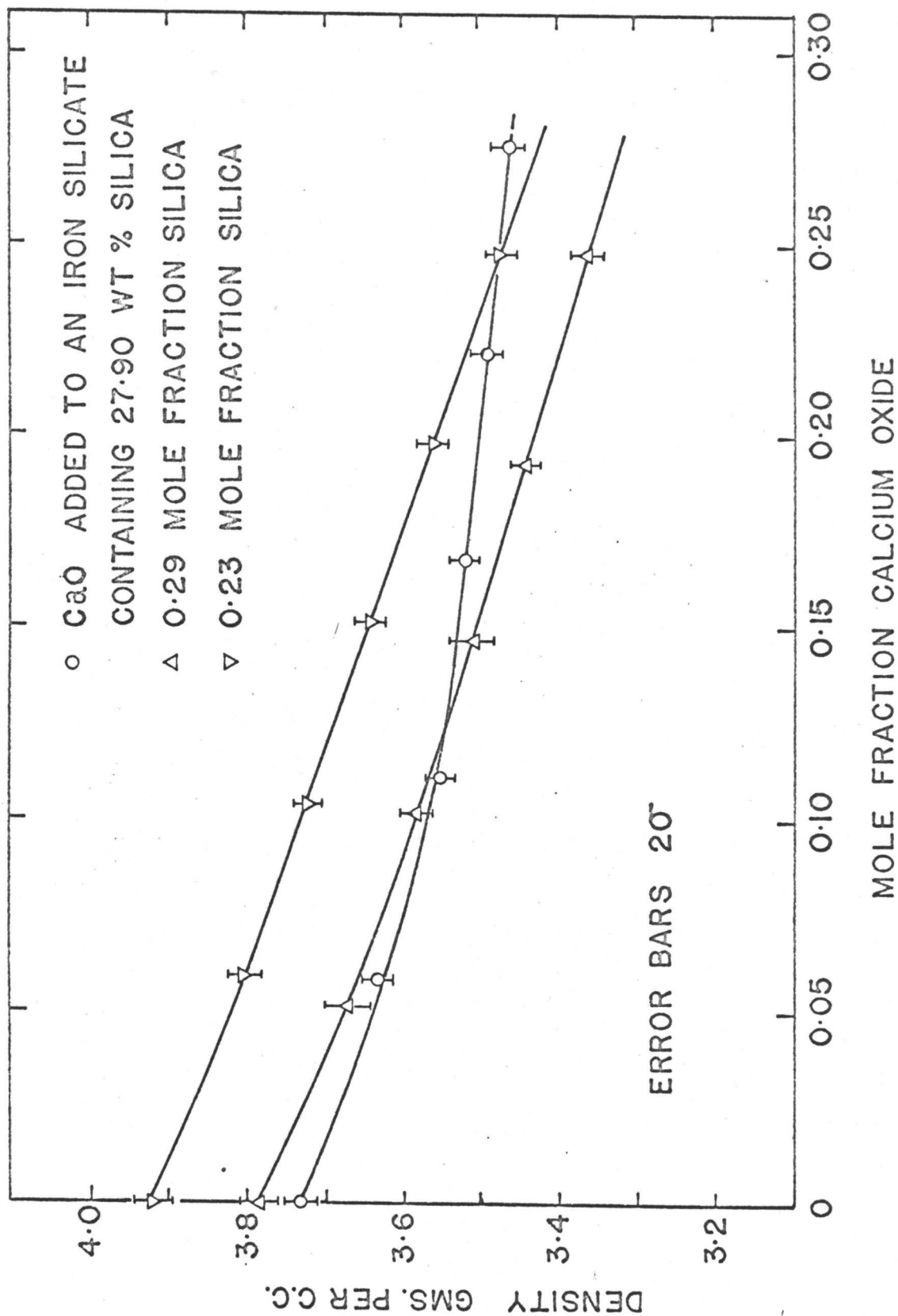


Figure 33. The density-composition relationships in the system $\text{CaO}'\text{-FeO}'\text{-SiO}_2$ at 1410°C .

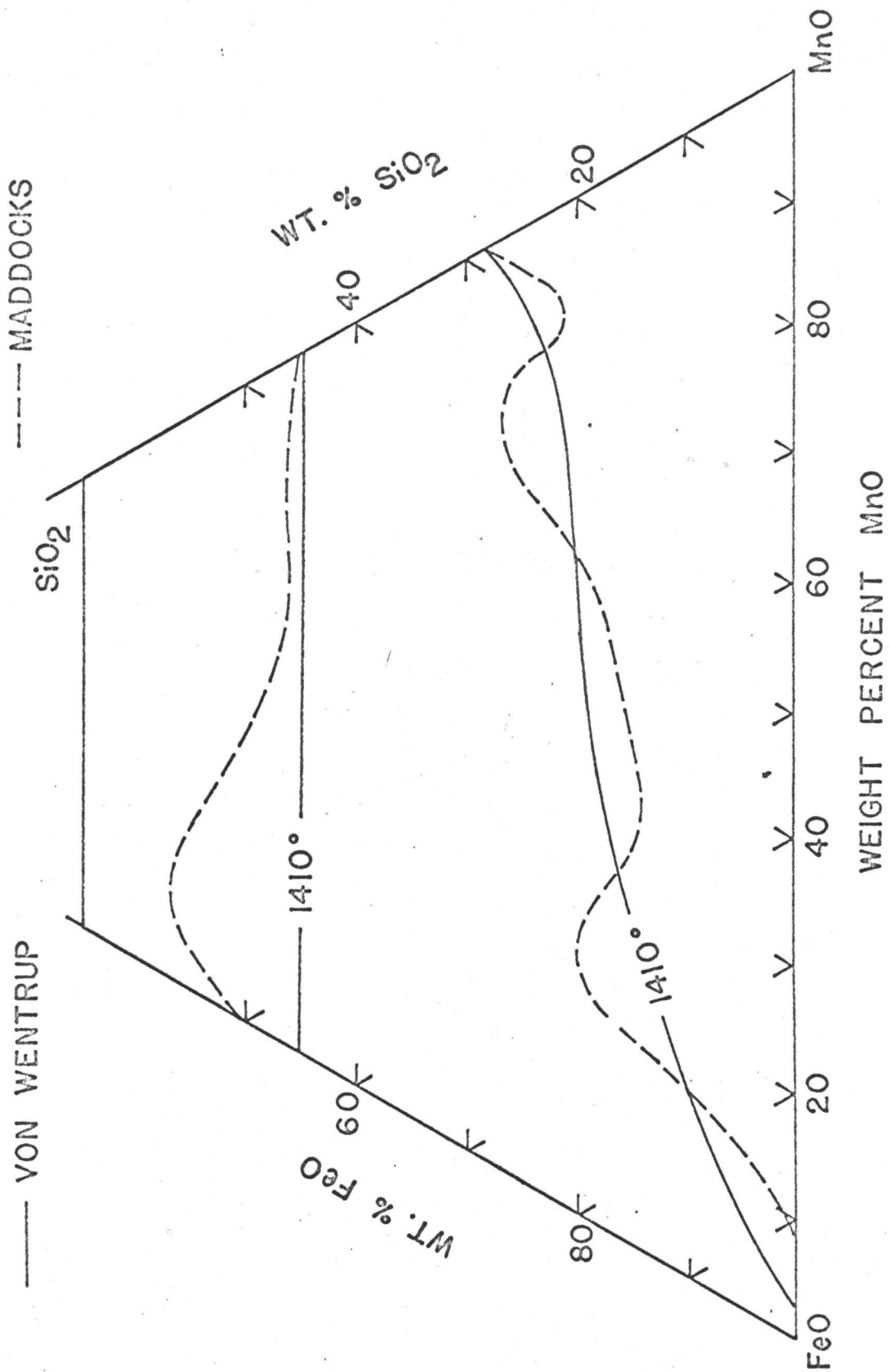


Figure 34. The liquid phase field in the system MnO-FeO-SiO₂ at 1410°C.

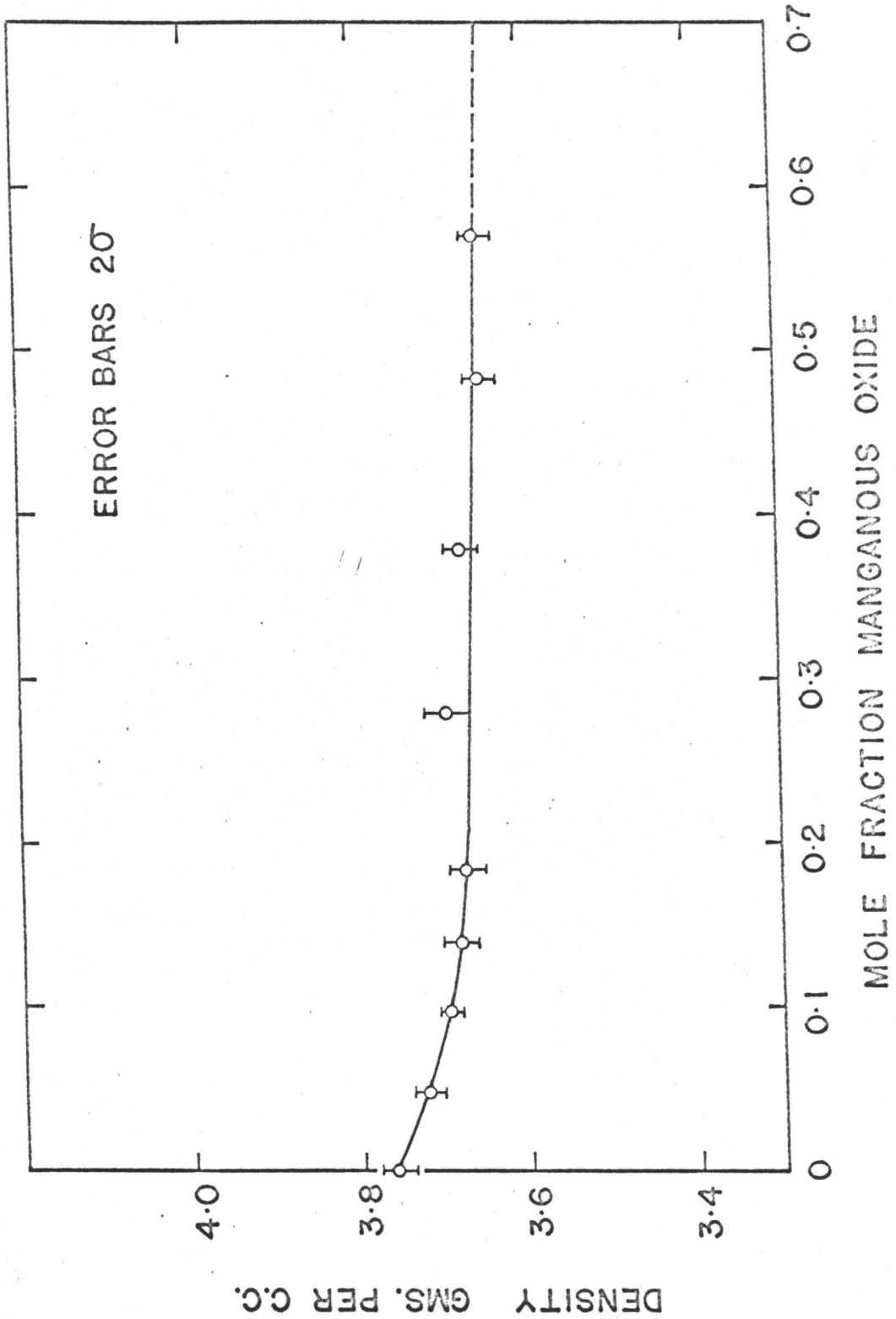


Figure 35. The density-composition relationship in MnO-FeO-SiO₂ melts in which $N_{\text{SiO}_2} = 0.29$ at 1410°C.

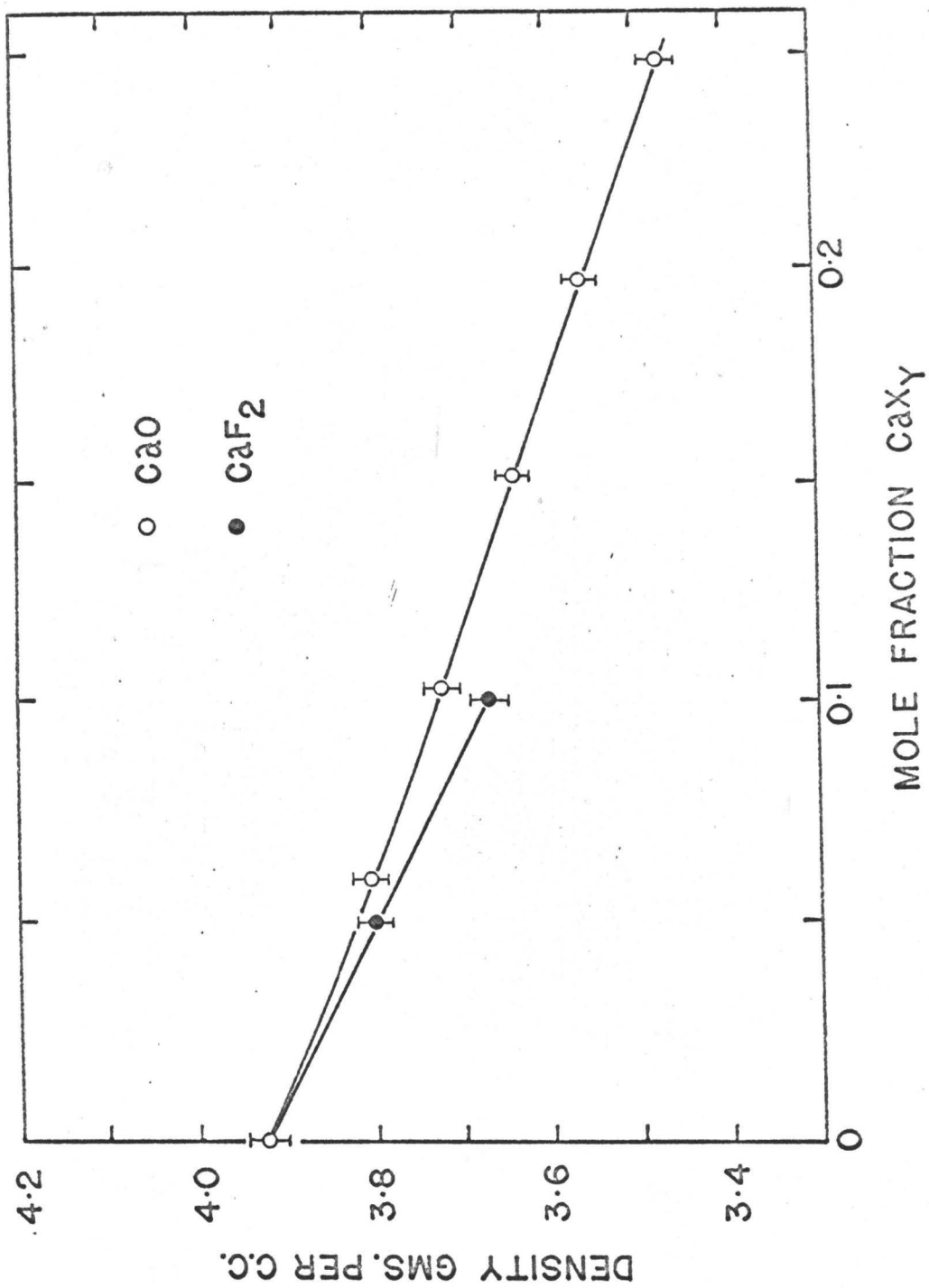


Figure 36. The density-composition relationship in CaF_2 - FeO - SiO_2 melts in which $N_{\text{SiO}_2} = 0.29$ at 1410°C .

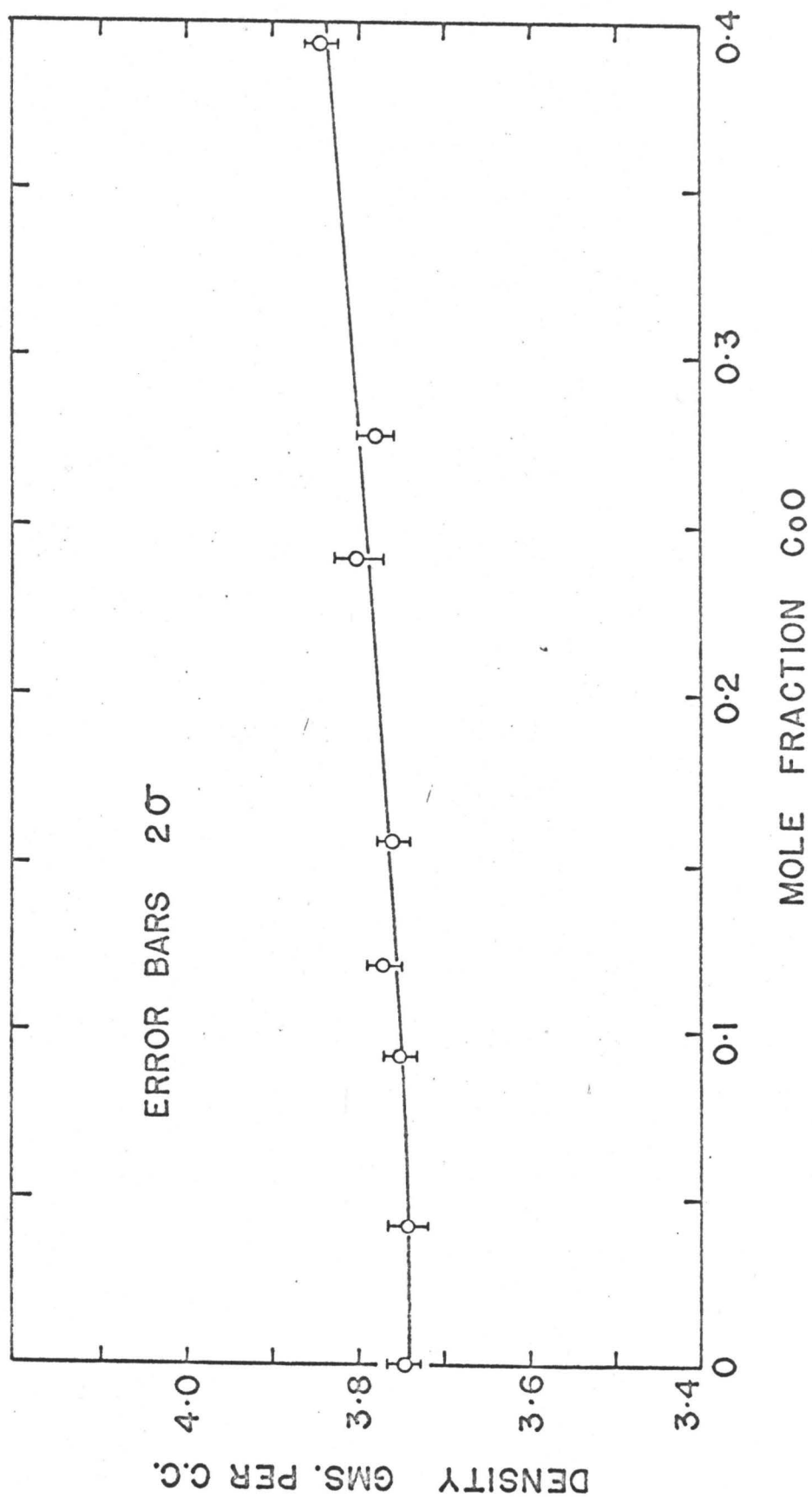


Figure 37. The density-composition relationship in CoO-FeO-SiO_2 melts in which $N_{\text{SiO}_2} = 0.29$ at 1410°C .

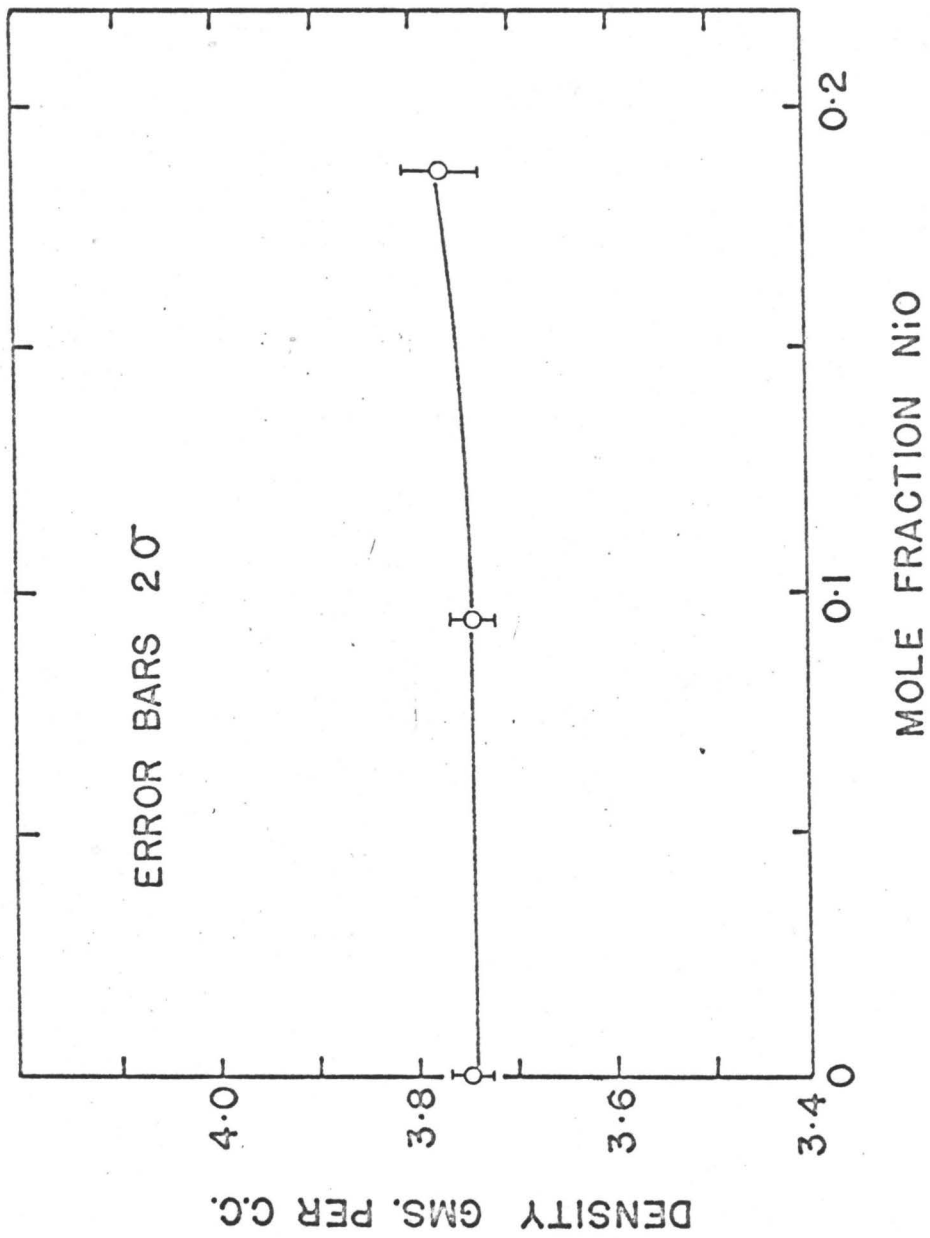


Figure 38. The density-composition relationship in NiO-FeO-SiO₂ melts in which $N_{\text{SiO}_2} = 0.29$ at 1410°C .

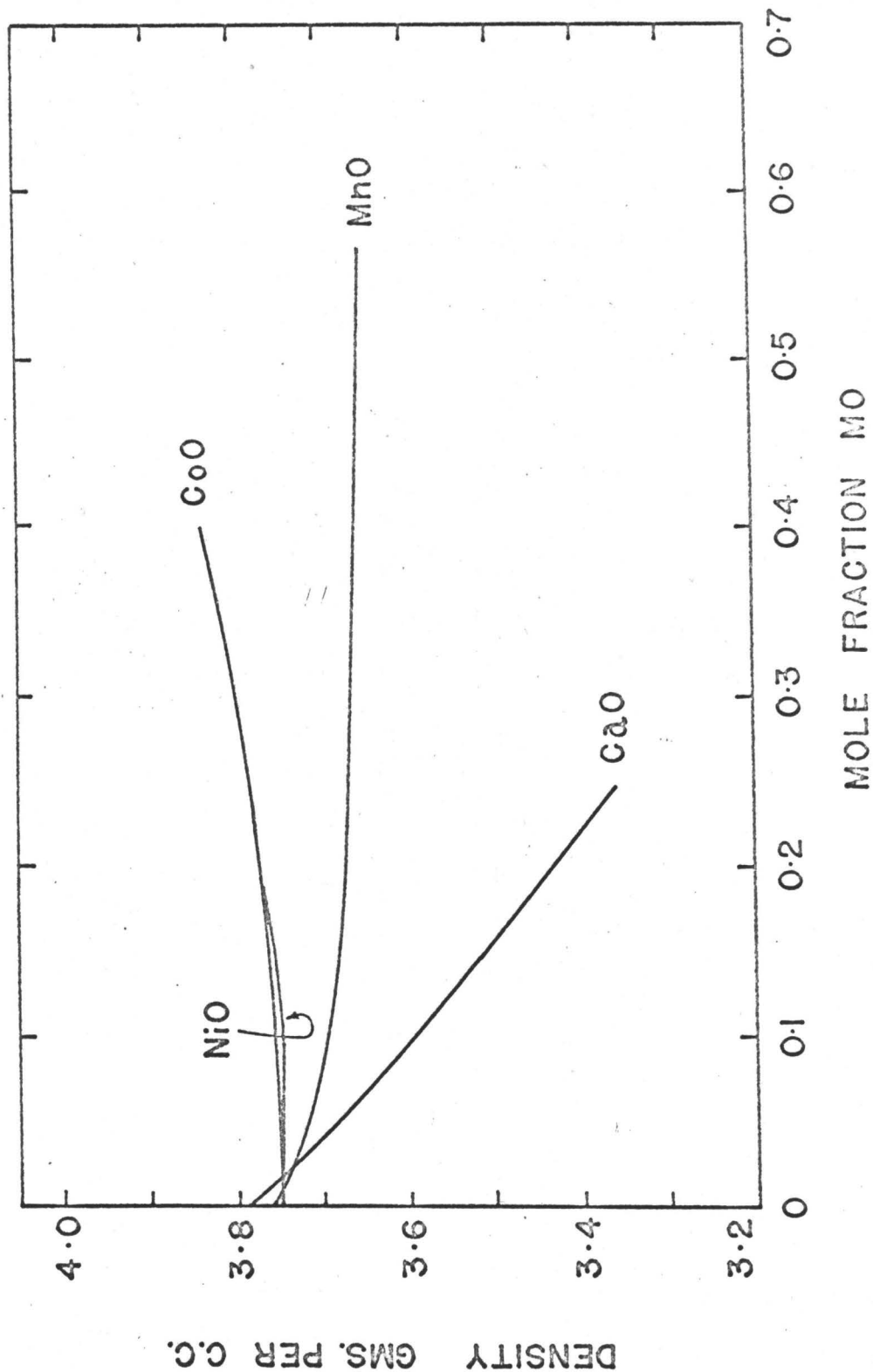


Figure 39. The effects of the replacement of Fe^{2+} ions by Ca^{2+} , Mn^{2+} , Co^{2+} and Ni^{2+} ions on the density of an iron silicate containing 29 mole percent silica.

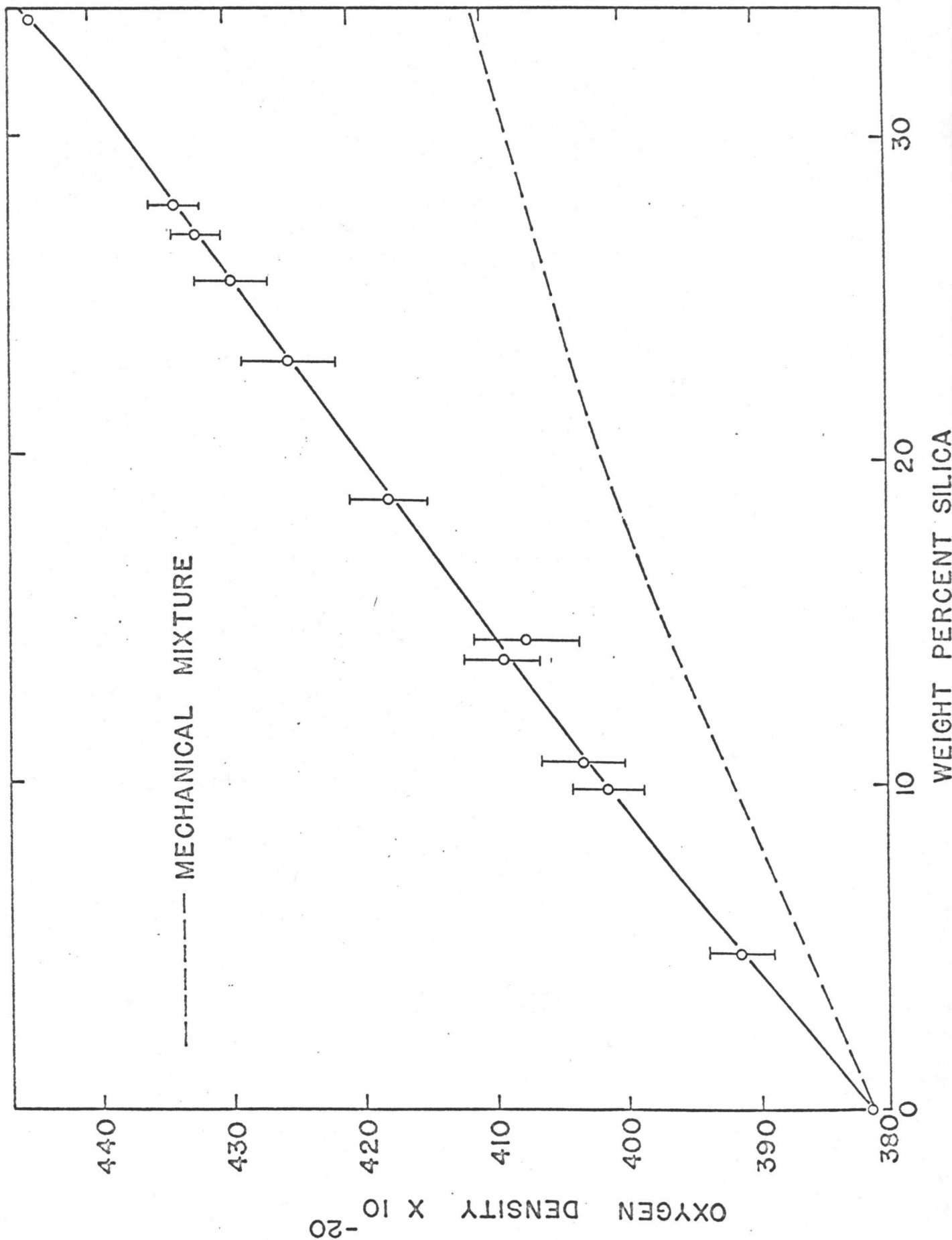


Figure 40. The oxygen density-composition relationship occurring in the system FeO-SiO₂ at 1410°C.

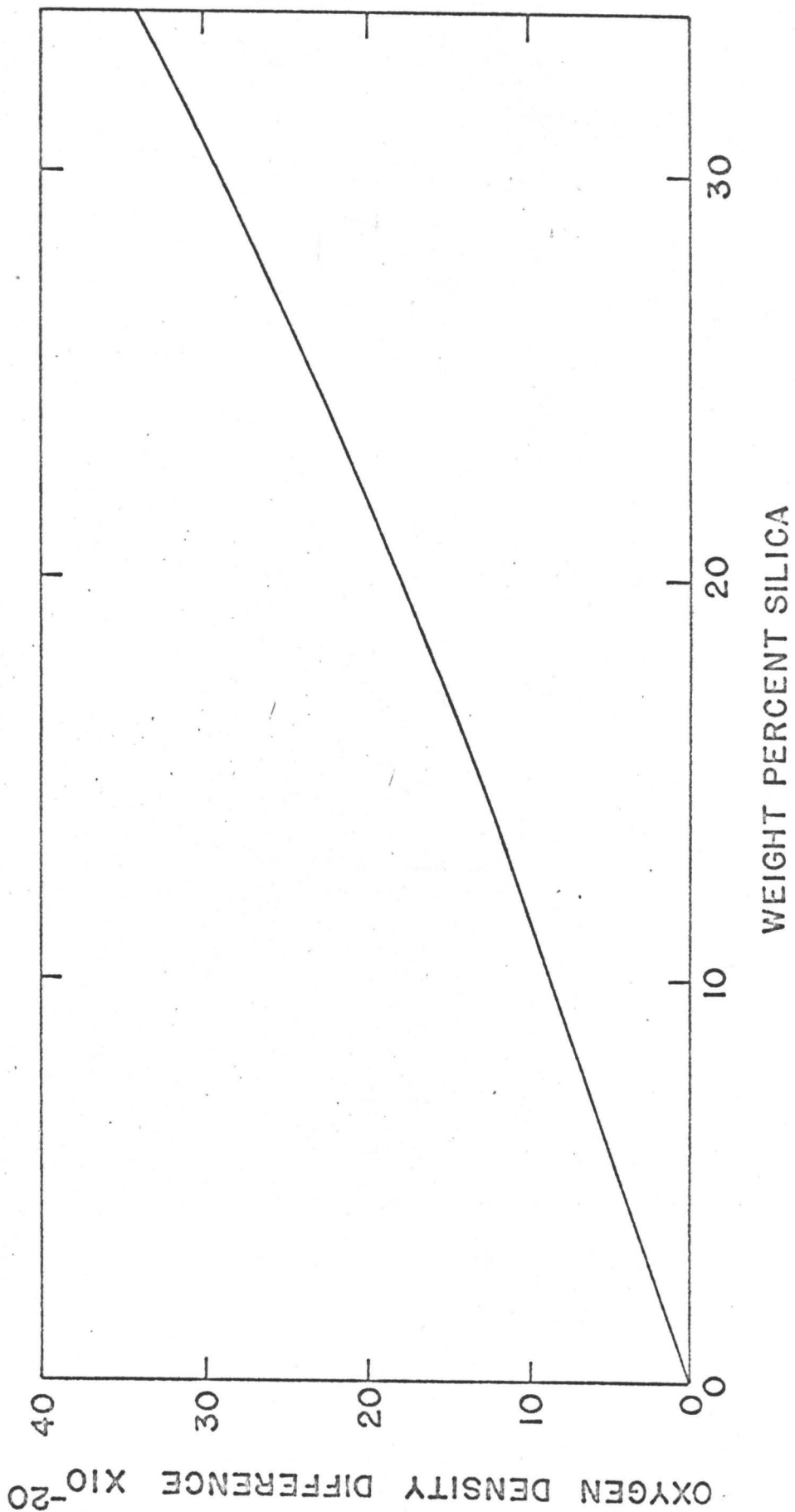


Figure 41. The difference in oxygen density between solutions and mechanical mixtures of iron silicates.

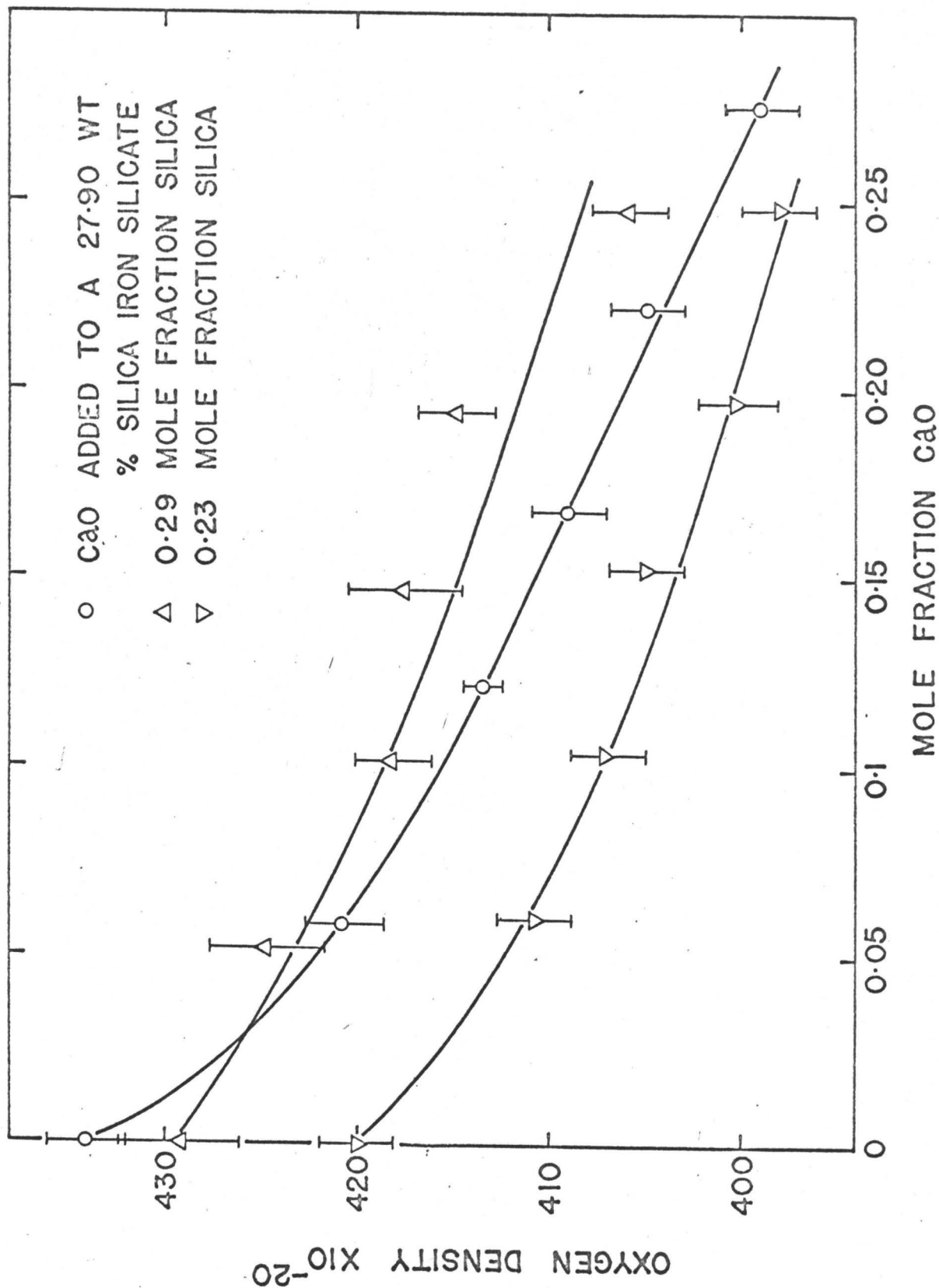


Figure 42. The oxygen density-composition relationships in the system $\text{CaO}-\text{FeO}-\text{SiO}_2$ at 1410°C .

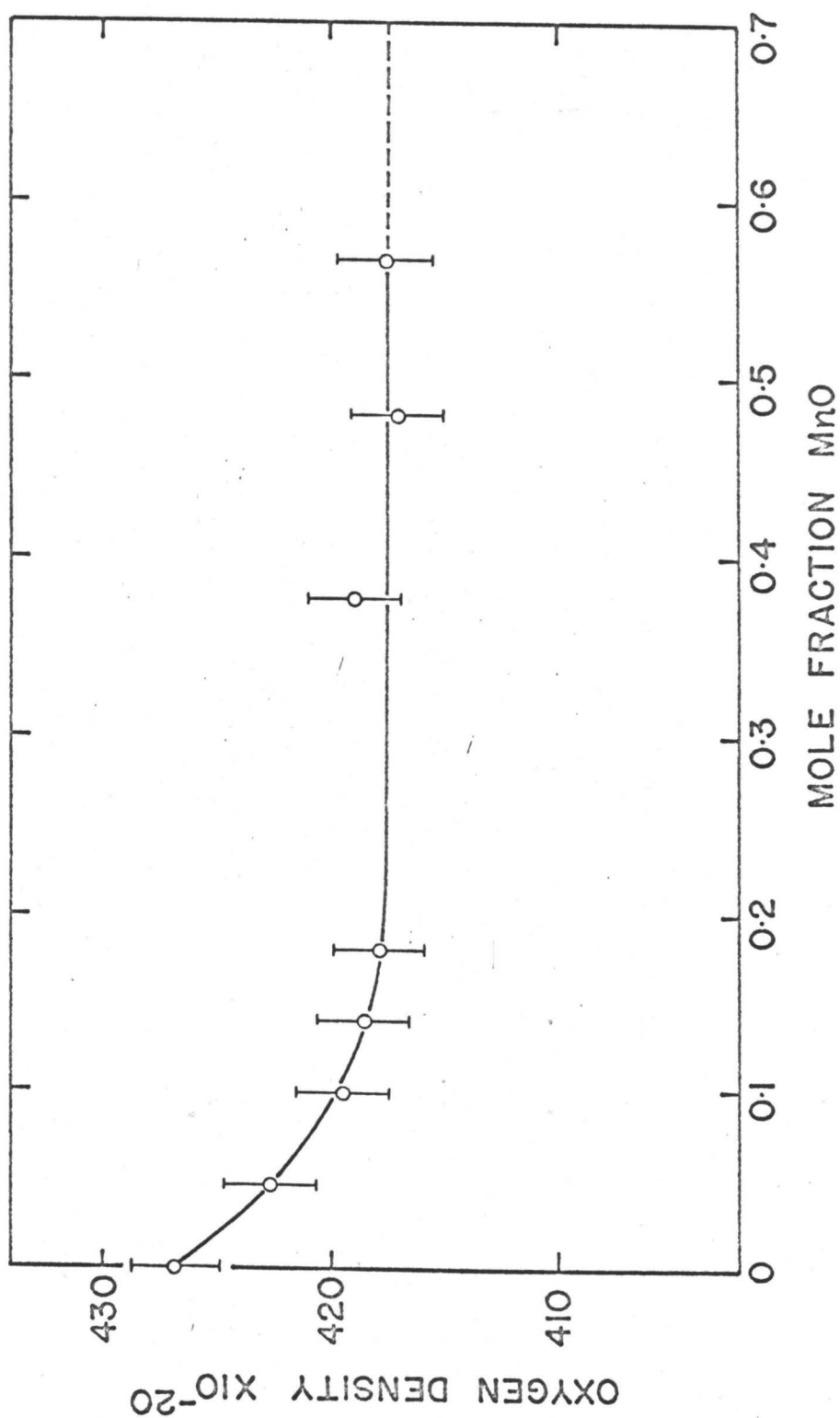


Figure 43. The oxygen density-composition relationship occurring in MnO-'FeO'-SiO₂ melts in which $N_{\text{SiO}_2} = 0.29$ at 1410°C.

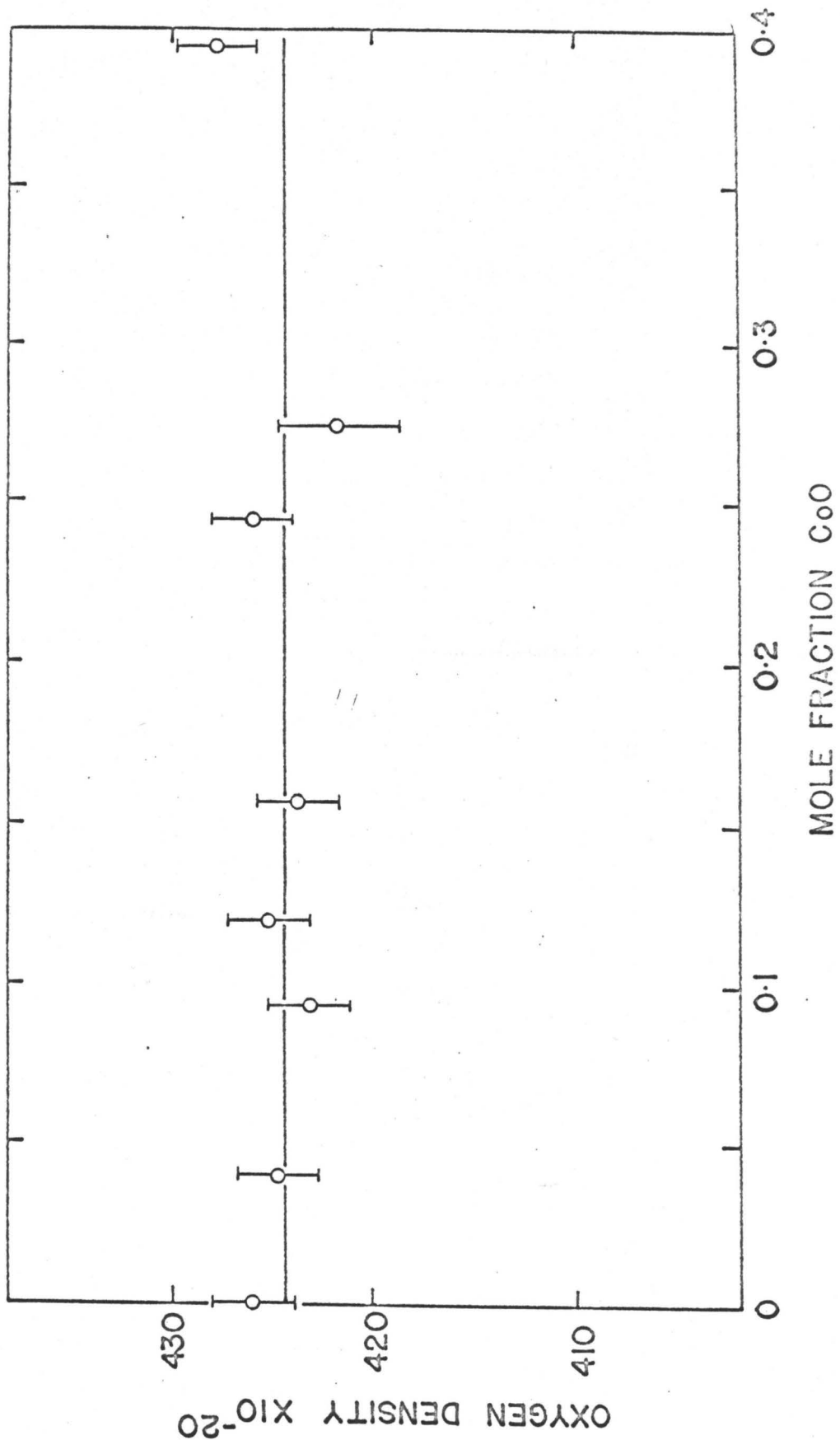


Figure 44. The oxygen density-composition relationship occurring in MnO-'FeO'-SiO₂ melts in which $N_{SiO_2} = 0.29$ at 1410°C

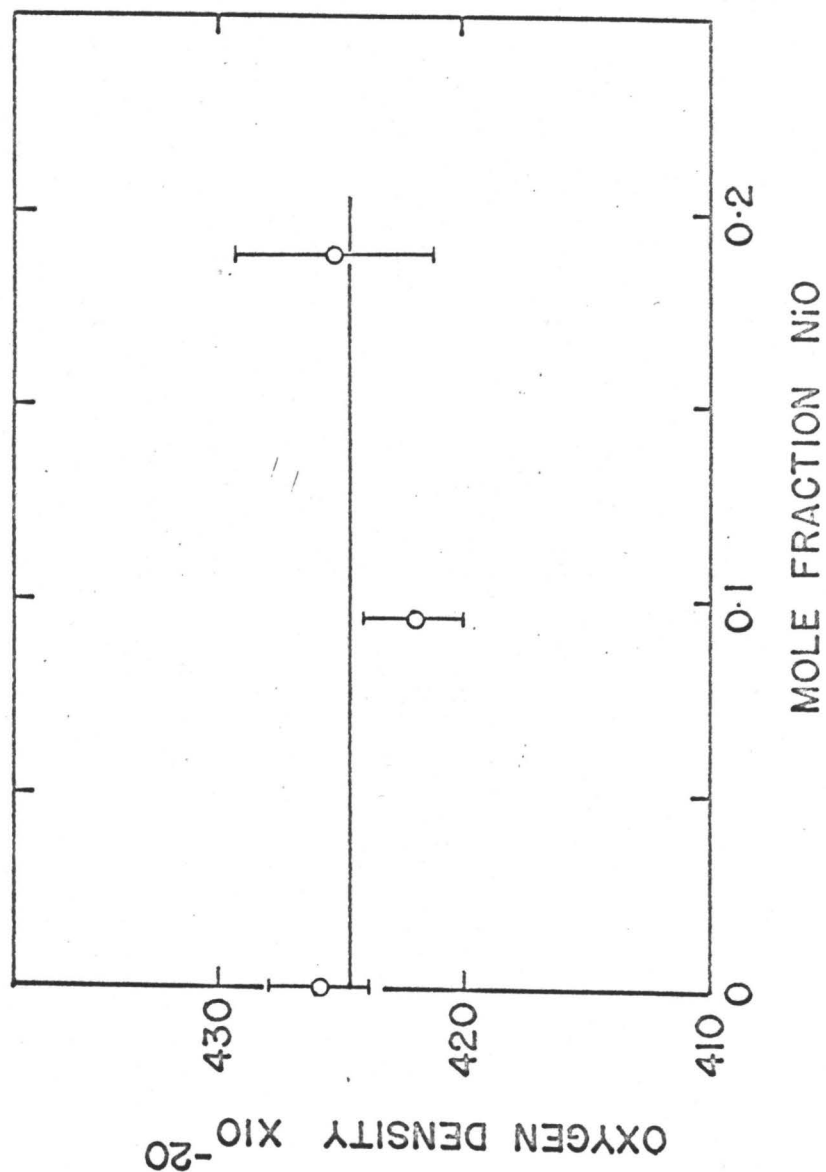


Figure 45. The oxygen density-composition relationship occurring in NiO-FeO-SiO₂ melts in which $N_{SiO_2} = 0.29$ at 1410°C.

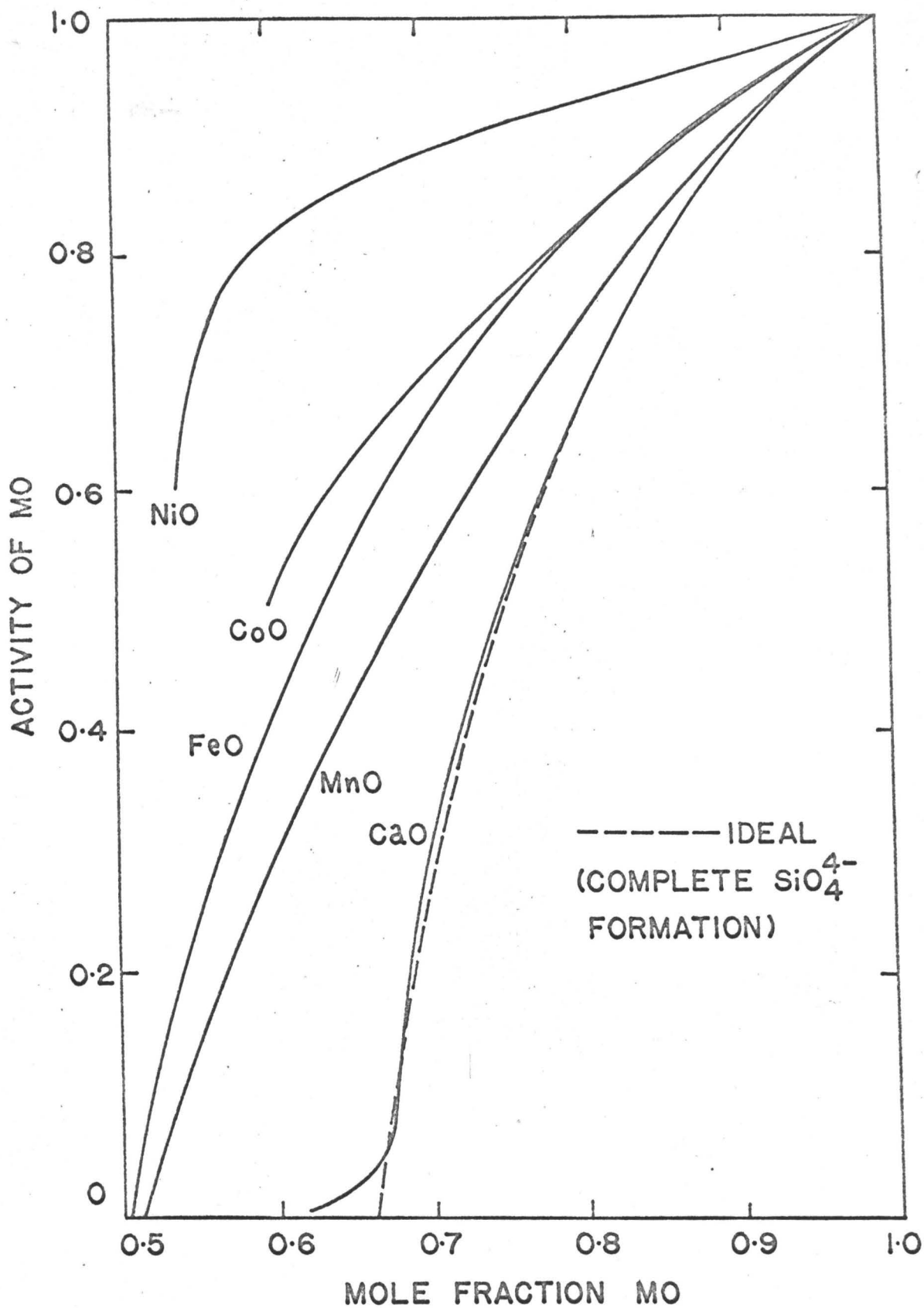


Figure 46. The activity-composition relationships of various metal oxides in binary silicate solution.

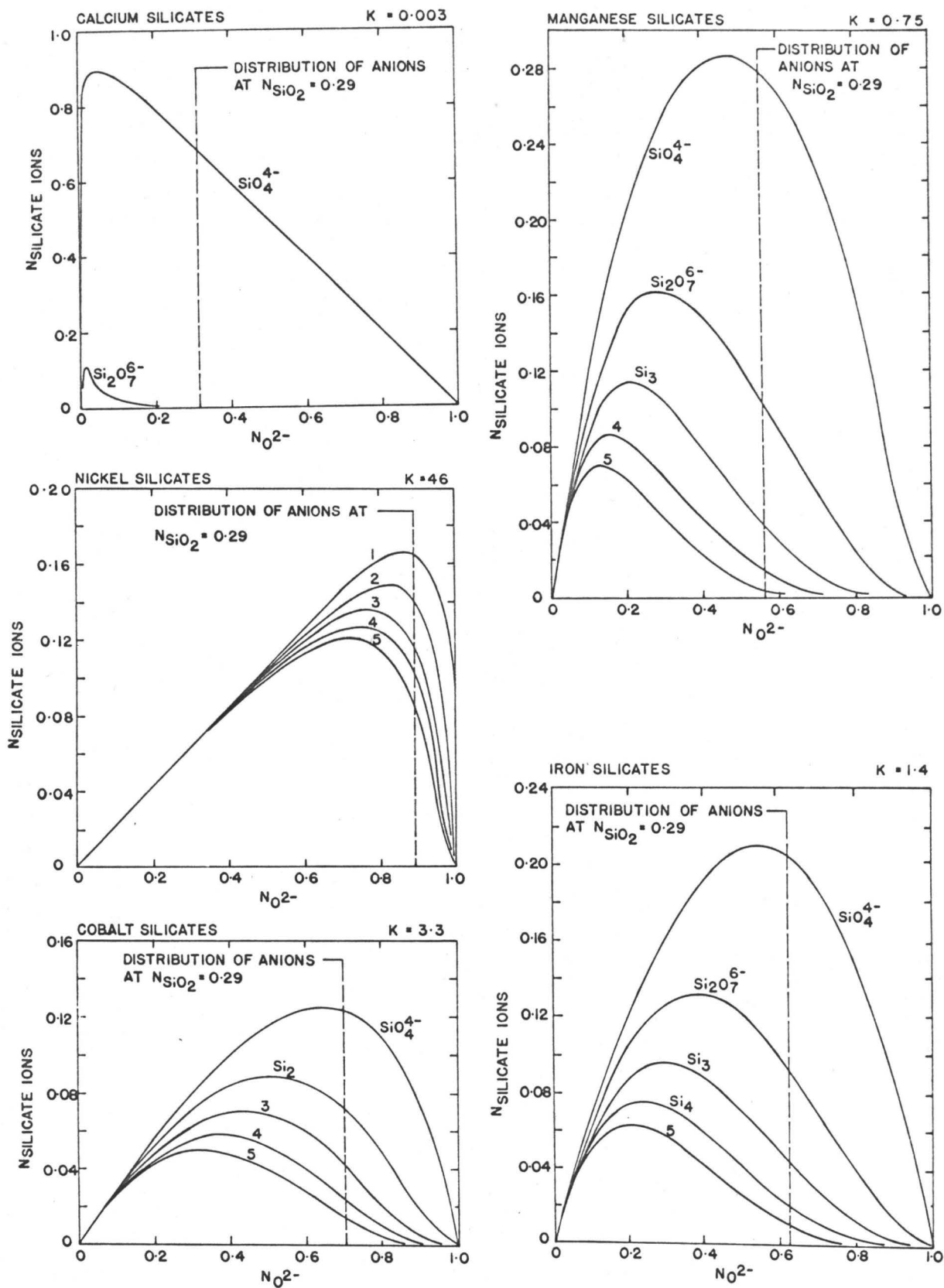


Figure 47. The theoretical distribution of anions occurring in various binary silicate systems.

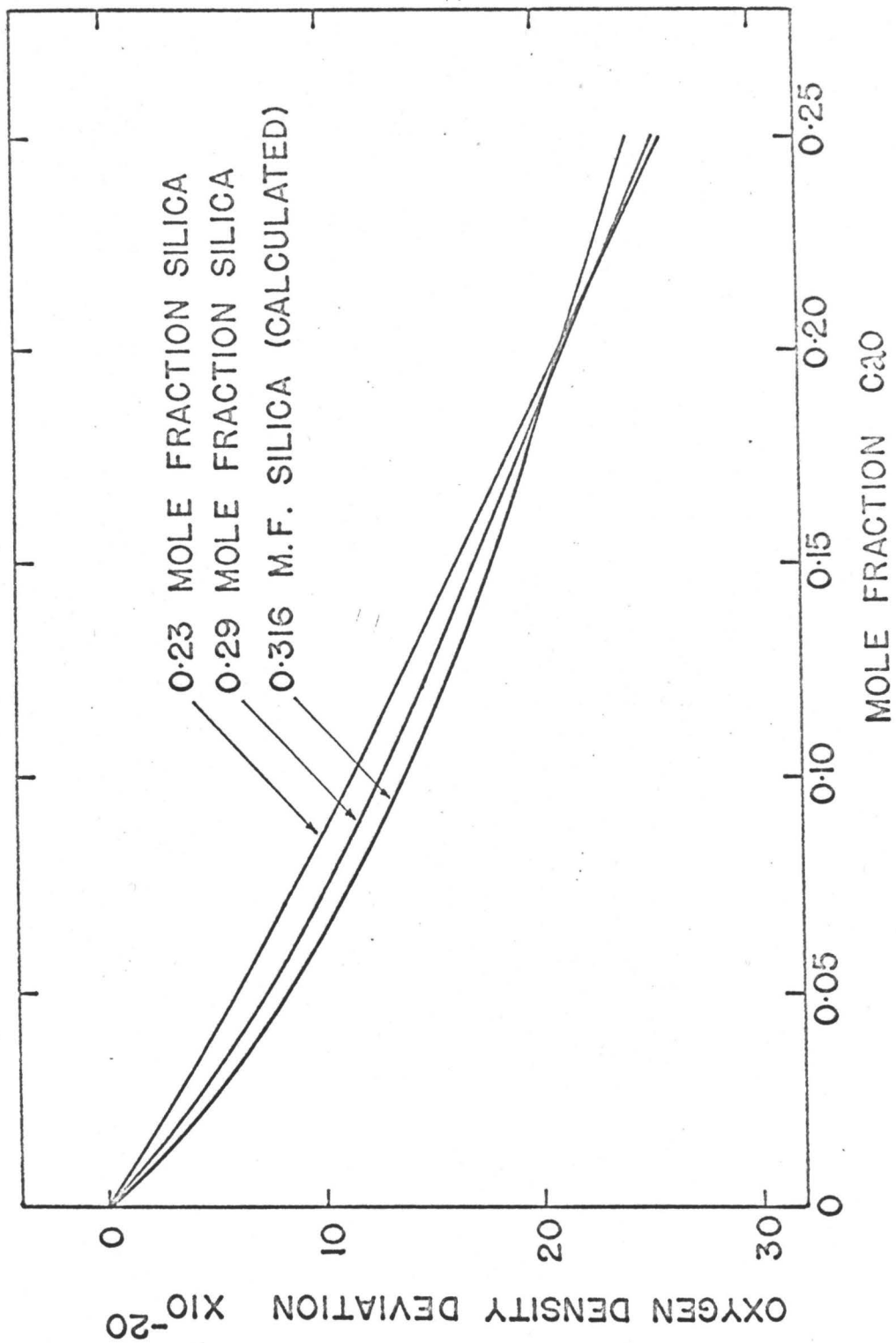


Figure 48. The oxygen density deviation due to cation replacement in the system $\text{CaO}-\text{FeO}-\text{SiO}_2$ at 1410°C .

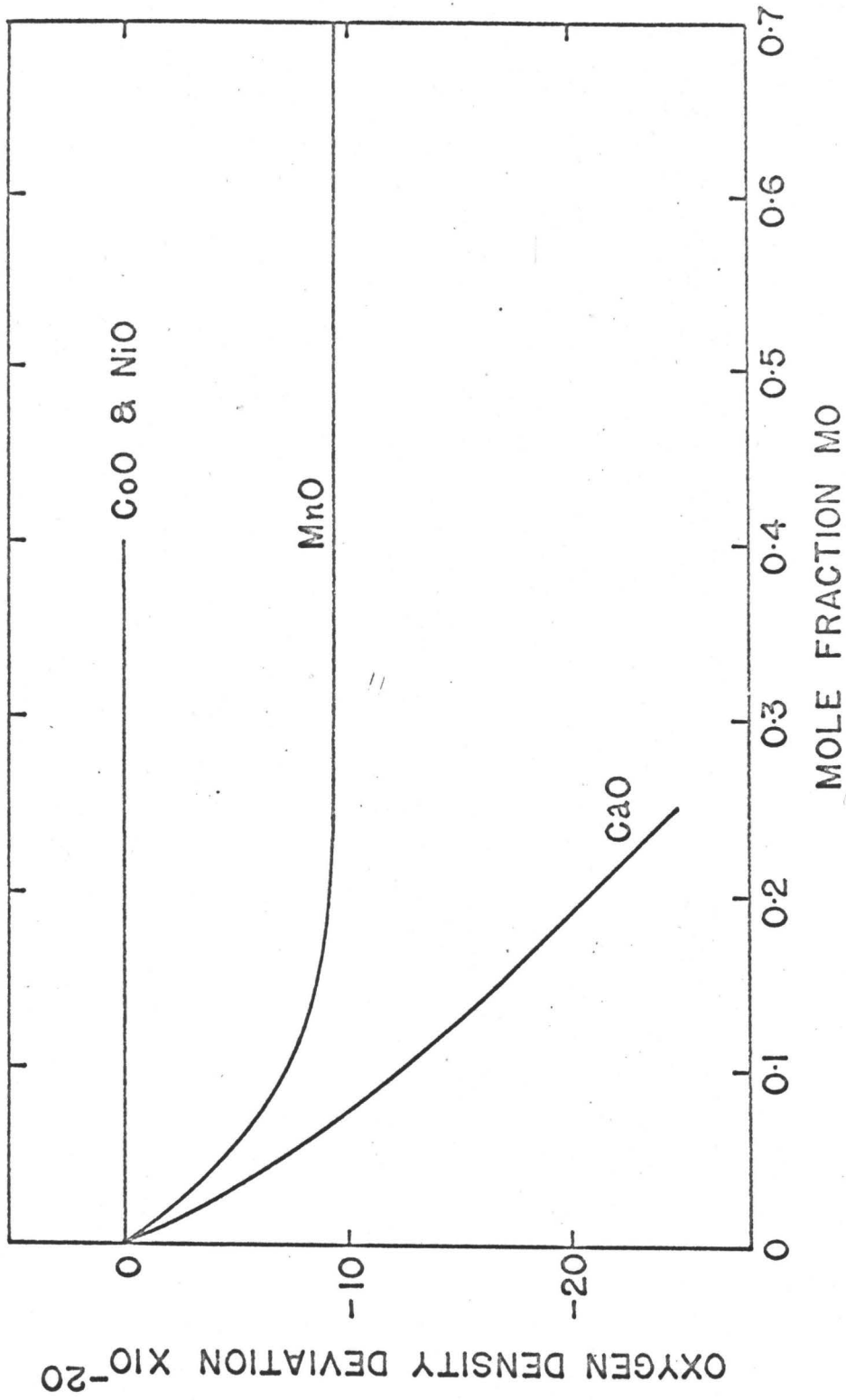


Figure 49. The oxygen density deviations due to the replacement of Fe^{2+} ions by Ca^{2+} , Co^{2+} , Mn^{2+} and Ni^{2+} ions along the $N_{\text{SiO}_2} = 0.29$ composition path at 1410°C .

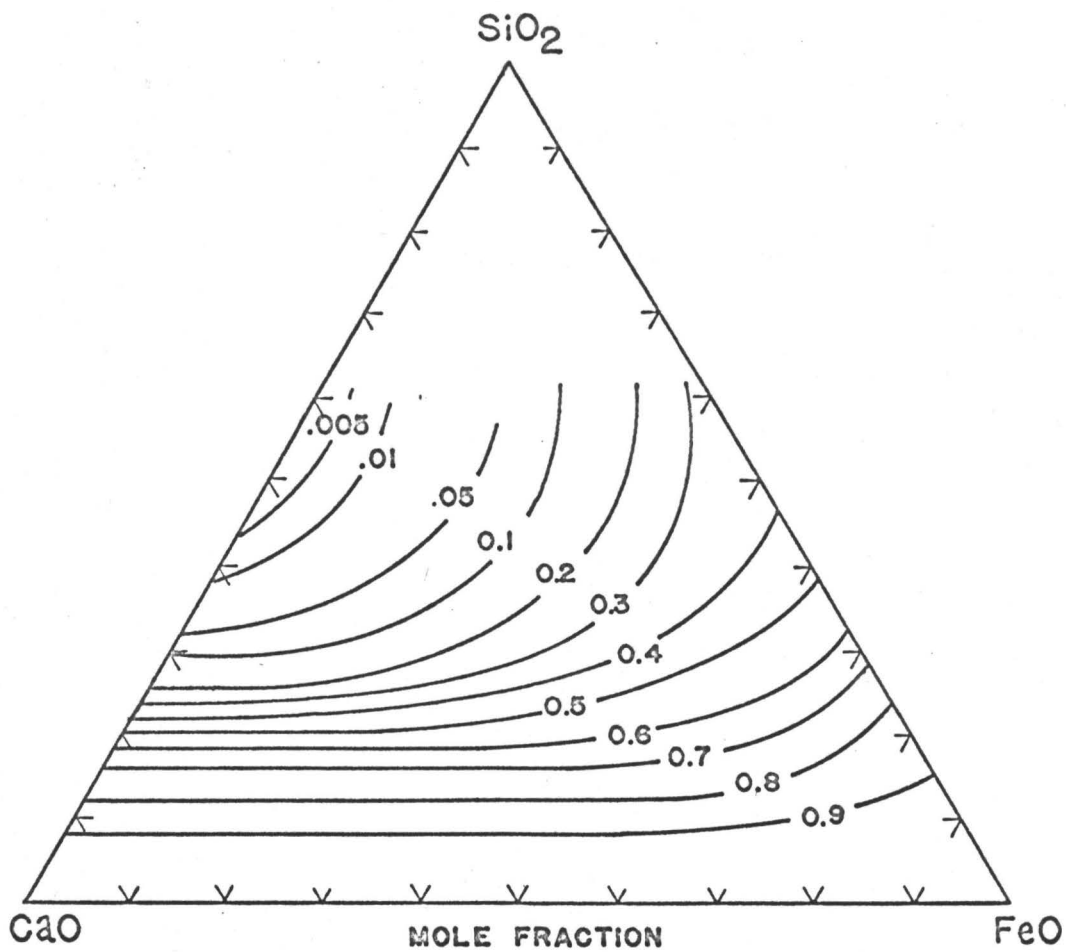
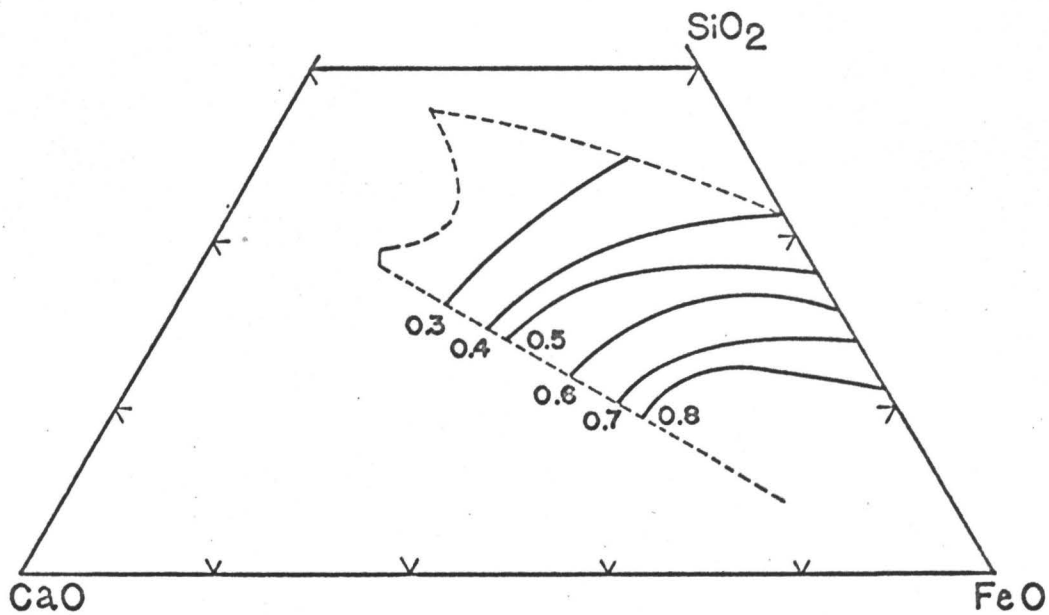


Figure 50. Iso-free oxygen ion activity lines in the system CaO-'FeO'-SiO₂ at 1600°C.⁽⁶¹⁾



— EXPERIMENT (BODSWORTH)
 - - - IDEAL MIXING WITH NO CHANGE IN DEGREE OF POLYMERISATION
 - · - · IDEAL MIXING WITH DEGREE OF POLYMERISATION DECREASING

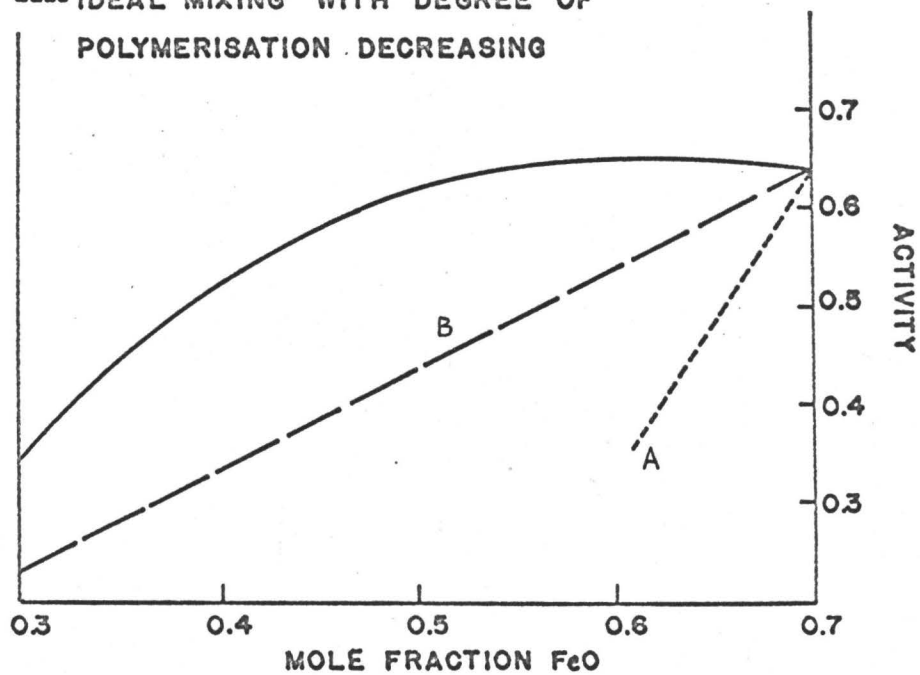


Figure 51. The activity of iron oxide in CaO-FeO-SiO₂ melts at 1365°C. (49)

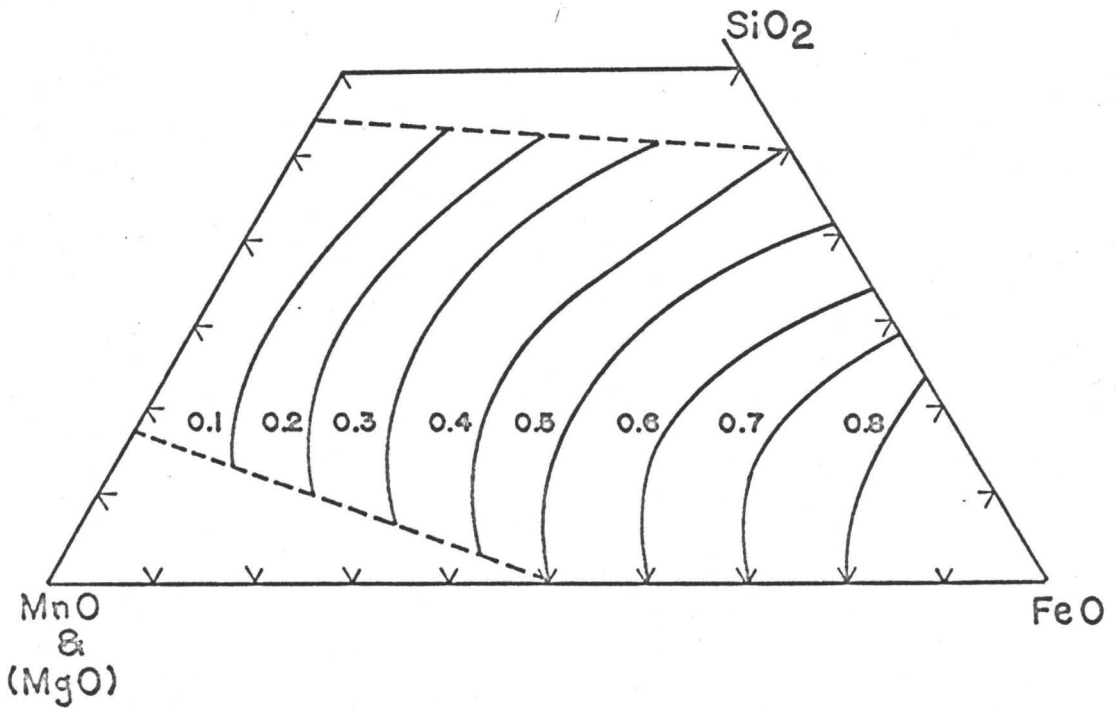
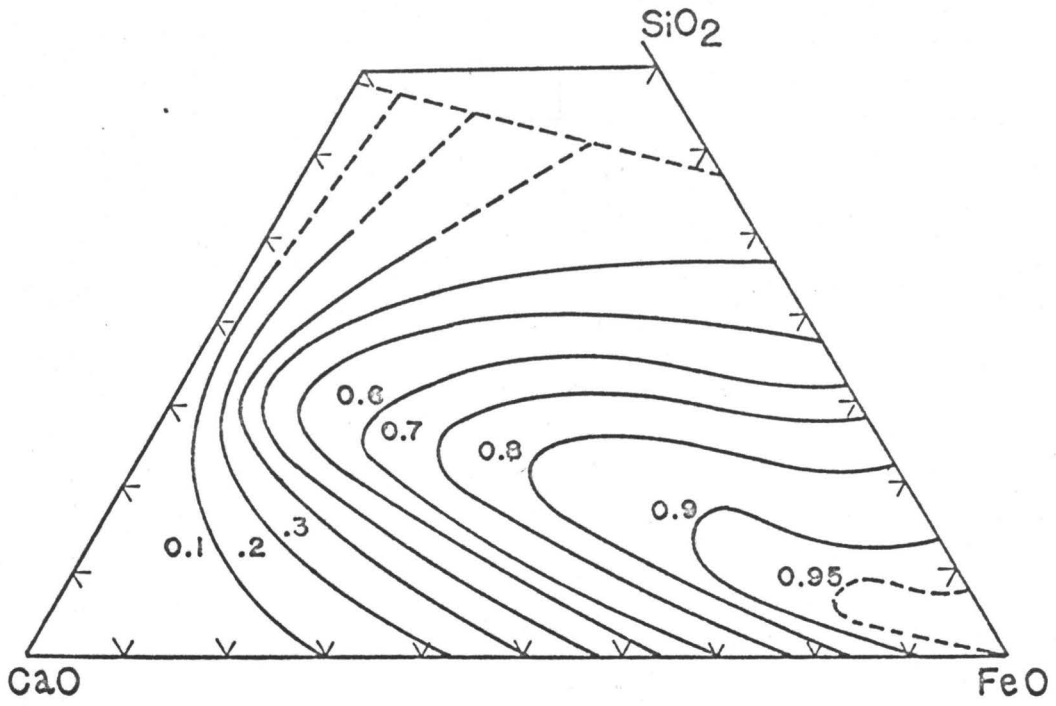


Figure 52. Iso-iron oxide activity lines in the systems CaO-'FeO'-SiO₂⁽¹¹³⁾ at 1600°C and MnO-'FeO'-SiO₂ at 1550°C.⁽¹⁰⁴⁾

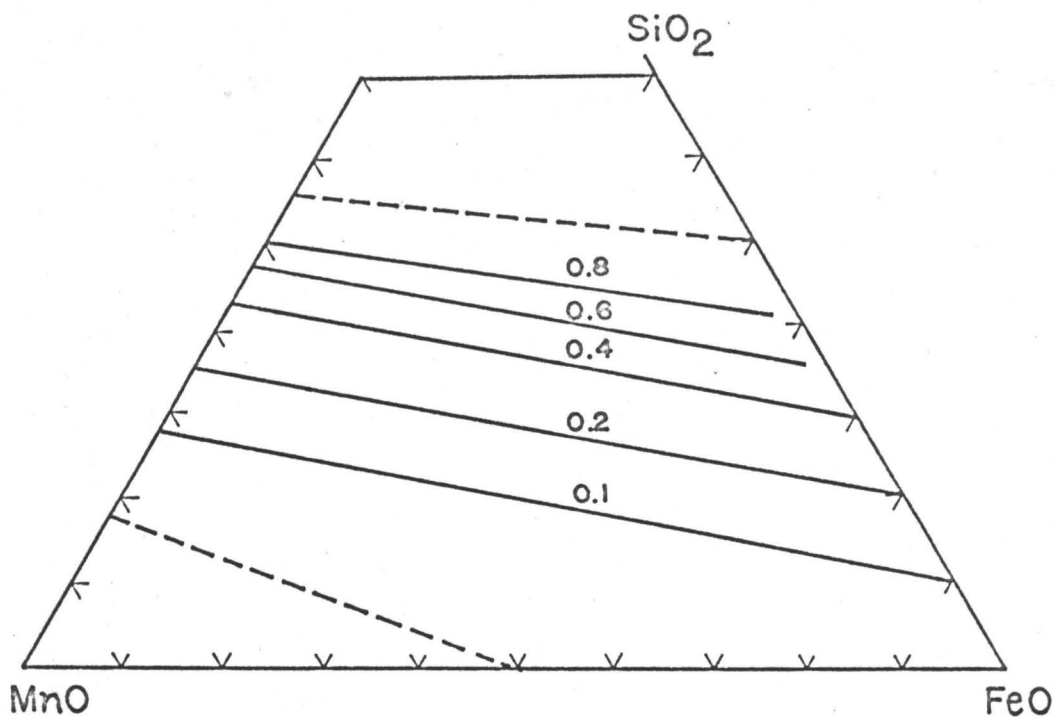


Figure 53(a). Iso-activity lines for SiO_2 in the system $\text{MnO}-\text{FeO}-\text{SiO}_2$ at 1550°C .⁽¹⁰⁴⁾

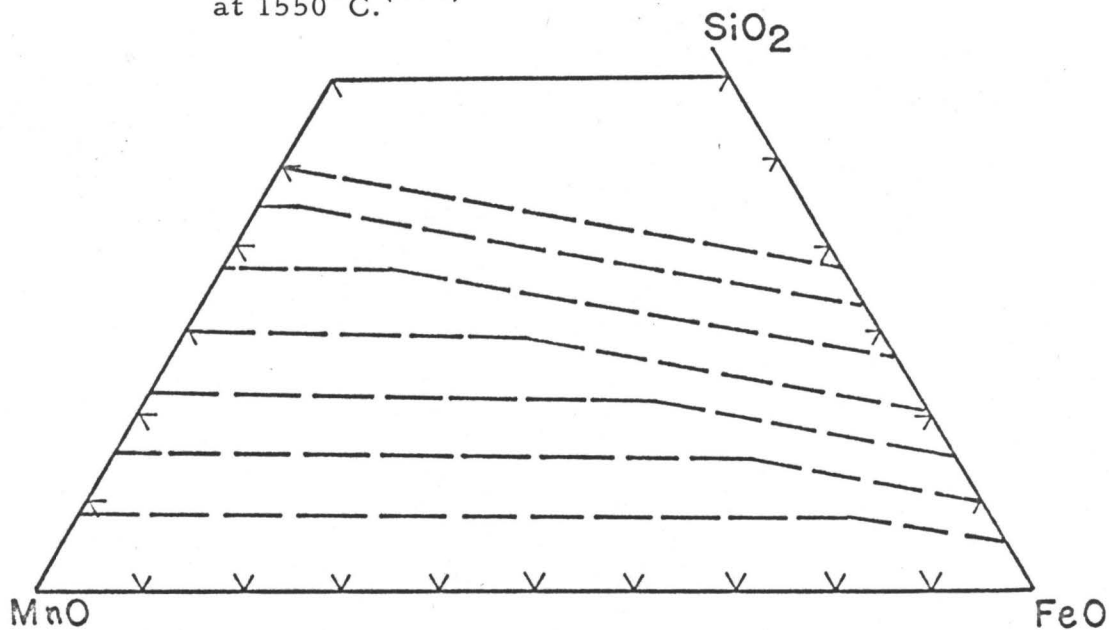


Figure 53(b). Proposed iso-degree of polymerisation lines in systems such as $\text{MnO}-\text{FeO}-\text{SiO}_2$.